Ruth SCHMIDT B.Sc.

Application of biological control agents in the rhizosphere of *Matricaria recutita* (L.): Their influence on the flavonoid production and non-target microorganisms

Master thesis

A thesis submitted in partial fulfilment of the requirements

for the degree of Master of Science (M.Sc.)

in „Biotechnology”

Institute of Environmental Biotechnology

Graz University of Technology

Supervisor: Univ.-Prof. Dipl.-Biol. Dr.rer.nat. Gabriele Berg

November 2012

EIDESSTATTLICHE ERKLÄRUNG

Ich erkläre an Eides statt, dass ich die vorliegende Arbeit selbstständig verfasst, andere als die angegebenen Quellen/Hilfsmittel nicht benutzt, und die den benutzten Quellen wörtlich und inhaltlich entnommene Stellen als solche kenntlich gemacht habe.

Graz, am …… ……
(Unterschrift)

STATUTORY DECLARATION

I declare that I have authored this thesis independently, that I have not used other than the declared sources / resources, and that I have explicitly marked all material which has been quoted either literally or by content from the used sources.

…….... ……
date (signature)

Acknowledgement

The research presented in this master thesis was carried out at the Laboratory of Environmental Biotechnology, Graz University of Technology between November 2011 and October 2012 and the Laboratory of Pharmacognosy, Graz University. A period of three months in winter 2011 was spent at the Sekem farm laboratories. The project was financially supported by UNCHAIN.

First, I would like to express my gratitude to my supervisor Prof. Gabriele Berg for giving me an insight into the fascinating area of microbial ecology and for her intellectual support during this time. Especially, I would like to thank her for giving me the opportunity to get acquainted with the everyday working life of Sekem, while experiencing a foreign culture first hand at the same time.

I am also very thankful to my co-supervisor, Prof. Elshahat M. Ramadan from the Microbiology Department Sekem who supported me during my stay in Egypt with scientific issues. Prof. Rudolf Bauer from the Institute of Pharmaceutical Sciences gave me the opportunity to conduct part of my work at his laboratory and provided me help in scientific questions. I would like to express my gratitude for this.

I am grateful for the scientific support from M.Sc. Martina Köberl. Also, Dr. Massimiliano Cardinale and Dr. Anastasia Bragina are to be acknowledged for their contribution to this thesis. I would like to thank Dr. Marlene Monschein for supporting me in the analytical part and Dr. Henry Müller for proofreading the thesis. Furthermore, I would like to express my gratitude to all co-workers from the Sekem companies and the Heliopolis University for their support.

The whole group of researchers, teachers and students have earned my compliments for the atmosphere they have created to the laboratories in Graz as well as in Cairo. Especially, I would like to thank my exchange partner Amr Mostafa and his family for their hospitality and for giving me an insight into the Egyptian way of living. Finally I would like to thank my friends for the help and support during my work. I am deeply grateful to my parents for giving me the opportunity to study and for supporting me in my choices and their endless patience with me.

Abstract

The influence of biological control agents (BCAs) on the production of flavonoids as well as on the indigenous plant-associated bacteria of *Matricaria recutita* (L.) was investigated. Chamomile seedlings were inoculated with three Gram-positive strains *Streptomyces subrutilus* Wbn2-11, *Bacillus subtilis* Co1-6, *Paenibacillus polymyxa* Mc5Re-14 and three Gram-negative strains *Pseudomonas fluorescens* L13-6-12, *Stenotrophomonas rhizophila* P69 and *Serratia plymuthica* 3Re4-18. Molecular fingerprints of microbial communities as well as real-time PCR analysis showed no significant differences for all applied bacterial antagonists compared with the uninoculated control. A pyrosequencing approach revealed *Proteobacteria*, *Actinobacteria*, *Acidobacteria*, *Chloroflexi*, *Verrucomicrobia*, *Bacteroidetes*, *Planctomycetes*, *Gemmatimonadetes* and *Firmicutes* as the most abundant phyla in all analysed samples (>1% of all sequences). When bacteria were analysed at the genus level, the relative abundances of different genera belonging to phyla *Proteobacteria*, *Bacteroidetes* and *Actinobacteria* varied among the samples under different treatments. Investigations of the secondary metabolites of chamomile showed a higher content of apgenin-7-*O*-glucoside and apigenin for the treatments with Gram-positive strains.

Kurzfassung

Im Rahmen der Masterarbeit wurde der Einfluss von biologische Bekämpfungsmitteln (BCAs) auf die Produktion von Flavonoiden, sowie auf die indigenen pflanzenassoziierten Bakterien von *Matricaria recutita* (L.) untersucht. Dazu wurden Kamillenkeimlinge mit drei Gram-positive Stämmen *Streptomyces subrutilus* Wbn2-11, *Bacillus subtilis* Co1-6, *Paenibacillus polymyxa* Mc5Re-14 und mit drei Gram-negativen Stämmen *Pseudomonas fluorescens* L13-6-12, Stenotrophomonas rhizophila P69 und *Serratia plymuthica* 3Re4-18 inokuliert. Molekulare Fingerprints der mikrobiellen Gemeinschaften, sowie real-time PCR Analysen zeigten keine signifikanten Unterschiede für alle eingesetzten bakteriellen Antagonisten verglichen mit der nicht inokulierten Kontrolle. Ein Pyrosequenzierungsansatz ließ *Proteobacteria*, *Actinobacteria*, *Acidobacteria*, *Chloroflexi*, *Verrucomicrobia*, *Bacteroidetes*, *Planctomycetes*, *Gemmatimonadetes* und *Firmicutes* als die am häufigsten vorkommende Stämme in allen untersuchten Proben erkennen (>1% aller Sequenzen). Die Analyse der Bakterien auf Gattungsebene zeigte, dass die relativen Häufigkeiten der verschiedenen Gattungen, die zu den Phyla *Proteobacteria*, *Bacteroidetes* und *Actinobacteria* zählen, unter den Proben der verschiedenen Behandlungen variierten. Untersuchungen der Sekundärmetaboliten von Kamille zeigten einen höheren Gehalt an Apgenin-7-*O*-glucosid und Apigenin für die Behandlungen mit Gram-positiven Stämmen.

List of contents

1. Introduction

1.1. Biological control: a solution for sustainable agriculture

The increase in world's population and the resulting demand for more food led to an intensification of agriculture production over the past few decades. However, increasing use of chemicals fertilizers and pesticides causes several negative effects, such as development of pathogen resistance to the applied agents, lethal effects on non-target species, environmental pollution, destruction of natural habitats and risks to human health (Compant et al., 2005; Rigby et al., 2001). Moreover, the increasing cost of chemical pesticides, especially in less affluent regions of the world, and consumer demand for healthy food without pesticides has led to a search for alternatives in sustainable agriculture (Yiridoe et al., 2005). Biological control of plant pathogens as well as plant growth promotion with naturally occurring microorganisms is thus being considered as an alternative for an environmentally friendly agriculture (Berg, 2009; Whipps, 2001). Presently, several microbial inoculants have been successfully commercialised and are currently marketed, dependent on their mode of action and effects, as biopesticides, plant strengtheners, biofertilisers, and phytostimulators (Berg, 2009).

1.2. Plant-associated bacteria and their use in agriculture

Biological control agents (BCAs) and plant growth promoting bacteria (PGPBs) (Compant et al., 2005; Emmert & Handelsman, 1999; Weller, 2007; Whipps, 2001) perform beneficial effects on plants via direct and indirect mechanisms. Direct mechanisms involve the interaction between beneficial bacteria and their host plant by serving the plant with supplying nutrients, such as the fixation of nitrogen, the phosphate solubilisation or the synthesis of phytohormones, including indole acetic acid (IAA), ethylene (ET), abscisic acid, cytokinin, and gibberellin (Bloemberg & Lugtenberg, 2001; Faure et al., 2008; Gull et al., 2005). Indirect mechanisms are based on the antagonistic activity against plant pathogens by competition for nutrients and niches (CNN), antibiosis or the induction of systemic resistance (ISR) in host plants (Chin-A-Woen et al., 2000; Loon, 2007; Lugtenberg & Kamilova, 2009).

The rhizosphere, comprising plants roots and the surrounding area of soil influenced by the roots, represents a hot spot for microorganisms due to the presence of root exudates and rhizodeposits (Bais et al., 2006; Shaw et al., 2006; Smalla et al., 2006). Moreover, the endosphere describing the microenvironment inside the plant represents a niche for the colonization of BCAs or PGPBs (Berg, 2009; Hardoim et al., 2008).

Despite their positive effects, if applied to plant roots in sufficient numbers, BCAs or PGPBs may perturb indigenous microbial populations. Therefore, unwanted, unspecific actions of the introduced beneficial microorganisms against non-target organisms have to be assessed (Scherwinski et al. 2008). It is an important task to gain knowledge about the microbial ecology of the target habitat for risk assessment studies relating to the release of beneficial microorganisms.

1.2.1. Streptomyces subrutilus

Streptomyces spp. are Gram-positive bacteria that have been studied as potential biocontrol agents (BCA) against fungal phytopathogens (Sabaratnam & Traquair, 2002). For instance, *Streptomyces sp.* HRO-71 was described as an efficient biological control organism towards several plant pathogenic fungi by the production of siderophores, antibiotics, indole-3-acetic acid (IAA), and chitinases (Berg et al., 2001). Mycostop®, based on a selected *Streptomyces griseoviridis* isolate from Finnish *Sphagnum* peat, is commercially available bio-pesticide that inhibits several seedborn and soilborne fungal pathogens (White, 1990). Moreover, control of *Rhizoctonia*-induced damping-off disease by *Streptomyces sp.* Di-944 was superior to Mycostop® (Fravel, 2005). A combination of lyophilized spores of the antibiosis strain *Streptomyces melanosporofaciens* EF-76 with plant defence-eliciting chitosan was shown to control potato scab (Jobin et al., 2005). Furthermore, Streptomyces species were shown to produce a variety of volatile organic compounds (VOCs) that can influence the growth of fungi (Alstrom, 2001). Schöller et al. (2002) screened twenty-six *Streptomyces* spp. and identified a total of 120 different VOCs, comprising alkanes, alkenes, alcohols, esters, ketones, sulfur-containing compounds and terpenoids.

1.2.2. Bacillus subtilis

The Gram-positive genus of Bacillus comprises a number of species that were among the first successful bio-pesticides for the control of insects and pathogens (Sarker and Mahbub, 2012). *Bacillus thuringiensis* (*Bt*), represents probably the most prominent member that accounts for over 90% of all market bio-insecticides (Fernández-Ruvalcaba et al., 2010). During sporulation, crystals of the Cry protein are formed that act toxic to many insects by forming pores of the membrane in the insect gut (Sarker and Mahbub, 2012). In Germany, FZB24® *Bacillus subtilis* (ABiTEP GmbH Berlin) has been on the market since 1999 and is used mainly as a seed dressing for potatoes (Kilian et al., 2000). Effective disease suppression of *Fusarium* and *Rhizoctonia* spp. on various crops such as cotton is achieved by seed treatment with Kodiak®, a formulated concentrate of *Bacillus subtilis* GB03 spores combined with traditional fungicides (Francis et al., 2010; Fravel, 2005). Moreover, Kodiak® protects the plant and stimulates plant growth and root proliferation (Spaepe et al., 2007; Tsavkelova et al., 2006). Several Bacillus strains have also been reported to be capable of producing VOCs leading to a promotion of plant growth (Ryu et al., 2004). For instance, VOCs emitted by *Bacillus subtilis* GB03 and *Bacillus amyloliquefaciens* IN937 were reported to promote the growth of *Arabidopsis thaliana* (Insam & Seewald, 2010; Ryu et al., 2003). Furthermore, the first enzyme of phenylpropanoidbiosynthesis pathway leading to the formation of flavonoids, phenylalanine ammonia-lyase (PAL), has been shown to increase due to seed treatment with *Bacillus subitilis* AF1 (Podile & Laxmi, 1998).

1.2.3. Paenibacillus polymyxa

Paenibacillus spp. represent Gram-positive bacteria that comprise a number of species used as biological control agents. Due to its broad host range and its ability to form endospores, *Paenibacillus polymyxa* is a potential commercially useful biocontrol agent (Timmusk et al., 2005). Moreover, the endophytic strain *Paenibacillus* sp. HKA-15 was reported to produce antifungal peptide antibiotics that protect soybean against *Rhizoctonia bataticola* that causes charcoal rot disease (Lal & Tabacchioni, 2009). Likewise, the impact of *Paenibacillus polymyxa* on plant growth is strong through the production of phytohormones such as cytokinin and auxin (Lal & Tabacchioni, 2009). Verginer et al. (2010) described the impact of

several *Paenibacillus* species on fruit flavour of grapes cultivated on different vineyards in Austria. Moreover, half of the grape-associated microorganisms were shown to produce a broad spectrum of VOCs. *Paenibacillus polymyxa* PB71 showed effective suppression of powdery mildew, a disease of the Styrian oil pumpkin (Fürnkranz et al., 2012). Timmusk & Wagner (1999) reported the induction of mild biotic stress by *Paenibacillus polymyxa* B2, suggesting that genes associated with plant defences against abiotic and biotic stress may be co-regulated. Recently, Selim et al. (2010) reported the upregulation of genes involved in the biosynthesis of phytoalexins, antifungal activity or cell wall in roots or cells after treatment with antagonistic lipopolypeptides (paenimyxin) from *Paenibacillus sp.* strain B2.

1.2.4. Pseudomonas fluorescens

Pseudomonas spp. are aerobic, Gram-negative bacteria that live ubiquitous in agricultural soils and are well adapted to growing in the rhizosphere (Weller, 2007). Particularly, fluorescent *Pseudomonas* spp. have been studied for decades for their plant growth-promoting effects through effective suppression of soilborne plant pathogens (Bakker et al., 2007). It has been described that *Pseudomonas fluorescens* enhanced biomass yield and ajmalicine production in *Catharanthus roseus* under draught stress (Jaleel et al., 2007). Moreover, certain fluorescent *Pseudomonas* spp. improved the growth of potato sugar beet and radish when applied to seeds or seed piece (Kloepper, 1981; Schroth & Hancock, 1982). A major mechanism of control of soilborne plant pathogens by fluorescent pseudomonads is the production of antibiotics, such as 2,4-diacetylphloroglucinol (DAPG), phenazine, pyoluteorin, and pyrrolnitrin (Viebahn et al., 2003). However, the major weakness of pseudomonads as biocontrol agents is their inability to produce resistant spores, as do many *Bacillus* spp., which therefore leads to complications during formulation process (Weller, 2007).

1.2.5. Stenotrophomonas rhizophila

The Gram-negative genus *Stenotrophomonas* comprises important species that used as BCAs. Especially *Stenotrophomonas maltophilia* and *Stenotrophomonas rhizophila* are known for their beneficial interactions with plants (Ryan et al., 2009). However, *Stenotrophomonas maltophilia* represent an emerging human pathogen that is responsible for fatal infections in humans (Berg et al., 2005). The plant growth

promoting effect of *Stenotrophomonas* spp. through the fixation of nitrogen was reported by Dobbelaere et al. (2003). Xanthobaccins, antifungal compounds produced by *Stenotrophomonas* sp. strain SB-K88, were shown to suppress sugar beet damping-off disease (Hashidoko et al., 1999). Wolf et al. (2002) described the antifungal properties of *Stenotrophomonas rhizophila*, which exclusively comprises strains isolated from the rhizosphere of plants, for the first time. Furthermore, the negative influence on mycelial growth of the soil-borne phytopathogenic fungus *Rhizoctonia solani* through the release of VOCs from *Stenotrophomonas rhizophila* P69 was reported previously (Kai et al., 2007). Recently, the accumulation of the compatible solutes glucosylglycerol (GG) and trehalose under salt stress conditions by *Stenotrophomonas rhizophila* was reported (Hagemann et al., 2008).

1.2.6. Serratia plymuthica

The genus *Serratia* comprises Gram-negative gamma-proteobacteria, which are associated with plant roots (Kai et al., 2007). *Serratia plymuthica* isolated were shown to produce antibiotics such as prodigiosin or pyrrolnitrin (Kalbe et al., 1996). Others secrete mycolytic enzyme, such as chitinases and glucanases (Berg et al., 2001). Kamensky (2003) described the use of *Serratia plymuthica* IC14 for the biocontrol of *Botrytis cinerea* and *Sclerotinia sclerotiorum* diseases. The strain *Serratia plymuthica* HRO-C48, isolated from the *Brassica napus* rhizosphere, proved to be an effective antagonistic bacterium due to its plant growth promoting and chitinolytic activity and was successfully developed as a commercially available product called Rhizostar® (Scherwinski et al., 2006). Rhizostar® acts against the phytopathogens *Verticillium dahlia*, especially by the secretion of so called *N*-acyl homoserine lactones (AHLs) that allow bacteria to use quorum sensing; a mechanism that is based on the monitoring of their own population density and the coordination of the regulation of gene expression (Müller et al., 2009).

1.3. *Matricaria recutita* (L.) as a model plant

Matricaria recutita (L.) (syn: *M. chamomilla* (L.); German chamomile) belongs to the family of Asteraceae (Compositae) and is one of the most widely used medicinal plants in the world (Salamon, 1992). The medical plant is widespread in various countries in the world particularly in Eastern Europe, Egypt and Argentina (Mulinacci, 2000). Infusions and essential oils from fresh or dried flower heads have been largely

used in herbal medicine for centuries due to its anti-inflammatory, spasmolytic, sedative, antibacterial and antifungal properties (Emmert & Handelsman, 1999). Moreover, chamomile has moderate antioxidant activities and significant antiplatelet activity *in vitro* (Abdoul-Latif et al. 2011; McKay and Blumberg, 2006). Sesquiterpenes (α-bisabolol, bisabololoxides A and B, farnesene), sesquiterpenelactones (chamazulene, with intense blue colour), acetylene-derivatives (spiroethers) as well as the flavonoids (apigenin, quercetin, patuletin, luteolin) and their glucosides are some of the many compounds that are responsible for those medicinal properties (Ganzera et al., 2006; McKay & Blumberg, 2006).

1.3.1. Properties and functions of flavonoids

Flavonoids are a widespread class of secondary metabolites including more than 6000 different structures (Ferrer et al., 2008). All flavonoids identified in the chamomile flowers to date are listed in Table 1 and their chemical reference structure is also reported (Fig. 1). By definition, they all share the same basic skeleton, the flavan-nucleus, consisting of two aromatic rings with six carbon atoms (ring A and B) interconnected by a hetero cycle including three carbon atoms (ring C) (Schijlen et al., 2004).

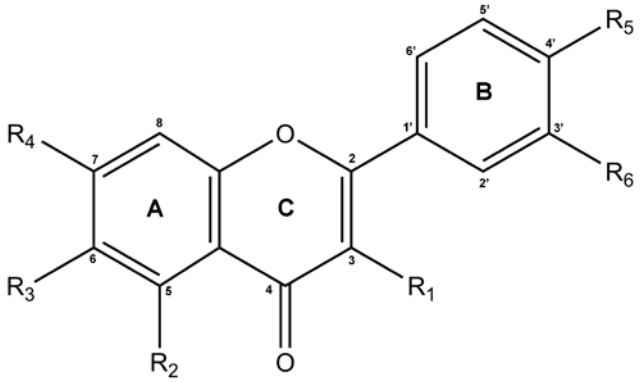

Fig. 1: Chemical structure of flavonoids

Table 1: List of phenolic compounds previously identified in Chamomilla recutita L. head flowers. Chemical reference structure and corresponding molecular weights also reported. glu = Glucose, rut = Rutinose, apio = Apiose, gal = Galactose (Mulinacci et al., 2000).

Substance	R1	R2	R3	R4	R5	R6	MW
Apigenin	H	OH	H	OH	OH	H	270
Apigenin-7-O-β-glucoside	H	OH	H	O-glu	OH	H	432
Apigenin-7-O-apiosyl-glucoside	H	OH	H	O-glu-apio	OH	H	564
Apigenin-7-O-glucosyl-6"-acetate "	H	OH	H	O-glu-6"ac	OH	H	474
Apigenin-7-O-glucosyl-2"-acetate "	H	OH	H	O-glu-2"ac "	OH	H	474
Apigenin-7-O-glucosyl-2",3"-diacetate "	H	OH	H	O-glu-2",3"-diac	OH	H	516
Apigenin-7-O-glucosyl-3",4"-diacetate "	H	OH	H	O-glu-3",4"-diac	OH	H	516
Luteolin	H	OH	H	OH	OH	OH	286
Luteolin-7-O-β-glucoside	H	OH	H	O-glu	OH	OH	448
Luteolin-4'-O-β-glucoside	H	OH	H	OH	O-glu	OH	448
Luteolin-7-O-β-rutinoside	H	OH	H	O-rut	OH	OH	594
6-Hydroxy-luteolin-7-glucoside	H	OH	OH	O-glu	OH	OH	464
Quercetin	OH	OH	H	OH	OH	OH	302
Quercetin-7-O-β-glucoside	OH	OH	H	O-glu	OH	OH	464
Quercetin-3 -O-β-rutinoside	O-rut	OH	H	OH	OH	OH	610
Quercetin-3 -O-β-galactoside	O-gal	OH	H	OH	OH	OH	464
Patuletin	OH	OH	OCH_3	OH	OH	OH	332
Patuletin-7-O-β-glucoside	OH	OH	OCH_3	O-glu	OH	OH	494
Isorhamnetin	OH	OH	H	OH	OH	OCH_3	316
Isorhamnetin -7-O-β-glucoside	OH	OH	H	O-glu	OH	OCH_3	478
Chrysoeriol-7-O-β-glucoside	H	OH	H	O-glu	OH	OCH_3	462
Jaceidin	OCH_3	OH	OCH_3	OH	Oil	OCH_3	360
Chrysosplenol	OCH_3	OH	OCH_3	OCH_3	OH	OH	360
Eupatoletin	OH	OH	OCH_3	OCH_3	OH	OH	360
Spinacetin	OH	OH	OCH_3	OH	OH	OCH_3	346
Axillarin	OCH_3	OH	OCH_3	OH	OH	OH	346
Eupalitin	OH	OH	OCH_3	OCH_3	OH	H	330
Chrysosplenetin	OCH_3	OH	OCH_3	OCH_3	OH	OCH_3	374
Astragalin	O-glu	OH	H	OH	OH	OH	286

The different flavonoids have different metabolic functions in plants including protection against ultraviolet (UV) radiation and phytopathogens, reproduction, auxin transport, as well as the coloration of flowers as a visual signal that attracts pollinators (Falcone et al., 2012). They also induce root nodulation when excreted by symbiotic nitrogen-fixing rhizobia (Mandal et al., 2010). Flavonols are probably the most important flavonoids participating in stress responses of plants (Stafford, 1991). Flavonoids are synthesized through the phenylpropanoid pathway, transforming phenylalanine into 4-coumaroyl-CoA, which finally enters the flavonoid biosynthesis pathway. Due to the beneficial effects of flavonoids there have been several attempts

to stimulate their biosynthesis and accumulation by genetic modification of the flavonoid pathway (Treutter, 2006). Furthermore, approaches to support the plant's defence mechanisms by stimulation of the flavonoid production have been made (Fischer et al. , 1997; Yu et al., 2003; Jeandet et al., 2002).

1.4. Objectives of the study

The aim of this study was to investigate the influence of six bacterial antagonists introduced into naturally chamomile field (Fig. 2) on the flavonoid production of the plant and to analyse their impact on the indigenous plant-associated bacteria. In a previous study (Köberl, 2010), several Gram-positive bacteria with antagonistic capacity toward phytopathogens such as *Verticillium dahliae*, *Rhizoctonia solani* und *Fusarium culmorum* were isolated from the rhizosphere and endorhiza of *Matricaria recutita*, *Calendula officinalis* and *Solanum distichum* was well as from the desert soil in Sinai. Surprisingly, Gram-positive strains were more abundant in the agricultural soil than Gram-negative strains, which is against the study of Janssen (2006). Therefore it was of great interest to test the three Gram-positive strains *Streptomyces subrutilus* Wb2n-11, *Bacillus subtilis* Co1-6, and *Paenibacillus polymyxa* Mc5Re-14 against three Gram-negative strains *Pseudomonas fluorescens* L13-6-12, *Stenotrophomonas rhizophila* P69 and *Serratia plymuthica* 3Re4-18 that were already described as biological control agents (Kai et al., 2007; Wolf et al., 2002; Zachow, 2010).

Fig. 2: Study site at Adlia farm / Sekem

The investigation of the microbial communities as well as the influence on the native community structure of *Matricaria recutita* (L.) were assessed by molecular fingerprinting using Single Strand Conformation Polymorphism (SSCP)-analysis. A deeper insight into the microbial community composition was employed by the use of a pyrosequencing approach. Furthermore, an attempt to quantify the abundances of total bacteria and *Firmicutes* gene copies in the rhizosphere of *Matricaria recutita* (L.) was performed by quantitative real time PCR (q-PCR). Due to the importance of gaining knowledge of root colonization by antagonists while developing effective biocontrol strategies (Zachow et al., 2010), the colonization pattern of *Serratia plymuthica* 3Re4-18 in the rhizosphere of greenhouse-grown chamomile plants was analysed by Confocal Laser Scanning Microscopy (CLSM).

The evidence that beneficial rhizobacteria may have influence on the on the secondary metabolism of plants was tested by qualifying and quantifying apigenin7-*O*-glucoside and apigenin in the chamomile flower heads with analytical methods such as High Performance Thin Layer Chromatography (HPTLC), High Performance Liquid Chromatography (HPLC) and Liquid Chromatography-Mass Spectrometry (LC-MS).

2. Materials and Methods

2.1. Sources of supply

If not explicitly stated, all chemicals, culture media, ready-for use kits and hardware were obtained from the following companies: Applied Biosystems (Foster City, USA), Biolife (Milan, Italy), Braun (Melsungen, Germany), Duchefa (Haarlem, Netherlands), Eppendorf (Hamburg, Germany), Fermentas (St. Leon-Rot, Germany), Fluka (Buchs, Switzerland), Greiner Bio-One (Kremsmünster, Austria), Inotech Biosystems (Rockville, USA), Invitrogen (Lofer, Austria), Lactan (Graz, Austria), Leica Microsystems (Wetzlar, Germany), Merck (Darmstadt, Germany), MP Biomedicals (Eschwege, Germany), Promega (Mannheim, Germany), Qiagen (Wien, Austria), Roth (Karlsruhe, Germany), Sarstedt (Nümbrecht, Germany), Sifin (Berlin, Germany), Sigma-Aldrich (St. Louis, USA), Whatman (Maidstone, UK).

2.2. Growth media and solutions

All used media and solutions were autoclaved at 121 °C for 15 min to ensure sterility.

2.2.1. Growth media

LB medium (Roth; Karlsruhe; Germany)

10 g tryptone

5 g yeast extract

10 g NaCl

Filled up with 1 l deionised water

Nutrient broth (Sifin; Berlin; Germany)

1 g beef extract

2 g yeast extract

5 g peptone

5 g NaCl

Filled up with 1 l deionised water

2.2.2. Solutions

Vanadate-molybdate reagent

25 g ammonium molybdate

1.25 g ammonium metavandate

250 ml of conc. HNO_3

Up to 300 ml deionised water

Crush and Soak buffer: (50 ml) (Sambrook / Fritsch / Manatio, 1989)

105.75 mg magnesium acetate

1.93 g ammonium acetate

18.5 mg EDTA (pH 8.0)

250 µl 20% SDS

Up to 50 ml deionised water

0.5 M EDTA-Stock-solution (pH 8.0, 180 ml)

37.3 g EDTA

12 g 10 M NaOH

8 g 1 M NaOH

Filled up with 18 ml deionised water

Loading-buffer 6x (Sambrook / Fritsch / Manatio, 1989)

30% glycerol in deionised water

0.25% bromphenol blue

0.25% xylencyanol

50x TAE buffer

242 g Tris (99.9%)

57 ml glacial acetic acid

100 ml 0.5 M EDTA

Filled up with 1 l deionised water

5x TBE buffer

54 g Tris HCl

27.5 g boric acid

20 ml 0.5 M EDTA

Filled up with 1 l deionised water

NaCl Solution 0.9%

9 g/l NaCl

2.2.3. Chemical standards

Apigenin (Fig. 3) and Apigenin-7-*O*-glucoside (Fig. 4) were obtained as analytical standards (over 95% purity) from Sigma Aldrich (St. Louis, USA).

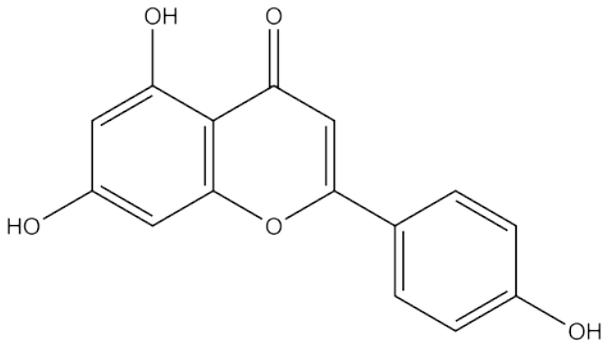

Fig. 3: Chemical structure of Apigenin

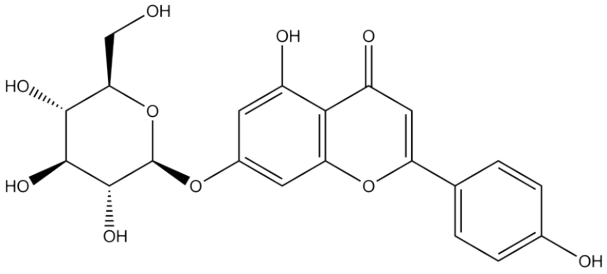

Fig. 4: Chemical structure of Apigenin-7-*O*-glucoside

2.3. Bacterial strains

From a hierarchical screening (Köberl et al., 2010), the following three Gram-positive strains were selected: (1) *Streptomyces subrutilus* Wb2n-11 isolated from desert soil in Sinai, (2) *Bacillus subtilis* subsp. *subtilis* Co1-6 obtained from the rhizosphere of *Calendula officinalis*, and (3) *Paenibacillus polymyxa* Mc5Re-14 isolated from the endorhiza of *Matricaria recutita* (L.). These Gram-positive strains were tested for their plant growth promoting effect in comparison to three Gram-negative strains, which were already described as biological control agents (BCA's; Wolf et al., 2002; Kai et al., 2007; Zachow et al., 2010): (4) *Pseudomonas fluorescens* L13-6-12 isolated from the rhizosphere of potato (Lottmann and Berg, 2001), (5) *Stenotrophomonas rhizophila* P69 isolated from the rhizosphere of *Brassica napus* (Wolf et al., 2002), and (6) *Serratia plymuthia* 3Re4-18 isolated from the endorhiza of *Solanum tuberosum* (Grosch et al., 2005).

For the preparation of inoculums, several colonies of each bacterial strain were inoculated in 500 ml liquid LB medium and grown at 30°C and 150 rpm for 24 h (Co1-6, L13-6-12, P69 and 3Re4-18) and for 48 h (Wb2n-11 and Mc5Re-14). To harvest the cells, the bacterial suspensions were centrifuged at 12,000 rpm for 20 min. Pellets were dissolved in 2 ml sucrose solution (1%), serving as cryoprotectant agent, and frozen to -70°C for 5 h. Tubes containing the frozen bacterial suspension

were put into ampules and connected to a freeze-dryer (Labconco FreeZone 4.5 Liter Benchtop, USA) for 12 h under vacuum at <0.1 Pa.

2.4. Field experiment

In October 2011, 4 week-old chamomile seedlings were planted in a field located in the north-eastern desert region of Egypt near Bilbeis (30°22'88"N; 31°39'41"E). Single treatments of the freeze-dried bacterial strains as well as a water control were applied. The plots were arranged in randomized block design (Fig. 5), with a distance of 50 cm within a row and five replicates per treatment. Each plot, comprising an area of height 1 m and width 2 m, contained 14 seedlings. Prior to planting, plant roots were dipped into the bacterial suspensions and water (control) for 15 to 20 min. During the growth stage, the field was irrigated with water (2,607 l m^{-3} on average per year) coming from the Nile or from local groundwater drillings - drip irrigation systems were used. Compost, produced on a composting facility by using rice straw, water hyacinth, wood chips, organic waste, clay, chicken and cow manure as input materials, was applied once (January).

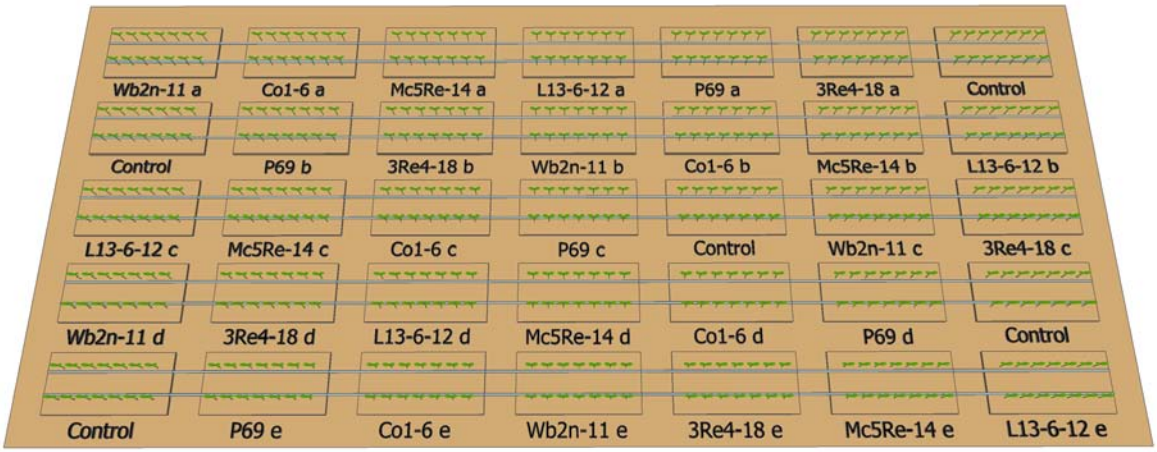

Fig. 5: Field design at Adlia farm/Sekem. Treatments: *Streptomyces subrutilus* Wb2n-11, *Bacillus subtilis* Co1-6, *Paenibacillus polymyxa* Mc5Re-14, *Pseudomonas fluorescens* L13-6-12, *Stenotrophomonas rhizophila* P69, *Serratia plymuthica* 3Re4-18 and Control (water).

2.5. Soil analysis

2.5.1. Soil sampling

Soil sampling was conducted in November 2011. Composite soil samples were collected from each plot at a surface depth of 0-5 cm and dried in a forced-air oven at

50°C for 24 h. Dried samples were sieved (<2 mm), homogenized and analysed for physico-chemical properties.

2.5.2. Soil texture

100 g of soil was weighted in a 1000 ml glass beaker and filled with distilled water. The solution was shaken several times and incubated for 24 h at room temperature to allow particles to sediment. The percentage of each constituent was determined by using the United States Department of Agriculture (USDA) soils classification scheme (Fig. 6).

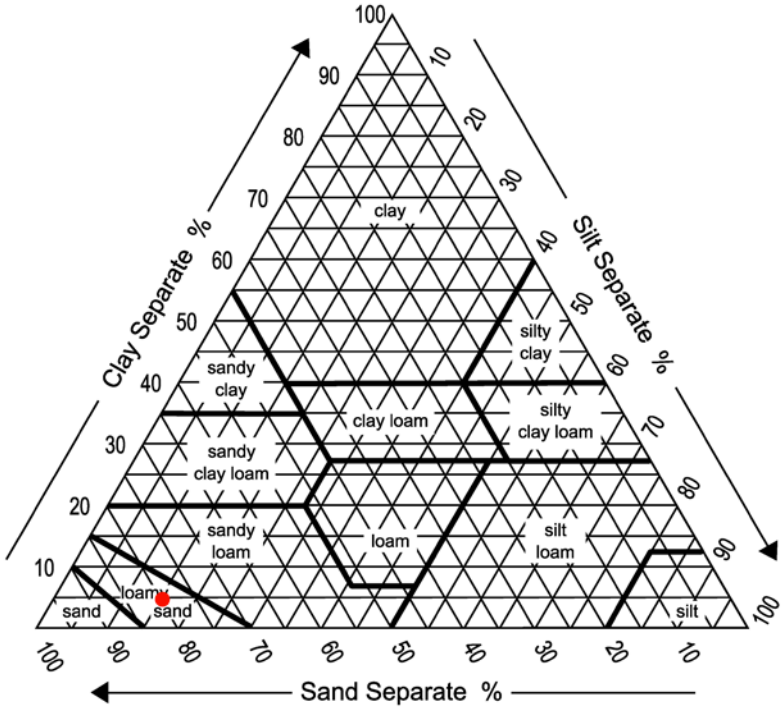

Fig. 6: Triangle for classification of soil texture. Percentage of each constituent was drawn resulting in three lines, one from each side of the triangle according to the relative percentages. The point where these three lines meet describes the description of the soil texture classes.

2.5.3. pH and electrical conductivity

Soil pH and electrical conductivity were measured in a 1:5 soil-water suspension according to Singh et al. (1999).

2.5.4. Organic matter and organic carbon

The weight of an empty porcelain dish was recorded, followed by weighing 1-2 g of soil into the porcelain dish and recording the weight of porcelain dish with the sample. The dish was placed in a muffle furnace and the temperature had gradually been increased to 650°C for 6 hours. After cooling down, the mass of the dish

containing burned soil was determined. Organic matter was calculated, using Equation 1.

Equation 1: Formula for calculating organic matter. w1 = dish without sample, w2 = dish with sample before burning, w3 = dish with sample after burning

Organic carbon was calculated using Equation 2.

Equation 2: Formula for calculating organic carbon.

2.5.5. Total nitrogen

The total nitrogen was determined according to the method of Kjeldahl. 20 ml of concentrated H_2SO_4 and 2 ml of NaOH were added to 1 g of soil into a digestion tube. The mixture was heated in a digestion block to 400°C until the mixture became transparent. After cooling to room temperature, the solution was quantitatively transferred to a 100 ml volumetric flask and 40% NaOH was added until the colour went blackish, followed by distillation. The distillate was collected into about 20 ml of 2% boric acid solution and titrated against a 0.01 N H_2SO_4 solution until pink colour started to appear. The total amount of nitrogen was calculated, using Equation 3.

Equation 3: Formula for calculating the total amount of nitrogen. N= Normality of acid, V Titration = Volume of acid used for titration, 14 = Molecular weight of nitrogen, Vol volumetric flask = Total volume in volumetric flask, W = weight of sample, Vol distillation = Volume of sample used for distillation, 1000 = conversion factor g into kg, 100 = conversion into %

2.5.6. Sample preparation for elemental analysis

2 ml of concentrated HNO_3 were added to 1 g of soil into a digestion tube and the sample was digested at 145°C for 1 h. 4 ml of $HClO_4$ were added and the sample was heated to 240°C for another 1 h. After cooling to room temperature, the solution was filtered (Whatman No. 42) and the volume was adjusted to 50 ml.

2.5.6.1. Total phosphorous

The total amount of phosphorus was measured by a colorimetric method which uses vanadate-molybdate reagent. 10 ml of acid digest was transferred into a 50 ml volumetric flask, and 10 ml of vanadate-molybdate reagent were added. The volume was adjusted to 50 ml and well shaken. After 10 min the absorbance at 420 nm was measured, using a solution of 0.2195 mg/ml KH_2PO_4 and 25 ml 7N H_2SO_4 as a standard. Total amount of phosphorous was calculated, using Equation 4.

Equation 4: Formula for calculating the total amount of phosphorous. R = reading of spectrophotometer P mg/l. 10 = volume of acid digest used for colour development. 50 = Volume make up for colour development. 100 = Volume make up after acid digestion. g = Sample weight (g) for acid digestion. 100 = conversion into %.

2.5.6.2. Total potassium

5 g of soil were weighted into a 1000 ml flask and 25 ml of 1N ammonium acetate was added. The solution was shaken and filtered (Whatman No. 42) after 5 min. The concentration of potassium in the filtrate was measured, using a flame photometer. The total amount of potassium was calculated using Equation 5.

Equation 5: C = Concentration of potassium in filtrate. mcf = Moisture correction factor. 25 = Volume of ammonium acetate. 100 = conversion into %.

2.6. Cultivation-independent approach

2.6.1. Sampling

Samples with five replicates per treatment were taken after 4 weeks and 8 weeks of the growth stage of *Matricaria recutita* (L.). A sample consisted of 5 g roots with adhering soil for rhizosphere and endorhiza analysis.

2.6.2. Total community DNA isolation

The bacterial fraction, associated with *Matricaria recutita* (L.) was extracted according to the protocol of Opelt & Berg (2004). For the extraction of microorganisms from the rhizosphere, 5 g of roots with adhering soil were mixed with 45 ml NaCl solution (0.85%) and vortexed for 5 min. A total volume of 4 ml of the

suspension was centrifuged at 13,000 rpm at 4°C for 20 min. For extraction of microorganisms from the endorhiza, 5 g of root material was surface sterilised with NaOCl solution (4%) for 5 min. Roots were washed with deionized water three times and transferred to a sterile Whirl-Pak® bag (eNasco, Fort Atkinson, USA). After adding 10 ml NaCl solution (0.85%), roots were disrupted using mortar and pestle. A total volume of 4 ml of the suspension was centrifuged at 13,000 rpm at 4°C for 20 min. The pellets obtained from extraction of the rhizosphere and the endorhiza were used for isolation of the total community DNA.

2.6.3. Total DNA extraction

The total DNA from the rhizosphere and the endorhiza was extracted using FastDNA® SPIN Kit for Soil (MP Biomedicals, Solon, USA) according to the manufacturer`s protocol. For mechanical lysis, the cells were homogenised in a FastPrep FP120 Instrument (QBiogene, BIO101, Carlsbad, USA) at speed 6.0 m sec^{-1} for 40 s (Opelt and Berg, 2004).

2.6.4. DNA isolation from bacterial cells

Pure cultures of the tested bacterial strains were used as standards for SSCP analysis. DNA from bacterial strains, *Streptomyces subrutilus* Wbn-11, *Bacillus subtilis* Co1-6, *Paenibacillus polymyxa* Mc5Re-14, *Pseudomonas fluorescens* L13-6-12, *Stenotrophomonas rhizophila* P69 and *Serratia plymuthica* 3Re4-18 was isolated according to Gomes et al., 2000. Several colonies were mixed with 500 µl lysis buffer containing 1.40% CTAB, 1 M NaCl, 7 mM Tris and 30 mM EDTA in 2-ml Ribolyzer tubes containing 0.5 g of a mixture of ceramic and silica beads. The tubes were agitated in a Ribolyzer at 6.5 m sec^{-1} for 15 s and incubated at 65°C for 60 min. For deproteinisation, 500 µl of chloroform / isoamyl alcohol (24:1 v/v) were added and centrifuged at 13,000 rpm for 5 min until phase separation took place. The water phase, containing the DNA, was transferred into a new Eppendorf tube and the chloroform / isoamyl alcohol extraction was repeated. DNA was precipitated by adding 1000 µl of precipitation buffer containing 0.50% CTAB and 40 mM NaCl and incubated at room temperature for 1 h. After centrifugation at 13,000 rpm for 5 min, the supernatant was discarded and the pellet was resuspended in 350 µl 1.2 M NaCl. Again, 500 µl of chloroform / isoamyl alcohol (24:1 v/v) were added, followed by centrifugation at 13,000 rpm for 5 min. The upper phase was transferred to a new Eppendorf tube and 210 µl of cold isopropanol were added and incubated at -21°C

over night. The tubes were centrifuged at 13,000 rpm at 4°C for 20 min. The supernatant was discarded and 200 µl of ethanol (80%) were added, followed by centrifugation at 13,000 rpm at 4°C for 5 min. The supernatant was removed and the pellet was dried und laminar flow. The DNA was dissolved in 50 µl nuclease free water.

2.6.5. Microbial fingerprinting by SSCP analysis

Single Strand Conformation Polymorphism (SSCP)-analysis of bacteria associated with *Matricaria recutita* (L.) was carried out according to Schwieger & Tebbe (1998). All used primers are listed in Table 2. Bacterial 16S rRNA gene sequences were amplified by PCR using the universal eubacterial primer pair Unibac-II-515f/ Unibac-II-927r^{P} (Lieber et al., 2002). The 60 µl reaction mixture contained 1×Taq-&Go™ Ready-to-use PCR Mix (MP Biomedicals, Solon, USA), 3 mM $MgCl_2$, 0.2 µM of each primer and 1 µl DNA template. Reaction conditions consisted of an initial denaturation at 95°C for 5 min, followed by 32 cycles of 95°C for 20 sec, 54°C for 15 sec, and 72°C for 30 sec, with a final extension of 72°C for 10 min.

To obtain genetic fingerprints of *Pseudomonas* and *Firmicutes* communities, a nested PCR was performed. In the first PCR, the *Pseudomonas* specific primer pair F311Ps/1459rPs (Milling et al., 2004) was used in a 20 µl reaction mixture containing 1×Taq-&Go™ Ready-to-use PCR Mix, 3 mM $MgCl_2$, 0.5 mg/ml BSA, 1.5% DMSO 0.2 µM of each primer and 1 µl DNA template. Reaction conditions consisted of an initial denaturation at 94°C for 7 min, followed by 30 cycles of 94°C for 45 sec, 56°C for 120 sec, and 72°C for 120 sec, with a final extension of 72°C for 10 min. For the second PCR, the universal eubacterial primer pair Unibac-II-515f/Unibac-II-927r^{P} was used in a 60 µl reaction mixture containing 1×Taq-&Go™ Ready-to-use PCR Mix, 3 mM $MgCl_2$, 0.2 µM of each primer and 2 µl of the product from the first PCR. Reaction conditions were set the same as those being described for universal eubacterial amplification before.

For the analysis of the *Firmicutes* community, the universal eubacterial primer pair 27f/1492r was used in a 20 µl reaction mixture containing 1×Taq-&Go™ Ready-to-use PCR Mix, 3 mM $MgCl_2$, 0.2 µM of each primer and 1 µl DNA template. Reaction conditions consisted of an initial denaturation at 95°C for 5 min, followed by 30 cycles of 95°C for 30 sec, 57°C for 30 sec, and 72°C for 90 sec, with a final extension of 72°C for 5 min. In the second PCR, the *Firmicutes* specific primer pair

BLS342f/BACr833r^{P} (Blackwood et al., 2005) was used in a 60 µl reaction mixture containing 1×Taq-&Go™ Ready-to-use PCR Mix, 0.2 µM of each primer and 3 µl of the product from the first PCR. Reaction conditions consisted of an initial denaturation at 95°C for 5 min, followed by 30 cycles of 95°C for 45 sec, 57°C for 60 sec, and 72°C for 45 sec, with a final extension of 72 °C for 10 min. The presence of PCR products was confirmed by electrophoresis in a 0.8% agarose gel run at 80 V in 1x TAE buffer.

The PCR products were purified by the Wizard® SV Gel and PCR Cleanup system (Promega, Mannheim, Germany), eluting the DNA in 30 µl nuclease-free water. The phosphorylated strands of the PCR products were selectively digested with lambda exonuclease by mixing 2.4 µl lambda exonuclease (Lambda Exonuclease, 5 U/ml, New England, Biolabs, Beverly, USA) and 3.6 µl 10x reaction buffer (Lambda Exonuclease Buffer 10x, New England Biolabs, Beverly, USA) with 30 µl of the eluted PCR product. The reaction mixtures were incubated at 37°C for 1 h. For denaturation and folding of the single strands, the loading buffer was prepared by mixing 950 µl formamide (95%), 4 µl 2.5 M NaOH (10 mM), 5 µl 5% bromophenol blue-solution (0.025%) and 41 µl deionized water. 30 µl of loading buffer was added to the samples, heated for 4 min at 98°C and incubated on ice for 5 min. Quintuplicates of each treatment along with pure cultures of the antagonistic strains and a Gene Ruler™ 1 kb DNA ladder (Ferments GmbH, St Leon-Rot) were loaded onto 8% (total bacteria and *Firmicutes*) or 9% (*Pseudomonas*) acrylamide gels (Table 3). Electrophoretic separation was performed 1x TBE buffer at 26°C and 400 V for about 26 h, using an INGENY phorU system (INGENY International BV, Goes Netherlands).

Table 2: Universal and specific primers used for SSCP analysis of the rhizosphere and endorhiza communities

Specificity	Primer	Primer sequence (5'-3')*	Reference
Eubacteria	Unibac-II-515f	GTG CCA GCA GCC GC	Lieber et al., 2002
	Unibac-II-927rP**	CCC GTC AAT TYM TTT GAG TT	Lieber et al. 2002
Eubacteria	27f	AGA GTT TGA TCC TGG CTC AG	Lane et al. 1991
	1492r	TAC GGY TAC CTT GTT ACG ACT T	Lane et al. 1991
Pseudomonads	F311Ps	CTG GTC TGA GAG GAT GAT CAG T	Milling et al., 2004
	1459rPs	AAT CAC TCC GTG GTA ACC GT	Milling et al., 2004
Firmicutes	BLS342F	CAG CAG TAG GGA ATC TTC	Blackwood et al., 2005
	BACr833rP**	CTA ACA CTT AGC ACT CAT	Blackwood et al., 2005

*IUPAC-code: Y = T/C; M = A/C
**5' phosphorylated primer

Table 3: Polyacrylamid gel components for SSCP analysis

Polyacrylamide gel components	8 %	9 %
Separating gel		
deionized H_2O	24.8 ml	27.9 ml
2 x MDE solution	19.6 ml	22 ml
5 x TBE	11.2 ml	12.6 ml
TEMED	26.4 µl	29.7 µl
10 % APS	264 µl	297 µl
Loading gel		
deionized H_2O	8.4 ml	9.4 ml
2 x MDE solution	7.2 ml	8.1 ml
5 x TBE	4.8 ml	5.4 ml
TEMED	40 µl	45 µl
10 % APS	96 µl	108 µl

Visualisation of the bands was performed by silver-staining according to (Bassam et al., 1991) with modifications (Opelt and Berg, 2004; Opelt et al., 2007).

2.6.6. Computer-analysis of SSCP gels

The silver-stained SSCP gels were digitalised using a transmissive scanner (Epson perfection 4990 Photo, USA) and band patterns were analysed using GelComparII® software (version 5.1, Applied Maths, Kortrijk, Belgium). In order to compare band profiles of different gels, background intensity was subtracted and the bands were normalised. For the cluster analysis, similarity matrices based on Pearson's correlation coefficients were constructed, and a dendrogram using the unweighted paired group means algorithm (UPGMA; Sokal & Sneath, 1963), was created. Relative positions and intensity of DNA bands were used for a principal component analysis (PCA).

2.6.7. Sequencing of SSCP bands

Dominant bands were excised from the SSCP gels according to Schwieger & Tebbe (1998) and incubated in 150 µl Crush and Soak buffer at 4°C for 4-5 days. After centrifugation at 13,000 rpm at 4°C for 10 min, 428.6 µl cold EtOH (70%) was added to supernatants and precipitated over night at -20°C. After centrifugation at 13,000 rpm at 4°C for 20 min, supernatants were discarded and the pellet was resuspended in 50 µl 10 mM Tris-HCl (pH 8) buffer. Extracted DNA fragments were re-amplified by PCR using the same primer pairs as described before. The PCR products were confirmed by electrophoresis in a 0.8% agarose gel with 1x TAE buffer, followed by purification with Wizard® SV Gel & PCR Clean–Up System according to the

manufacturer's protocol. The DNA concentration was quantified using a NanoDrop™ 2000c spectrophotometer (Nanodrop Technologies, Erlangen, Germany) and sequenced by LGC Genomics (Berlin, Germany). A sequence similarity search of the SSCP bands was performed using the BLAST-N program against the refseq_rna database (Altschul et al., 1997) of the National Center for Biotechnology Information (NCBI).

2.7. Pyrosequencing approach

A barcoded pyrosequencing approach was used for the characterisation of rhizosphere bacterial communities associated with *Matricaria recutita* (L.). The V4-V5 hypervariable region of the bacterial 16S rRNA gene was amplified with the set of eubacterial primers Unibac-II-515f/Unibac-II-927r (Zachow et al., 2008) containing the 454 pyrosequencing adaptors, linkers and sample specific tags (Table 4). The amplification was performed in 20 µl reactions containing 1 µl DNA template, 1× Taq-&Go™ Ready-to-use PCR Mix (MP Biomedicals, Solon, USA), 3 mM $MgCl_2$ and 0.5 µM of each primer. Reaction conditions consisted of an initial denaturation at 95 °C for 2 min, followed by 34 cycles of 95°C for 20 sec, 65°C for 15 sec, and 72°C for 29 sec, with a final extension of 72°C for 10 min. PCR products from four samples of the same treatment were purified using the Wizard® SV Gel and PCR Clean-Up System and quantified using a NanoDrop™ 2000c spectrophotometer. Subsequently, amplicons of each treatment were pooled together in an equimolar ratio and subjected to pyrosequencing using a Roche 454 GS-FLX+ Titanium™ platform executed by Eurofins MWG (Ebersberg, Germany).

Table 4: Custom primers including 454 pyrosequencing adaptors (bold), linkers (italic) and sample specific tags (underlined)

Name	Primer sequence
Unibac-II-515f_MID27	**CGTATCGCCTCCCTCGCGCCA***TCAG*ACGCGAGTAT GTGCCAGCAGCCGC
Unibac-II-515f_MID28	**CGTATCGCCTCCCTCGCGCCA***TCAG*ACTACTATGT GTGCCAGCAGCCGC
Unibac-II-515f_MID29	**CGTATCGCCTCCCTCGCGCCA***TCAG*ACTGTACAGT GTGCCAGCAGCCGC
Unibac-II-515f_MID30	**CGTATCGCCTCCCTCGCGCCA***TCAG*AGACTATACT GTGCCAGCAGCCGC
Unibac-II-515f_MID31	**CGTATCGCCTCCCTCGCGCCA***TCAG*AGCGTCGTCT GTGCCAGCAGCCGC
Unibac-II-927r_454	**CTATGCGCCTTGCCAGCCCGC***TCAG* CCCGTCAATTYMTTTGAGTT

2.7.1. Data analysis using RDP and QIIME

Raw sequencing reads were demultiplexed, quality and length filtered using Ribosomal Database Project's (RDP) Pyrosequencing Pipeline (Cole et al., 2009). Primers were cropped and all sequence reads shorter than 150 bp - with a minimum average quality score <20 and with any ambiguous characters were discarded. A total of 16,007 quality-filtered sequences were recovered. Due to different numbers of sequences between the samples, data was normalised to the same number of sequences (1,858 quality reads) using an in-house developed Perl script (10 times random re-samplings followed by subset formation). A further downstream analysis of normalised data was achieved using the QIIME (Quantitative Insights Into Microbial Ecology) toolkit (Caporaso et al., 2010), which allows for comparison and analysis of microbial community sequencing data.

2.7.2. QIIME protocol 1 - create a mapping file and assign samples to multiplex reads

Protocol 1 consists of acquiring a dataset of already normalized data, and assigning the DNA sequences. After having creating mapping files for each sample, the script `split_libraries.py` was used. As the sequences have already passed quality filtering, using RDP's pipeline, the same parameters (minimum quality score = 20, minimum/maximum length = 150/1000, error-correcting Golay of 12 nucleotide barcodes, no ambiguous base calls and no mismatches allowed in the primer sequence) were used. The output of this step is a quality-filtered set of sequences, wherein each sequence is assigned explicitly to one sample.

2.7.3. QIIME Protocol 2 - picking OTUs, assigning taxonomy, inferring phylogeny and creating an OTU table

Protocol 2 consists of picking Operational Taxonomic Units (OTUs) based on sequence similarity within the reads and picking a representative sequence from each OTU. The protocol also assigns taxonomic identities using reference database, aligns the OTU sequences, creates a phylogenetic tree and constructs an OTU table, representing the abundance of each OTU in each microbial sample. Protocol 2 requires demultiplexed sequences such as those generated in the `seqs.fna` file from Protocol 1. The `pick_otus_through_otu_table.py` workflow performs the following steps (Table 5):

Table 5: The Qiime script "pick_otus_through_otu_table"

Subscript	Description
pick_otus.py	clustering sequences of a given similarity into OTUs
pick_rep_set.py	choosing a representative sequence for each cluster
assign_taxonomy.py	aligns the representative sequences to a set of sequences
align_seqs.py	assigns a taxonomy to a sequence cluster
filter_alignment.py	filters the alignments for gaps
make_phylogeny.py	builds a phylogenetic tree based on a chosen method
make_otu_table.py	creates an OTU table

`pick_otus.py` clusters all the sequences from all the samples into Operational Taxonomic Units (OTUs). All the sequences that are clustered are of a certain similarity. OTUs in QIIME are clusters of sequences, frequently intended to represent particular levels of taxonomic classifications, such as phylum, family or genus. However, determining exactly how OTUs should be defined and what they represent, is an actively discussed issue in research. In this study bacterial sequences were clustered into OTUs using 97%, 95% and 80% similarity thresholds with UCLUST (Edgar, 2010).

`pick_rep_set.py` picks a representative sequence from each OTU for further downstream analysis. This representative sequence is used for taxonomic identification of the OTU and phylogenetic alignment. The default method was changed to search for the most abundant sequence in an OTU.

`assign_taxonomy.py` assigns representative sequences to taxonomic identities using established database. The taxonomy was assigned by using a QIIME-based wrapper of the RDP classifier program (Wang et al., 2007) against the RDP core set (Cole et al., 2007, 2009) using an 80% confidence threshold for taxonomic assignment. As the RDP database only allows for taxonomic classification until genus level, a QIIME supported greengenes file was used to classify until species level.

`align_seqs.py` aligns sequences using the default aligner PyNAST (Caporaso et al., 2010) where a set of pre-aligned sequences (Greengenes - http://greengenes.lbl.gov/cgi- bin/nph-index.cgi) is used as template.

`filter_alignment.py` filters the sequence alignment in order to remove columns composed of gaps only and locations known to be excessively variable.

`make_phylogeny.py` builds a phylogenetic tree, based on the filtered alignment file by using a FastTree algorithm as default. For visualisation of the obtained phylogenetic tree the program TopiaryExplorer (Pirrung et al., 2011) was used.

`make_otu_table.py` generates an OTU table, based on taxonomic assignments as well as the OTU map, which lists all OTUs created in the analysis together with their taxonomic identifiers.

Based on the OTU table, the script `summarize_taxa_through_plots.py` is used to create groups of different taxonomic levels (phylum, family etc.) depicted as bar charts.

2.7.4. Alpha diversity within samples and rarefaction curves

Alpha diversity is an important part of the community analysis and describes the biodiversity found within one sample or a community. The script `alpha_rarefaction.py` was used to calculate alpha diversity. This workflow performs the following steps (Table 6):

Table 6: The Qiime script "alpha_rarefaction.py "

Subscript	Description
multiple_rarefactions.py	generate rarefied OTU tables
alpha_diversity.py	compute measures of alpha diversity for each rarefied OTU table
collate_alpha.py	collate alpha diversity results
make_rarefaction plots.py	generate alpha diversity rarefaction plots

`multiple_rarefactions.py` perform subsamplings of the main OTU table creating smaller OTU tables of a user defined size by randomly choosing a given number of OTUs from the main list for each sub-table.

`alpha_diversity.py` calculates alpha diversity for each sub-table by a user defined metric. For this analysis Chao1 (Chao & Bunge, 2002), Shannon (Shannon, 1997) and observed OTU metrics at 97%, 95% and 80% similarity were calculated.

`collate-alpha.py` concatenates all files generated within the `alpha_diversity.py` script into a single combined table.

`make_rarefaction plots.py` visualise alpha rarefaction by creating rarefaction plots.

2.7.5. Beta diversity between samples and beta diversity plots

Beta diversity describes the dissimilarity within communities or between samples. The workflow `jackknifed_beta_diversity.py` consisting of the following steps (Table 7) and performing a series of analysis was used to calculated beta diversity:

Table 7: The Qiime script "jackknifed_beta_diversity.py"

Subscript	Description
multiple_rarefactions.py	build rarefied OTU tables
beta_diversity.py	compute distance matrices for rarefied OTU tables
upgma_cluster.py	build UPGMA trees from rarefied distance matrice
tree_compare.py	compare rarefied UPGMA trees and determine jackknife support for tree nodes
principal_coordinates.py	compute principal coordinates on each rarefied distance matrix
make_2d_plots.py	compare rarefied principal coordinates plots from each
make_3d_plots.py	rarefied distance matrix

`multiple_rarefactions.py` generates jackknifed OTU tables by subsampling the full available data set. To ensure that a random subset of sequences is selected from each sample, 100 sequences from each sample were selected. By default QIIME generates 10 jackknife replicates of the available data. Each replicate is a simulation of a smaller sequencing effort (100 sequences in each sample).

`beta_diversity.py` calculates the distance matrix for each jackknifed dataset resulting in two sets of 10 distance matrix files.

`upgma_cluster.py` uses each of the distance matrix files as a basis for hierarchical clustering with UPGMA (Unweighted Pair Group Method with Arithmetic Mean).

`tree_compare.py` compares jackknifed trees with a master tree constructed from `upgma_cluster.py`.

`principal_coordinates.py` compares groups of samples based on previously calculated jackknifed principal coordinates.

`make_2d_plots.py` and `make_3d_plots.py` construct a two-dimensional respectively three-dimensional plot based on the output of

`principal_coordinates.py`. A two-dimensional plot and a three-dimensional bi-plot were created in order to reveal the most abundant taxa in different areas of the PCoA plot. For the three-dimensional bi-plot taxonomic classification of 80% genetic distance was included.

2.7.6. Network analysis

To investigate the co-occurrence of OTUs in the rhizosphere samples, a network analysis was performed using Cytoscape version 2.2 (Shannon et al., 2003). This network analysis allows for visualisation of the OTUs that are either unique or shared by specific groups of samples. Connections were drawn between rhizosphere samples and OTUs using edge weights to calculate edge length or clustering nodes with common annotations together (Garcia et al., 2007). For clustering the OTUs and the treatments in the network, the edge-weighted spring embedded layout was used. This algorithm models edges as springs and nodes as like-charged particles, so nodes repel each other and edges spring, but connect nodes at a preferred length (Yeung et al., 2008). For visualisation purpose the number of OTUs was reduced by filtering out edge weights <2 and notes were coloured by taxonomic classification.

2.8. qPCR analyses

The abundances of total bacteria and *Firmicutes* gene copies in the rhizosphere of *Matricaria recutita* (L.) were quantified by a quantitative polymerase chain reaction (qPCR). For the total bacteria, the universal eubacterial primer pair used was Unibac-II-515f/Unibac-II-927r (Lieber et al., 2002), while the *Firmicutes* specific primer pair, BLS342f/BACr833rP (Blackwood et al., 2005), was used for *Firmicutes*. To estimate bacterial gene abundances, standard curves were generated using 10-fold serial dilutions of plasmid DNA containing a full-length copy of either the *P. polymyxa* PB71 16S rRNA gene or the *Bacillus subtilis* subsp. *subtilis* 16S rRNA gene (Köberl et al., 2011).

For the total bacteria, the qPCR 10 µl reaction mixture contained 1x KAPA^{TM} SYBR® FAST qPCR MasterMix Universal (PEQLAB, Polling, Austria), 0.25 µM of each primer and 1 µl of the standard and DNA template. PCR conditions were 95°C for 5 min, followed by 35 cycles of 95°C for 20 sec, 54°C for 15 sec, and 72°C for 30 sec, with a final extension of 72°C for 10 min.

For *Firmicutes*, the 10 µl qPCR reaction mixture contained 1x KAPA^{TM} SYBR$^{®}$ FAST qPCR MasterMix Universal (PEQLAB, Polling, Austria), 0.25 µM of each primer and 1 µl standard and DNA template. PCR conditions were 95°C for 5 min, followed by 30 cycles of 95°C for 45 sec, 56°C for 60 sec, and 72°C for 45 sec, with a final extension of 72°C for 10 min.

qPCR was performed in duplicate for each sample using the Rotor-Gene 6000 Rotor-GeneTM 6000 real-time rotary analyser (Corbett Research, Sydney, Australia). The melting curve analysis of the PCR products was performed immediately after the amplification. Bacterial copy numbers for each reaction were generated from the standard curves and calculated to copy number per g rhizosphere.

2.9. Confocal Laser Scanning Microscopy

2.9.1. Inoculation of chamomile seeds with DsRed2-labeled antagonists and bioassay

DsRed2-labeled bacteria (3Re4-18) were grown in 5 ml nutrient broth supplemented with tetracycline (40 µg ml^{-1}) at 30°C and 120 rpm for 24 h. Bacterial cells were collected by centrifugation at 13,000 rpm for 5 min and resuspended in fresh NB medium without addition of antibiotics. The cell suspension was adjusted to an optical density corresponding to a cell count of 10^9 cells ml^{-1}. Seeds were mixed with 1 ml of the cell suspension in 1.5 ml Eppendorf tubes and incubated at room temperature for 15 min followed by a washing step with sterile NaCl solution (0.85%). Seeds were placed on a filter paper in moist chambers which were kept at 22°C for 5 days. Seeds, incubated with sterile water served as control. Roots of chamomile were examined on a Leica TCS SPE confocal scanning microscope (Leica Microsystems GmbH, Wetzler, Germany).

2.10. Chemical analysis of *Matricaria recutita* (L.) secondary metabolites

2.10.1. Plant material

Fresh chamomile flowers were harvested in March 2012 at Adlia farm/Sekem and dried in a forced-convection oven at 40 °C. Dried chamomile flowers were shipped to Graz, Austria and stored at room temperature until the analysis took place. Prior to

extraction, dried flowers were milled to a fine powder using a universal IKA M 20 grinding mill (IKA®-Werke, Staufen, Germany).

2.10.2. Extraction

The extraction of chamomile flower heads was performed by using an accelerated solvent extractor, ASE 200 (Dionex Corporation, Sunnyvale, CA, USA). A cellulose filter was placed at the bottom of a 22 ml stainless steel extraction cell. 1 g of chamomile powder was mixed with diatomaceous earth in a proportion (4:1) and placed into the cell. The cell was filled up with sea sand to 90% and then closed tightly. The extraction was carried out at a temperature of 68°C, with a constant pressure of 69 bar and a static time of 5 min using 100 % methanol (v/v) as extraction solvent. Based on preliminary experiments, conditions of ASE 200 were set as follows: no preheating period; heating time of 5 min; flush volume at 30% of the extraction cell volume; three extraction cycles; nitrogen purge time of 60 s. The extracts were filtered (Whatman No. 42) into glass vials, adjusted to 50 ml volume with methanol and stored at 4 °C in darkness until the chromatographic analysis was made.

2.10.3. HPTLC analysis

A high performance liquid chromatography analysis of the extracts was performed on silica gel 60 F254 HPTLC plates (10 × 10 cm; Merck, Darmstadt, Germany). Standard and sample solutions were applied bandwise (bandlength 8 mm, track distance 6 mm, distance from left edge 15 mm and low edge 15 mm) using a CAMAG automatic TLC-sampler 4 (CAMAG, Muttenz, Switzerland) fitted with WinCATS 1.2.3 software. Plates were developed in a twin-trough glass chamber (24.5 cm × 8 cm × 22.5 cm) using concentrated acetid acid:water:butanol (17:17:66 v/v/v) as mobile phase. The development length was 80 mm. After the development had been finished, the plates were dried at 105°C for 5 min. Derivatisation was carried out by spraying the plates with a solution of diphenylboric acid-2-aminoethylester (100 mg) and PEG 400 (500 mg) in methanol (10 ml, Brasseur and Angenot, 1986), followed by drying at room temperature for 30 min. A ReproStar 3 with VideoStore 2 documentation software (Camag, Muttenz, Switzerland) was used for the imaging and archiving thin-layer chromatograms. All images were obtained by exposing the plate to direct UV light (λ=366 nm).

2.10.4. HPLC-DAD analysis

The high performance liquid chromatography (HPLC) was performed on an Agilent 1100 chromatographis system equipped with a diode array detector (DAD) (Agilent Technologies, Waldbronn, Germany). A LiChrospher® 100 RP-18 (125x4 mm, 5 µm) (Merck, Darmstadt, Germany) was employed for the separation. The binary mobile phase consisted of solvents A (water) and B (acetonitrile) according to the following profile: 0-17 min, 15-40% B; 17-18 min, 40-75% B; 18-29 min, 75% B. After having returned to initial conditions within 30 min, the system was equilibrated for 10 min. The flow rate was 1.0 ml/min and the injection volume was 5µl.

2.10.5. LC-MS analysis

A liquid chromatography analysis was performed on an UltiMate 3000 RS chromatographic system (Dionex, Sunnyvale, CA, USA). A LiChrospher® 100 RP-18 (125x4 mm, 5 µm) (Merck, Darmstadt, Germany) was employed for the separation. The HPLC conditions were set as described before.

For the mass analysis, a linear trap quadrupole (LTQ) XL mass spectrometer (Thermo Scientific, San Jose, CA) with an electrospray interface (ESI) was used. ESI negative ion mode conditions were set as follows: source voltage 3.0 kV, sheath gas flow rate 50 au, auxiliary gas flow rate 10 au, source current 100.0 µA, capillary voltage -45.0 kV and capillary temperature 330°C. The screening was performed in full scan, covering the range from m/z 50 up to 2000.

Apigenin and apigenin-7-*O*-glucoside were quantified based on peak areas calculated from their respective ion chromatograms using Xcalibur Quan Browser (Version 2.0, Thermo Fisher, San Jose, USA). Spectra of each treatment were overlaid with the control using MZmine (Version 2.8, Katajamaa et al., 2006) in order to identify new peaks arising from the treatments.

2.11. Statistical analysis

For the statistical analysis of the data the statistical package PASW Satistics 18 (SPSS Inc., Chicago, USA) was used. First, data were checked for Normal distribution and Homogeneity of variance. Second, an ANOVA analysis was performed with data that follows a Normal distribution. A Post Hoc test was applied depending on the Homogeneity of the variance index. Homogenous data with a variance $P>0.05$ was subjected to a Tukey honestly significant difference (HSD)

analysis of variance, while not homogenous data with a variance $P<0.05$ was subjected to a Games-Howell analysis.

3. Results

3.1. Soil analysis

The soil texture at Adlia farm / Sekem was classified as sandy-silt with an average pH of 8.48 ± 0.13, an electrical conductivity of 254.75 µS/m ± 42.75, an organic matter content of 1.44% ± 0.17, an organic carbon content of 0.82% ± 0.09, a total nitrogen content of 0.15% ± 0.02, a total phosphorous content of 0.01% ± 0.01 and a total potassium content of 0.07% ± 0.01 (Table 8).

Table 8: General physical and chemical properties of the soil at the study site at Adlia farm / Sekem.

pH	E.C. (µS/m)	O.M. (%)	O.C. (%)	T.N. (%)	T.P. (%)	T.K. (%)
8.48 ± 0.13	254.75 ± 42.75	1.44 ± 0.17	0.82 ± 0.09	0.15 ± 0.02	0.01 ± 0.01	0.07 ± 0.01

E.C. = Electrical conductivity, O.C. = Organic carbon, O.M. = Organic Matter, T.N. = Total Nitrogen, T.P. = Total Phosphorous, T.K. = Total Potassium

3.2. Analysis of chamomile-associated microbial communities

3.2.1. Computer-assisted comparison of SSCP profiles

For the analysis of microbial communities associated with *Matricaria recutita* (L.), microbial fingerprints from the rhizosphere and the endorhiza were accomplished by an SSCP analysis using universal eubacterial as well as *Pseudomonas* and *Firmicutes*-specific primers. Computer-assisted comparison (UPGMA) of the microbial profiles resulted in grouping of rhizosphere samples at different sampling times at 10% similarity (Fig. 7, Fig. 9 and Fig. 11). The differences between the two sampling times were also confirmed by a principal component analysis (Fig. 8, Fig. 10 and Fig. 12). Within the calculated dendrogram, the fingerprints of total bacteria from the rhizosphere showed similarities of 20% to 25% (Fig. 7), while *Pseudomonas* community patterns from the rhizosphere resulted in similarities of 38% to 60% (Fig. 9). An even higher degree of 51% to 60% similarity could be detected for *Firmicutes* samples from the rhizosphere (Fig. 11). Endorhiza communities showed similarities of 3% to 40% between different sampling times (Fig. 13 and Fig. 15). Within the cluster of *Pseudomonas*, samples from both sampling times joined a group. This overlap of microbial communities was also confirmed by a principal component

analysis (Fig. 14). *Firmicutes* communities showed similarities of 25% to 67% within the cluster trees.

In the fingerprints of the second sampling, derived from the rhizosphere communities, all five replicates of the treatment with *Bacillus subtilis* Co1-6 formed a separated cluster. Furthermore, *Pseudomonas* communities in the endorhiza of plants treated with *Streptomyces subrutilus* Wb2n-11 clustered together at the first and second sampling time.

In most cases samples from different treatments were found to be more similar to each other than the samples of the five replicates of each specific treatment, suggesting no significant differences arising from the bacterial inoculants. Moreover, no cluster group was found containing exclusively SSCP patterns of one specific treatment.

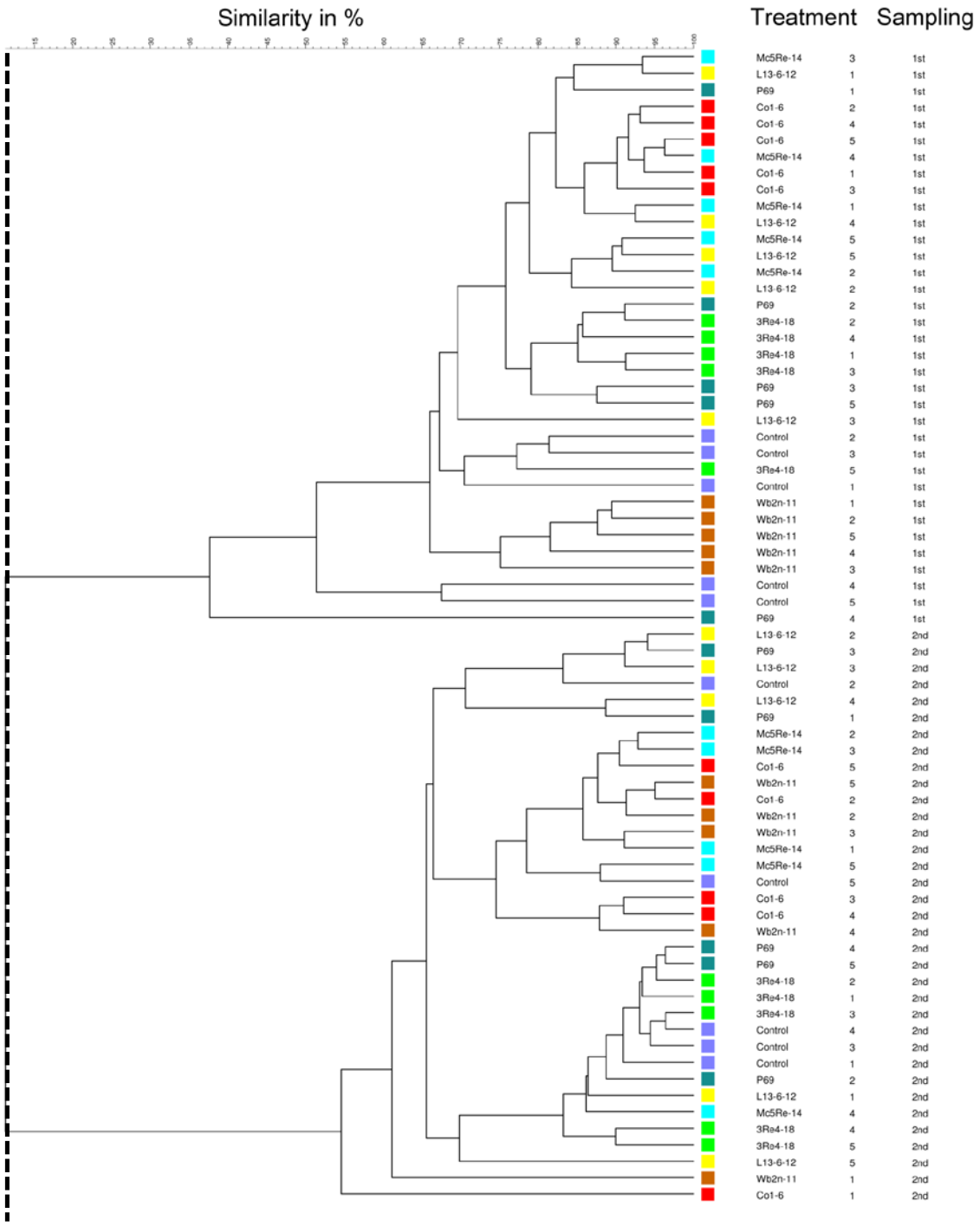

Fig. 7: Cluster analysis of eubacterial community fingerprints of rhizosphere samples after the various treatments (*Streptomyces subrutilus* Wb2n-11, *Bacillus subtilis* Co1-6, *Paenibacillus polymyxa* Mc5Re-14, *Pseudomonas fluorescens* L13-6-12, *Stenotrophomonas rhizophila* P69, *Serratia plymuthica* 3Re4-18 and water control) at the sampling time (i) after 4 weeks and (ii) after 8 weeks. Similarities between SSCP fingerprints were calculated using the curve-based Pearson correlation coefficient and grouped according to their similarity using the hierarchical UPGMA.

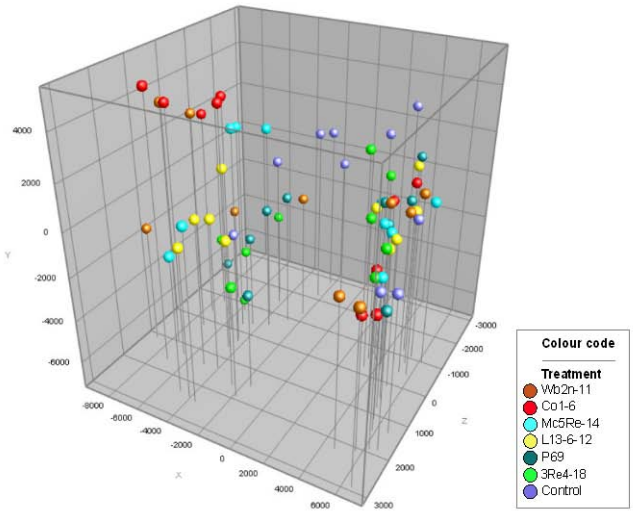

Fig. 8: Principal Component Analysis (PCA) of eubacterial community fingerprints of rhizosphere samples after the various treatments (*Streptomyces subrutilus* Wb2n-11, *Bacillus subtilis* Co1-6, *Paenibacillus polymyxa* Mc5Re-14, *Pseudomonas fluorescens* L13-6-12, *Stenotrophomonas rhizophila* P69, *Serratia plymuthica* 3Re4-18 and water control) at the sampling time (i) after 4 weeks (left) and (ii) after 8 weeks (right). PCA was calculated based on relative positions and intensity of DNA bands.

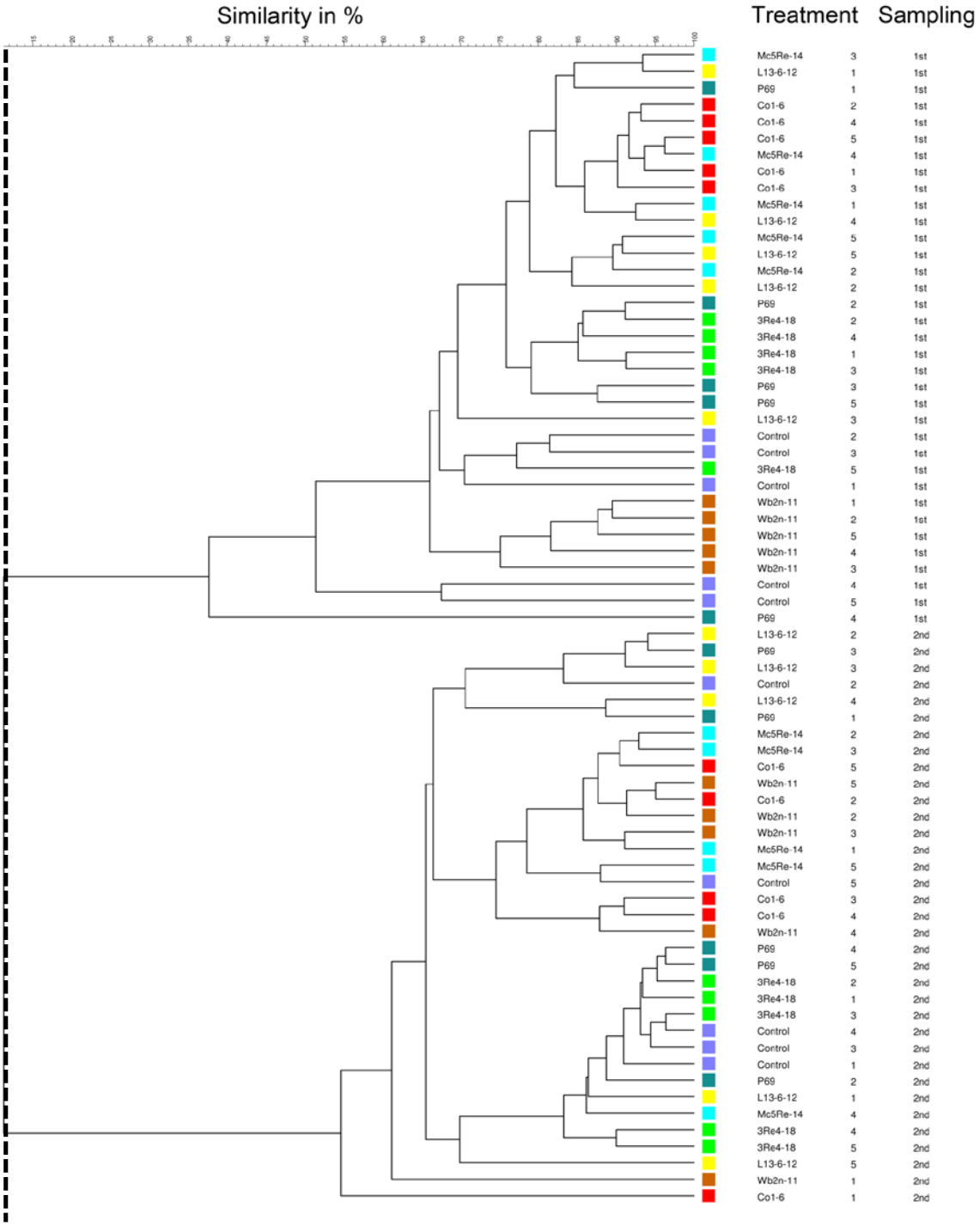

Fig. 9: Cluster analysis of *Pseudomonas* community fingerprints of rhizosphere samples after the various treatments (*Streptomyces subrutilus* Wb2n-11, *Bacillus subtilis* Co1-6, *Paenibacillus polymyxa* Mc5Re-14, *Pseudomonas fluorescens* L13-6-12, *Stenotrophomonas rhizophila* P69, *Serratia plymuthica* 3Re4-18 and water control) at the sampling time (i) after 4 weeks and (ii) after 8 weeks. Similarities between SSCP fingerprints were calculated using the curve-based Pearson correlation coefficient and grouped according to their similarity using the hierarchical UPGMA.

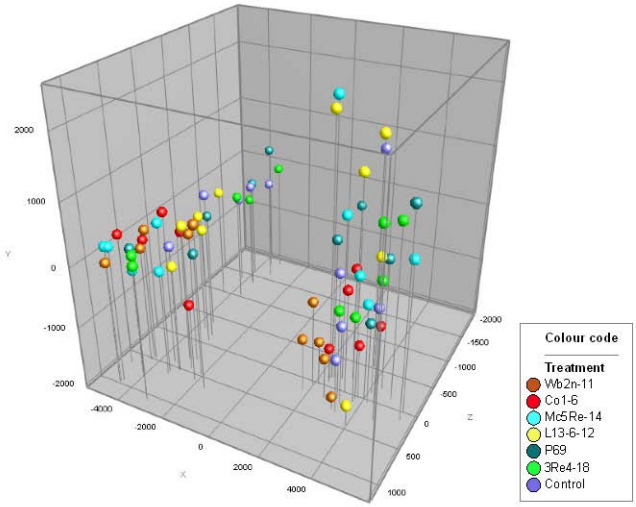

Fig. 10: Principal Component Analysis (PCA) of *Pseudomonas* community fingerprints of rhizosphere samples after the various treatments (*Streptomyces subrutilus* Wb2n-11, *Bacillus subtilis* Co1-6, *Paenibacillus polymyxa* Mc5Re-14, *Pseudomonas fluorescens* L13-6-12, *Stenotrophomonas rhizophila* P69, *Serratia plymuthica* 3Re4-18 and water control) at the sampling time (i) after 4 weeks (left) and (ii) after 8 weeks (right). PCA was calculated based on relative positions and intensity of DNA bands.

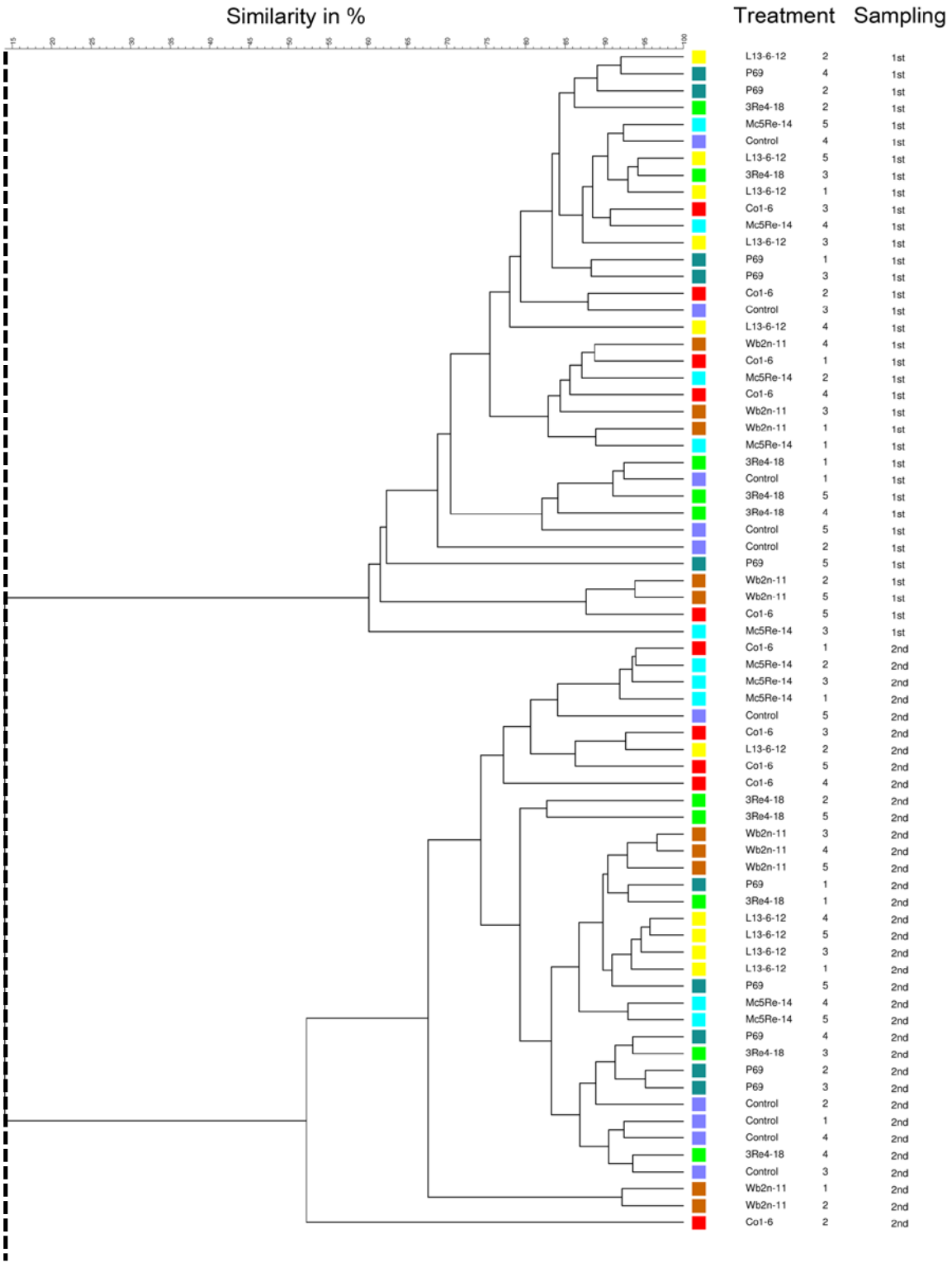

Fig. 11: Cluster analysis of the *Firmicutes* community fingerprints of rhizosphere samples after the various treatments (*Streptomyces subrutilus* Wb2n-11, *Bacillus subtilis* Co1-6, *Paenibacillus polymyxa* Mc5Re-14, *Pseudomonas fluorescens* L13-6-12, *Stenotrophomonas rhizophila* P69, *Serratia plymuthica* 3Re4-18 and water control) at the sampling time (i) after 4 weeks and (ii) after 8 weeks. Similarities between SSCP fingerprints were calculated using the curve-based Pearson correlation coefficient and grouped according to their similarity using the hierarchical UPGMA.

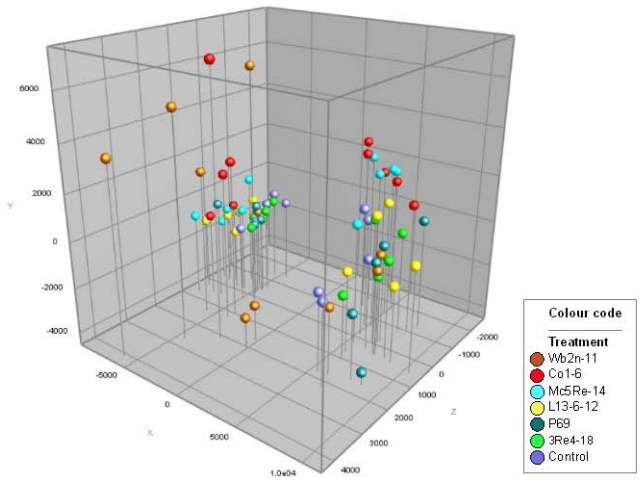

Fig. 12: Principal Component Analysis (PCA) of *Firmicutes* community fingerprints of rhizosphere samples after the various treatments (*Streptomyces subrutilus* Wb2n-11, *Bacillus subtilis* Co1-6, *Paenibacillus polymyxa* Mc5Re-14, *Pseudomonas fluorescens* L13-6-12, *Stenotrophomonas rhizophila* P69, *Serratia plymuthica* 3Re4-18 and water control) at the sampling time (i) after 4 weeks (left) and (ii) after 8 weeks (right). PCA was calculated based on relative positions and intensity of DNA bands.

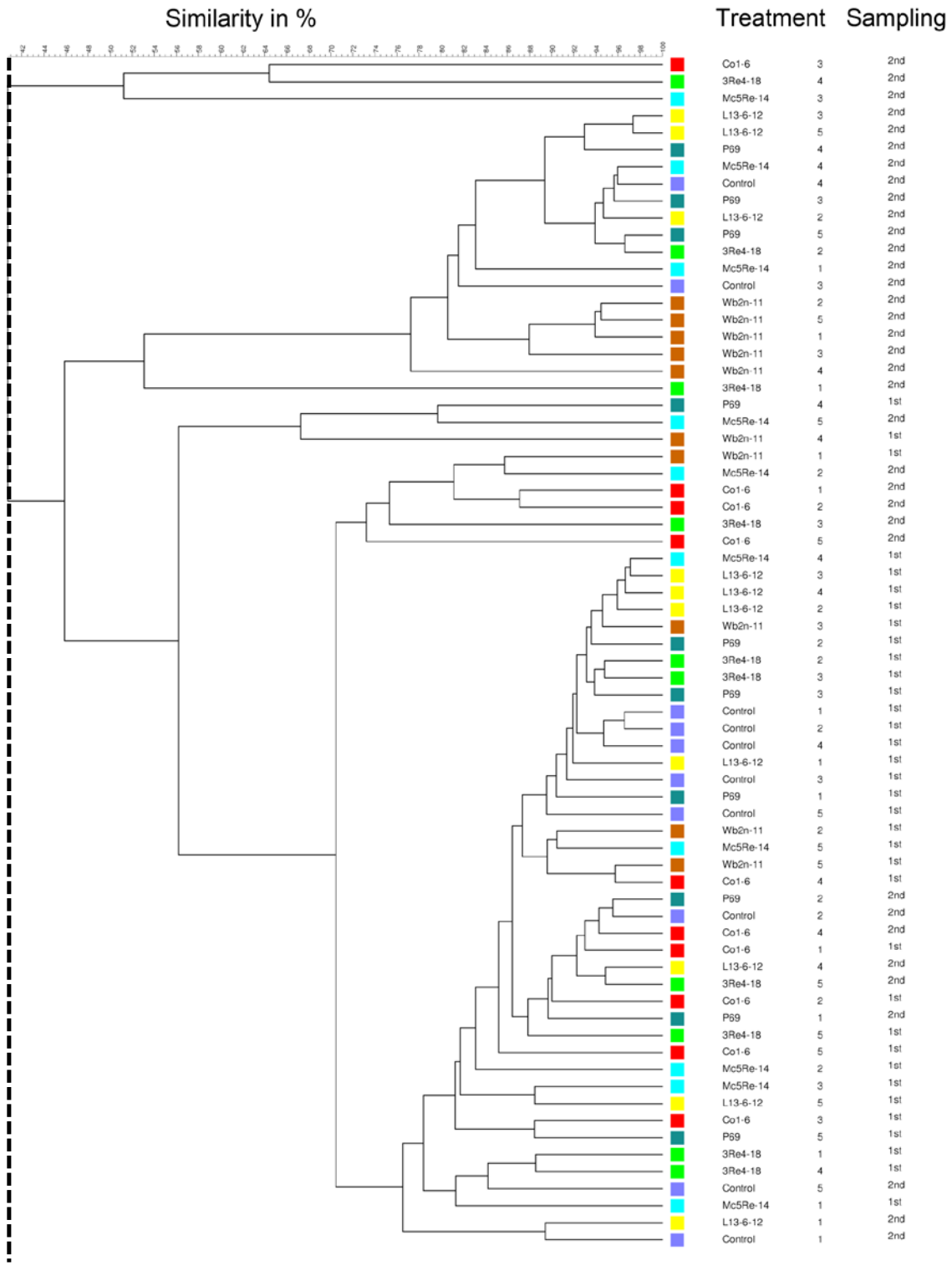

Fig. 13: Cluster analysis of the *Pseudomonas* community fingerprints of endorhiza samples after the various treatments (*Streptomyces subrutilus* Wb2n-11, *Bacillus subtilis* Co1-6, *Paenibacillus polymyxa* Mc5Re-14, *Pseudomonas fluorescens* L13-6-12, *Stenotrophomonas rhizophila* P69, *Serratia plymuthica* 3Re4-18 and water control) at the sampling time (i) after 4 weeks and (ii) after 8 weeks. Similarities between SSCP fingerprints were calculated using the curve-based Pearson correlation coefficient and grouped according to their similarity using the hierarchical UPGMA.

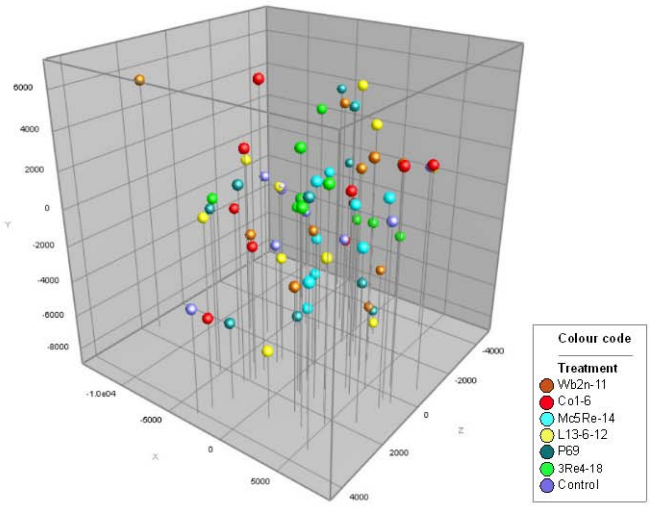

Fig. 14: Principal Component Analysis (PCA) of *Pseudomonas* community fingerprints of endorhiza samples after the various treatments (*Streptomyces subrutilus* Wb2n-11, *Bacillus subtilis* Co1-6, *Paenibacillus polymyxa* Mc5Re-14, *Pseudomonas fluorescens* L13-6-12, *Stenotrophomonas rhizophila* P69, *Serratia plymuthica* 3Re4-18 and water control) at the sampling time (i) after 4 weeks and (ii) after 8 weeks. PCA was calculated based on relative positions and intensity of DNA bands.

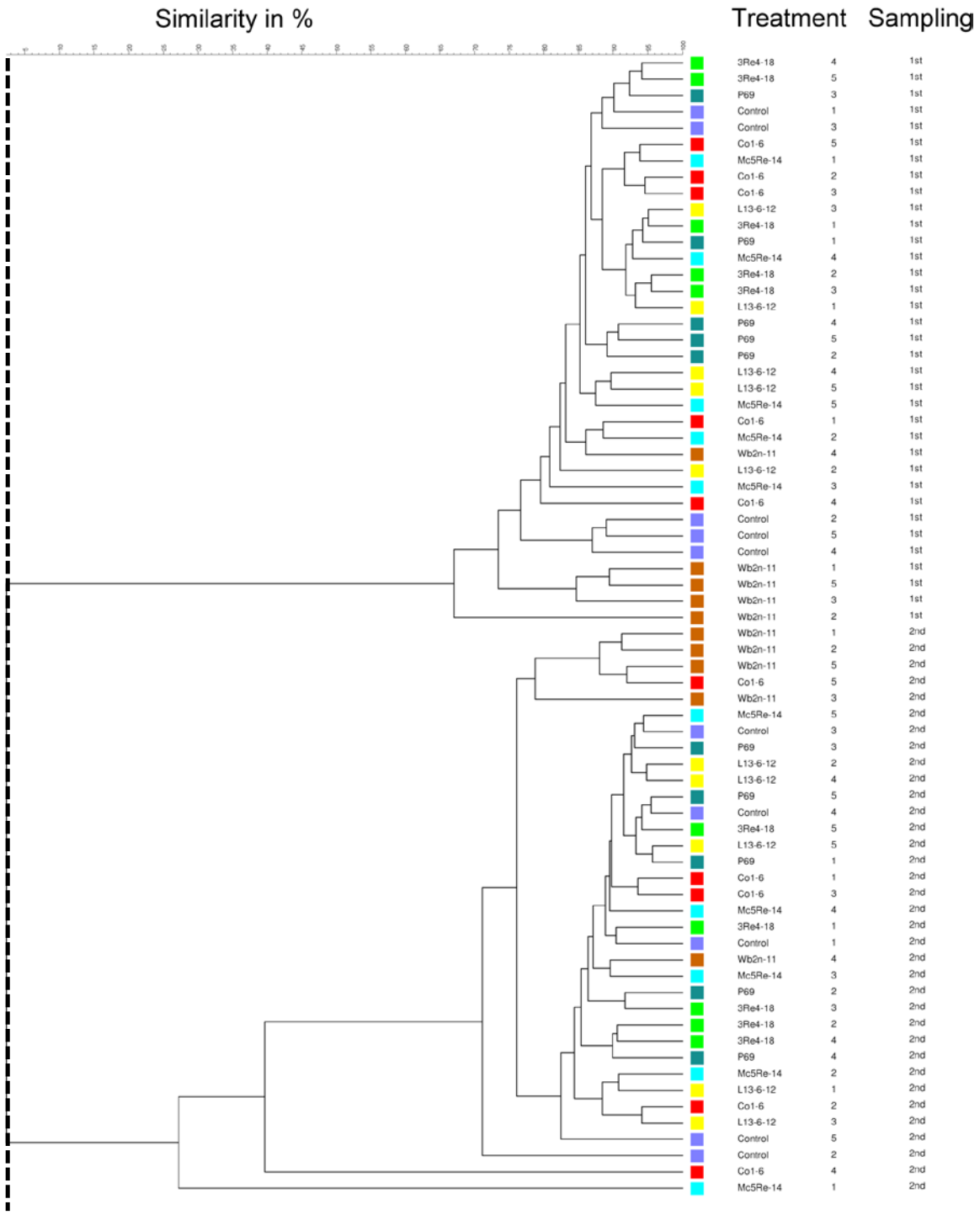

Fig. 15: Cluster analysis of the *Firmicutes* community fingerprints of endorhiza samples after the various treatments (*Streptomyces subrutilus* Wb2n-11, *Bacillus subtilis* Co1-6, *Paenibacillus polymyxa* Mc5Re-14, *Pseudomonas fluorescens* L13-6-12, *Stenotrophomonas rhizophila* P69, *Serratia plymuthica* 3Re4-18 and water control) at the sampling time (i) after 4 weeks and (ii) after 8 weeks. Similarities between SSCP fingerprints were calculated using the curve-based Pearson correlation coefficient and grouped according to their similarity using the hierarchical UPGMA.

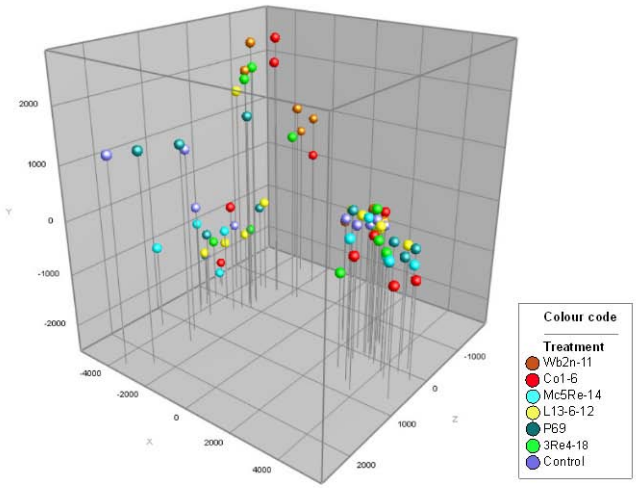

Fig. 16: Principal Component Analysis (PCA) of *Firmicutes* community fingerprints of endorhiza samples after the various treatments (*Streptomyces subrutilus* Wb2n-11, *Bacillus subtilis* Co1-6, *Paenibacillus polymyxa* Mc5Re-14, *Pseudomonas fluorescens* L13-6-12, *Stenotrophomonas rhizophila* P69, *Serratia plymuthica* 3Re4-18 and water control) at the sampling time (i) after 4 weeks (left) and (ii) after 8 weeks (right). PCA was calculated based on relative positions and intensity of DNA bands.

3.2.2. Molecular fingerprints of microbial communities

Using universal eubacterial primers, SSCP patterns showed a highly diverse composition of microbial communities in the rhizosphere of *Matricaria recutita* (L.) (Fig. 17 and Fig. 18), while using group-specific primers, *Pseudomonas* and *Firmicutes* community patterns showed a less diverse microbial community composition (Fig. 19, Fig. 20, Fig. 21 and Fig. 22). Between 20-30 bands were found for the total bacterial community patterns and about ten bands for *Pseudomonas* and *Firmicutes* community patterns. Generally, SSCP patterns showed a high similarity between the treatments and the control. Only few bands appeared occasionally, however those bands could not be related to any treatment. Using universal eubacterial primers, SSCP patterns showed a high content of chloroplast DNA in the endorhiza of *Matricaria recutita* (L.) (data not shown). Therefore, group-specific primers were used to avoid the amplification of chloroplast DNA. *Pseudomonas* and *Firmicutes* community patterns of the endorhiza showed a very low complexity,

where only 2-7 bands could be found (Fig. 23, Fig. 24, Fig. 25 and Fig. 26). Also, SSCP patterns of the endorhiza did not show any relation to the treatments.

Sequencing of the excised bands from the SSCP gel of total bacterial communities showed that nearly all samples contained *Bacillus sp.* (Table 9). Moreover, *Bacillus endophyticus* (closest database match *Bacillus endophyticus* strain p18_C12, 93% similarity to JQ833589.1), *Pantoea dispersa* (closest database match *Pantoea dispersa* strain p91_H01, 90-93% similarity to JQ829612.1) and *Serratia marcescens* (closest database match *Serratia marcescens* strain MUD-MaC2, 90% similarity to JX534512.1) were detected.

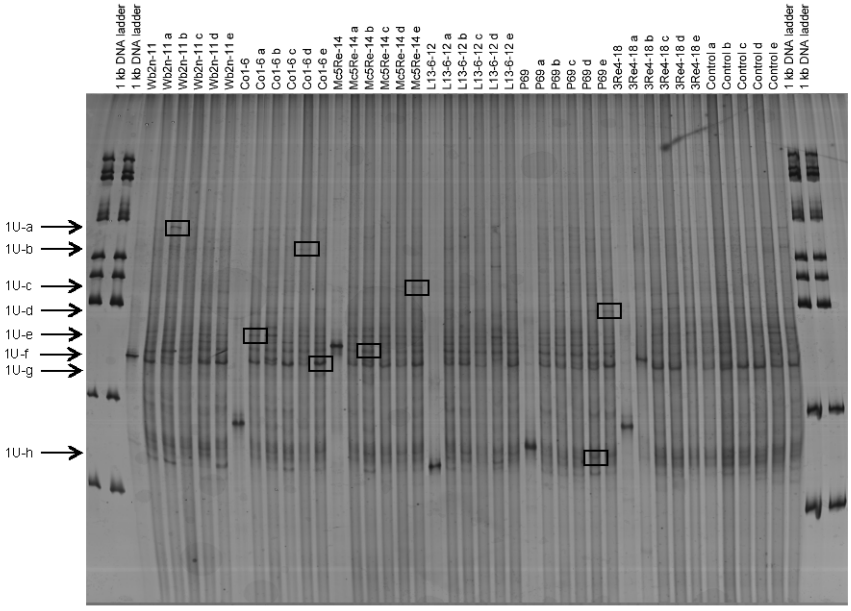

Fig. 17: SSCP pattern of the rhizosphere communities after the various treatments (*Streptomyces subrutilus* Wb2n-11, *Bacillus subtilis* Co1-6, *Paenibacillus polymyxa* Mc5Re-14, *Pseudomonas fluorescens* L13-6-12, *Stenotrophomonas rhizophila* P69, *Serratia plymuthica* 3Re4-18 and water control) using universal eubacterial primers at the sampling time (i) after 4 weeks. Lanes marked Wb2n-11, Co1-6, Mc5Re-14, L13-6-12, P69 and 3Re4-18 contain PCR-products from pure bacterial cultures; Black framed bands were excised for identification by sequencing.

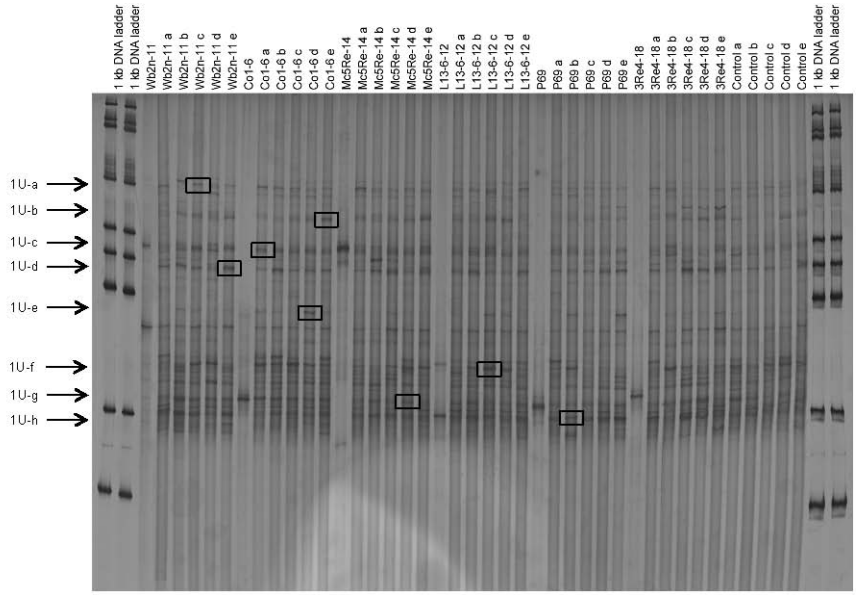

Fig. 18: SSCP pattern of the rhizosphere communities after the various treatments (*Streptomyces subrutilus* Wb2n-11, *Bacillus subtilis* Co1-6, *Paenibacillus polymyxa* Mc5Re-14, *Pseudomonas fluorescens* L13-6-12, *Stenotrophomonas rhizophila* P69, *Serratia plymuthica* 3Re4-18 and water control) using universal eubacterial primers at the sampling time (ii) after 8 weeks. Lanes marked Wb2n-11, Co1-6, Mc5Re-14, L13-6-12, P69 and 3Re4-18 contain PCR-products from pure bacterial cultures; Black framed bands were excised for identification by sequencing.

Table 9: Sequencing results of 16S rRNA gene fragments derived from selected SSCP bands using universal eubacterial primers

Band	Closest NCBI database match	Accession No.	Similarity (%)
1U-a	*Bacillus endophyticus* strain p18_C12	JQ833589.1	93
1U-b	*Serratia marcescens* strain MUD-MaC2	JX534512.1	90
1U-c	*Pseudomonas psychrotolerans* strain: C36	NR_042191.1	97
1U-d	No match	-	-
1U-e	*Bacillus flexus* strain p2_D03	JQ829837.1	90
1U-f	*Klebsiella pneumoniae* strain p95_F10	JQ830639.1	90
1U-g	*Pantoea dispersa* strain p91_H01	JQ829612.1	93
1U-h	*Pantoea dispersa* strain p91_H01	JQ829612.1	90
2U-a	*Flavobacterium flevense* strain: NBRC 14960	AB680723.1	99
2U-b	*Bacillus selenatarsenatis* strain A1-37c-12	JX517224.1	99
2U-c	*Bacillus sp.* SG22	JX402437.1	99
2U-d	*Bacillus cereus* strain p44_E01	JQ832456.1	99
2U-e	*Anoxybacillus sp.* D1021	EU926955.1	99
2U-f	*Bacillus sp.* SG22	JX402437.1	100
2U-g	*Bacillus sp.* S3-R6TC-BA1	GU325806.1	95
2U-h	*Bacillus sp.* S3-R6TC-BA1	GU325806.1	96

For the first sampling time of the *Pseudomonas* community, the two dominant bands 1P-b, 1P-c were identified as *Pseudomonas sp.* (closest database match *Pseudomonas sp.* MOC14, 100% similarity to JX122114.1). Furthermore, *Pseudomonas sp.* (closest database match *Pseudomonas mandelii strain* BJC15-C35, 100% similarity to JX469391.1), *Dokdonella sp.* (closest database match *Dokdonella sp.* CC-YHH031, 97% similarity to GQ281768.1), *Pseudomonas sp.* OF38, 99% similarity to HM626451.1), *Xanthomonadales sp.* (closest database match *Xanthomonadaceae* bacterium K-1-9 16S, 97% similarity to JQ963326.1) and *Lysobacter sp.* (closest database match *Lysobacter sp.* 7C-9, 97% similarity to JQ349048.1) were identified. *Pseudomonas sp.* MOC14 was present in several samples (Table 10). For the second sampling time, the three intensive bands 2P-b, 2P-e and 2P-f were identified as *Pseudomonas sp.* (closest database match *Pseudomonas sp.* MOC14, 100% similarity to JX122114.1), *Lysobacter sp.* (closest database match *Lysobacter sp.* ljh-29, 99% similarity to GU217698.1) and *Pseudomonas sp.* (*Pseudomonas mandelii* strain BJC15-C3, 99% similarity to JX469391.1), respectively. Also in the second sampling time, *Pseudomonas sp.* MOC14 was frequently present. Sequencing of the band 2P-e revealed a similarity of 99% to *Pseudomonas fluorescens* strain BIM B-187 (GU784932.1), however the applied strain *Pseudomonas fluorescens* L13-6-12 could not be detected.

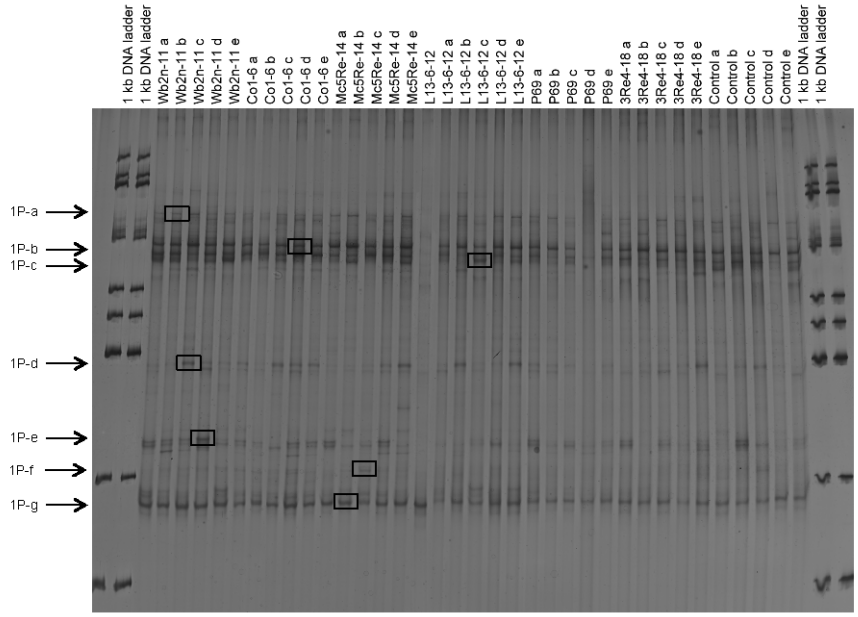

Fig. 19: SSCP pattern of the rhizosphere communities after the various treatments (*Streptomyces subrutilus* Wb2n-11, *Bacillus subtilis* Co1-6, *Paenibacillus polymyxa* Mc5Re-14, *Pseudomonas fluorescens* L13-6-12, *Stenotrophomonas rhizophila* P69, *Serratia plymuthica* 3Re4-18 and water control) using *Pseudomonas*-specific primers at the sampling time (i) after 4 weeks. Lane marked L13-6-12 contains PCR-product from pure bacterial culture; Black framed bands were excised for identification by sequencing.

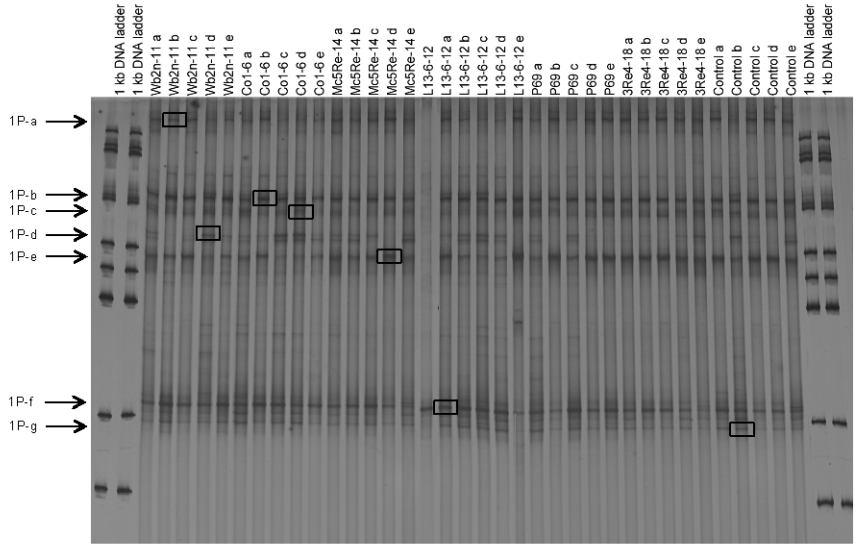

Fig. 20: SSCP pattern of the rhizosphere communities after the various treatments (*Streptomyces subrutilus* Wb2n-11, *Bacillus subtilis* Co1-6, *Paenibacillus polymyxa* Mc5Re-14, *Pseudomonas fluorescens* L13-6-12, *Stenotrophomonas rhizophila* P69, *Serratia plymuthica* 3Re4-18 and water control) using *Pseudomonas*-specific primers at the sampling time (ii) after 8 weeks. Lane marked L13-6-12 contains PCR-product from pure bacterial culture; Black framed bands were excised for identification by sequencing.

Table 10: Sequencing results of 16S rRNA gene fragments derived from selected SSCP bands using *Pseudomonas*-specific primers

Band	Closest NCBI database match	Accession No.	Similarity (%)
1P-a	*Pseudomonas sp.* MOC14	JX122114.1	100
1P-b	*Pseudomonas sp.* MOC14	JX122114.1	100
1P-c	*Pseudomonas mandelii* strain BJC15-C35	JX469391.1	100
1P-d	*Dokdonella sp.* CC-YHH031	GQ281768.1	97
1P-e	*Pseudomonas sp.* OF38	HM626451.1	99
1P-f	*Xanthomonadaceae* bacterium K-1-9	JQ963326.1	97
1P-g	*Lysobacter sp.* 7C-9	JQ349048.1	97
2P-a	*Pseudomonas sp.* MOC14	JX122114.1	100
2P-b	*Pseudomonas sp.* MOC14	JX122114.1	100
2P-c	*Lysobacter sp*. 9NM-14	JQ608331.1	100
2P-d	*Pseudomonas fluorescens* strain BIM B-187	GU784932.1	99
2P-e	*Lysobacter sp.* ljh-29	GU217698.1	99
2P-f	*Pseudomonas mandelii* strain BJC15-C35	JX469391.1	99
2P-g	*Pseudomonas sp.* MOC14	JX122114.1	99

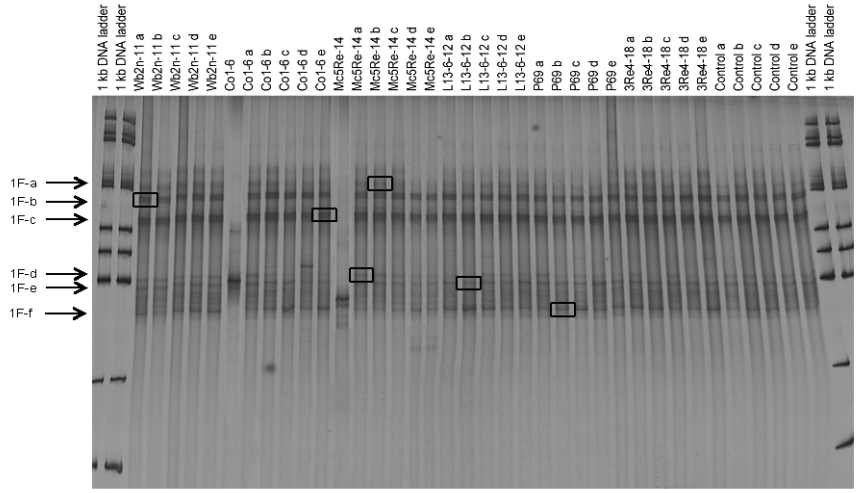

Fig. 21: SSCP pattern of the rhizosphere communities after the various treatments (*Streptomyces subrutilus* Wb2n-11, *Bacillus subtilis* Co1-6, *Paenibacillus polymyxa* Mc5Re-14, *Pseudomonas fluorescens* L13-6-12, *Stenotrophomonas rhizophila* P69, *Serratia plymuthica* 3Re4-18 and water control) using *Firmicutes*-specific primers at the sampling time (ii) after 8 weeks. Lanes marked Co1-6, Mc5Re-14 contain PCR-product from pure bacterial culture; Black framed bands were excised for identification by sequencing.

Sequencing of the excised bands showed that all samples contained *Bacillus sp.* (Table 11). In the first and the second sampling times, *Bacillus sp.* BMR7 and Bacillus sp. DV9-6 were the most frequent ones. Sequencing of the bands 1F-c, 1F-3 and 2F-e showed similarities of 99%, 100% and 98% to *Bacillus korlensis* (JX517217.1), *Bacillus megaterium* (JX455196.1) and *Bacillus flexus* (JX280923.1), which are natural inhabitants of soil.

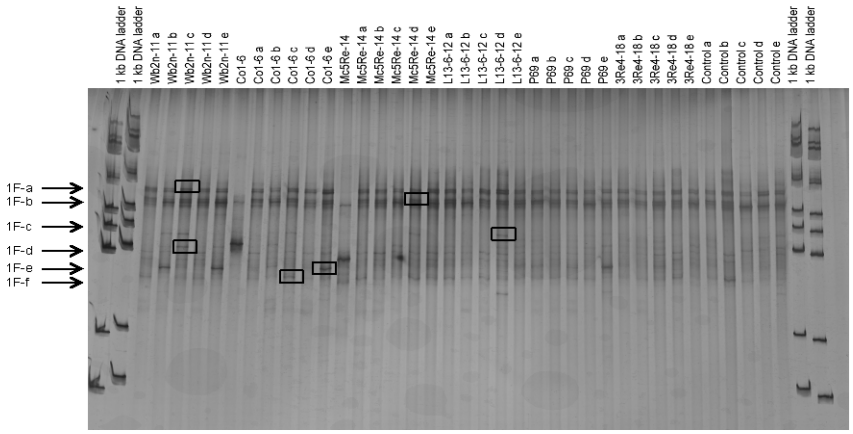

Fig. 22: SSCP pattern of the rhizosphere communities after the various treatments (*Streptomyces subrutilus* Wb2n-11, *Bacillus subtilis* Co1-6, *Paenibacillus polymyxa* Mc5Re-14, *Pseudomonas fluorescens* L13-6-12, *Stenotrophomonas rhizophila* P69, *Serratia plymuthica* 3Re4-18 and water control) using *Firmicutes*-specific primers at the sampling time (ii) after 8 weeks. Lanes marked Co1-6, Mc5Re-14 contain PCR-product from pure bacterial culture; Black framed bands were excised for identification by sequencing.

Table 11: Sequencing results of 16S rRNA gene fragments derived from selected SSCP bands using *Firmicutes*-specific primers

Band	Closest NCBI database match	Accession No.	Similarity (%)
1F-a	*Bacillus sp.* BMR7	JX434152.1	99
1F-b	*Bacillus sp.* BMR7	JX434152.1	100
1F-c	*Bacillus korlensis* strain A2-37c-4	JX517217.1	99
1F-d	*Bacillus sp.* DV9-6	GQ407151.1	99
1F-e	*Bacillus megaterium* strain BS2	JX455196.1	100
1F-f	*Bacillus sp.* DV9-6	GQ407151.1	99
2F-a	*Bacillus sp.* BMR7	JX434152.1	99
2F-b	*Bacillus sp.* NMLR7	JX434112.1	98
2F-c	*Bacillus sp.* D22-4C	EU931539.1	98
2F-d	*Bacillus sp.* DV9-6	GQ407151.1	99
2F-e	*Bacillus flexus* strain TAX4	JX280923.1	98
2F-f	*Bacillus sp.* SCSIO 15042	JX232168.1	99

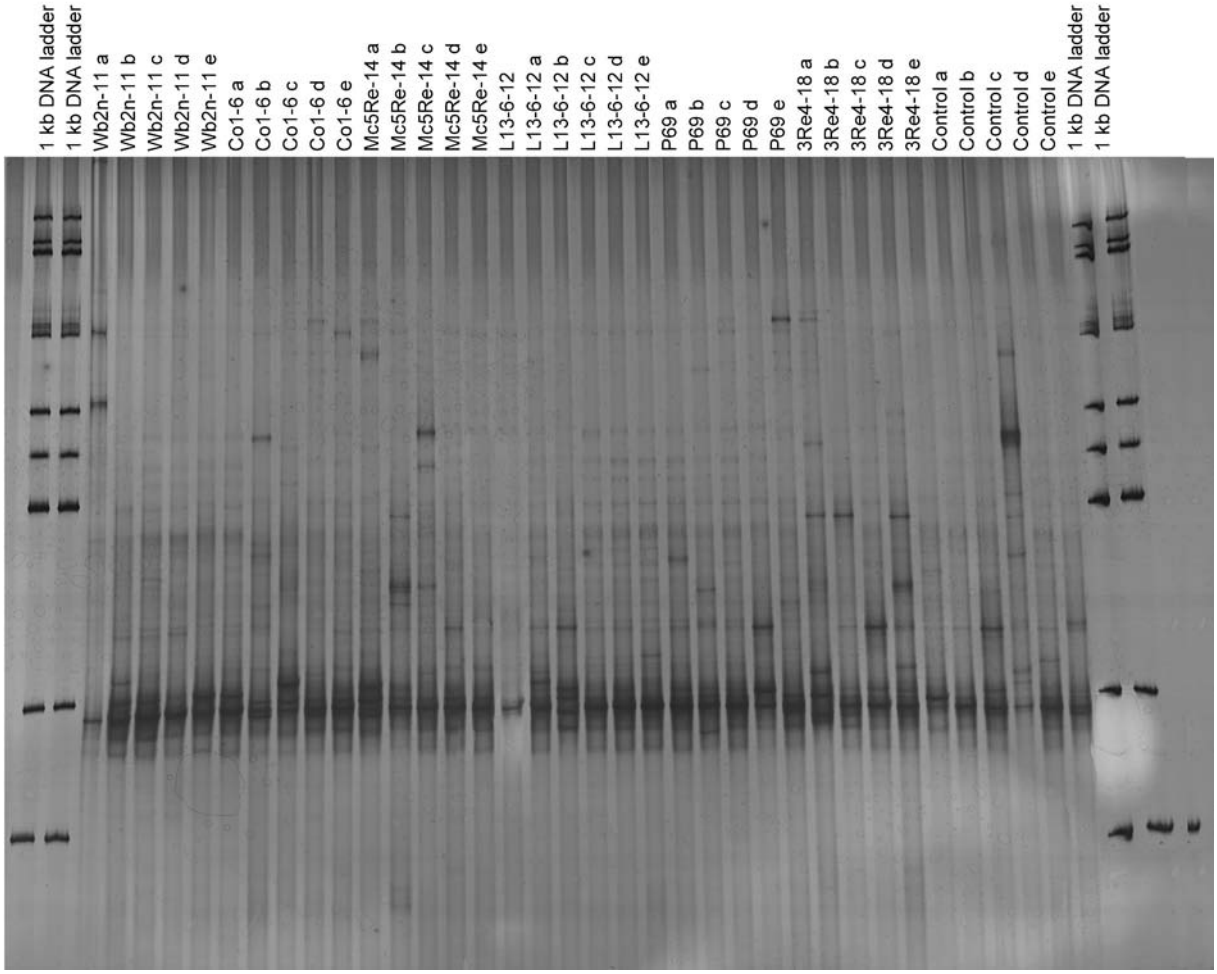

Fig. 23: SSCP pattern of the endorhiza communities after the various treatments (*Streptomyces subrutilus* Wb2n-11, *Bacillus subtilis* Co1-6, *Paenibacillus polymyxa* Mc5Re-14, *Pseudomonas fluorescens* L13-6-12, *Stenotrophomonas rhizophila* P69, *Serratia plymuthica* 3Re4-18 and water control) using *Pseudomonas*-specific primers at the sampling time (i) after 4 weeks. Lane marked L13-6-12 contains PCR-product from pure bacterial culture.

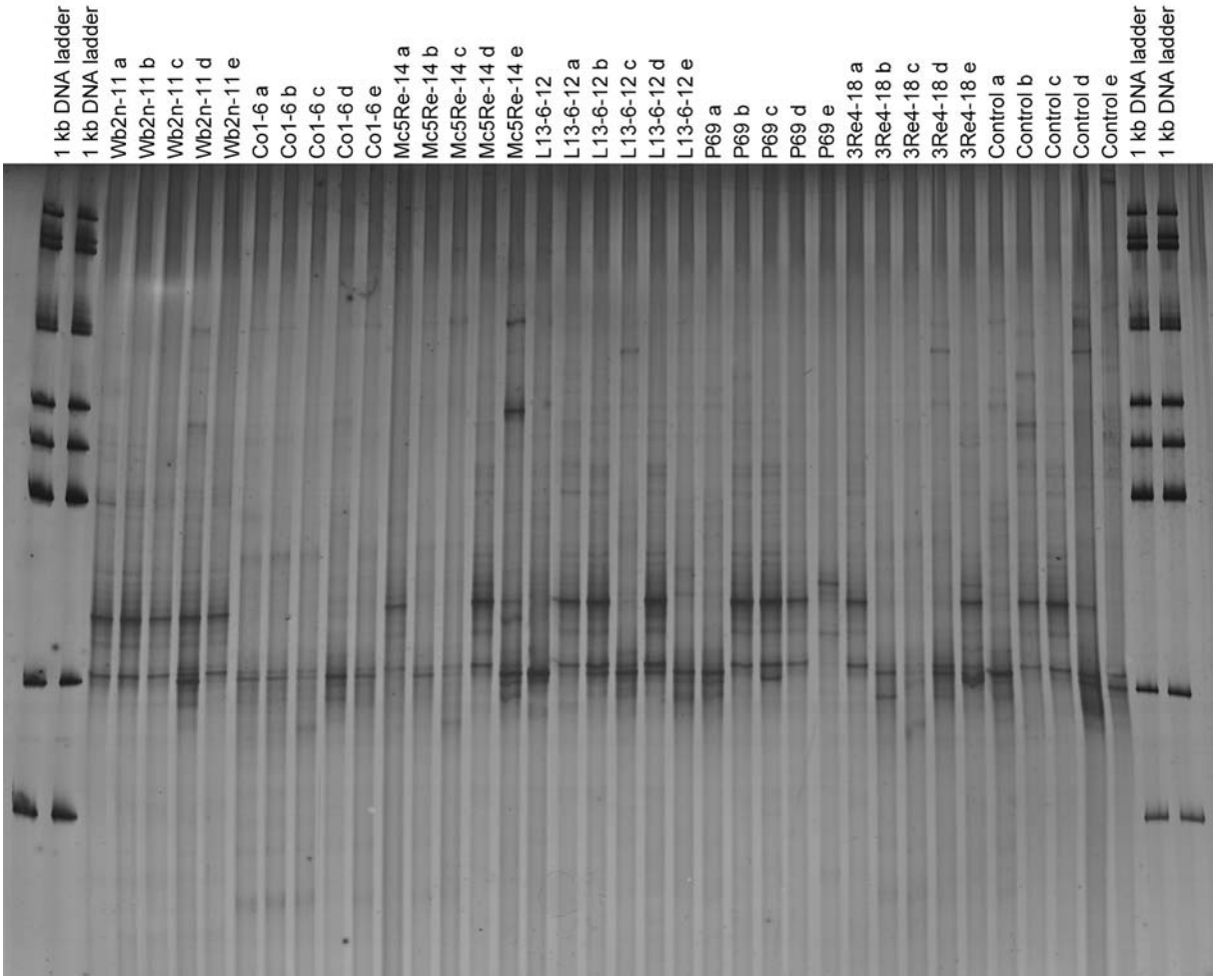

Fig. 24: SSCP pattern of the endorhiza communities after the various treatments (*Streptomyces subrutilus* Wb2n-11, *Bacillus subtilis* Co1-6, *Paenibacillus polymyxa* Mc5Re-14, *Pseudomonas fluorescens* L13-6-12, *Stenotrophomonas rhizophila* P69, *Serratia plymuthica* 3Re4-18 and water control) using *Pseudomonas*-specific primers at the sampling time (ii) after 8 weeks. Lane marked L13-6-12 contains PCR-product from pure bacterial culture.

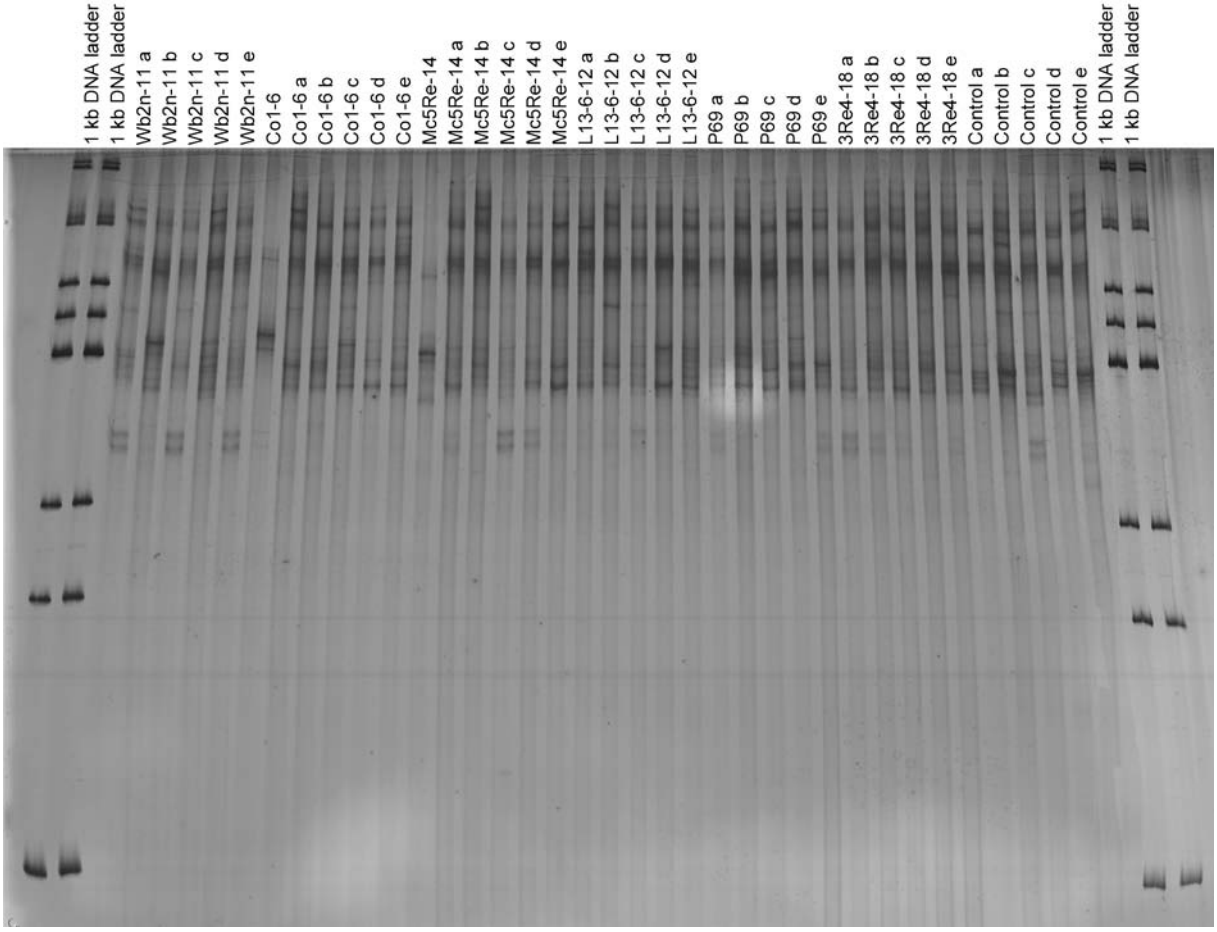

Fig. 25: SSCP pattern of the endorhiza communities after the various treatments (*Streptomyces subrutilus* Wb2n-11, *Bacillus subtilis* Co1-6, *Paenibacillus polymyxa* Mc5Re-14, *Pseudomonas fluorescens* L13-6-12, *Stenotrophomonas rhizophila* P69, *Serratia plymuthica* 3Re4-18 and water control) using *Firmicutes*-specific primers at the sampling time (i) after 4 weeks. Lanes marked Co1-6 and Mc5Re-14 contain PCR-products from pure bacterial culture.

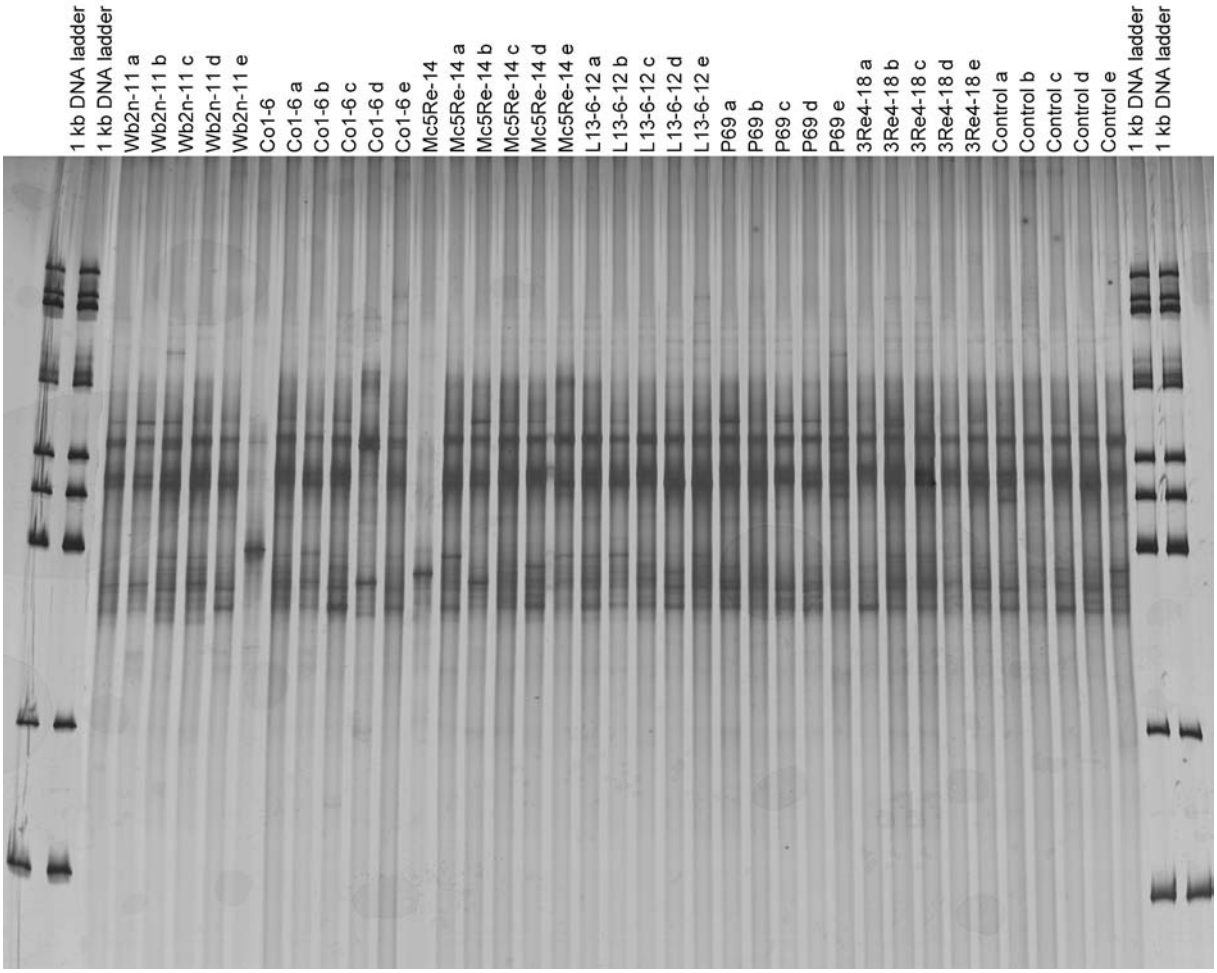

Fig. 26: SSCP pattern of the endorhiza communities after the various treatments (*Streptomyces subrutilus* Wb2n-11, *Bacillus subtilis* Co1-6, *Paenibacillus polymyxa* Mc5Re-14, *Pseudomonas fluorescens* L13-6-12, *Stenotrophomonas rhizophila* P69, *Serratia plymuthica* 3Re4-18 and water control) using *Firmicutes*-specific primers at the sampling time (ii) after 8 weeks. Lanes marked Co1-6 and Mc5Re-14 contain PCR-products from pure bacterial culture.

3.3. Pyrosequencing of total bacteria

Rarefaction analysis was performed to an extent of diversity coverage (Fig. 27). Assessment of richness revealed that pyrosequencing effort attained 35.8-46.5% of estimated richness at a genetic distance of 97% (Fig. 27). At the genetic distances of 95% and 80% amplicon libraries covered 41.7-49.7% and 56.6-88.8% of estimated richness, respectively. Taxonomic composition of bacterial communities (Fig. 28) was similar at phylum level comprising *Proteobacteria*, *Bacteroidetes*, *Firmicutes* and *Actinobacteria* as the most dominant phyla, which was also confirmed by a phylogenetic tree (Fig. 29). However, the phylum *Verrucomicrobia* was only present in the sample from the treatment with *Stenotrophomonas rhizophila* P69 (= DSM14405^T), considering only taxa covering more than 1% of quality sequences. *Acidobacteria* were observed in samples treated with *Bacillus subtilis* Co1-6, *Stenotrophomonas rhizophila* P69 and *Serratia plymuthica* 3Re4-18. At genus level, *Rhizobium* (phylum Proteobacteria), *Pseudoxanthomonas* (phylum Proteobacteria), *Pseudomonas* (phylum Proteobacteria), *Flavobacterium* (phylum *Bacteroidetes*) and *Arthrobacter* (phylum *Actinobacteria*) represented the most abundant genera showing a different composition according to different treatments.

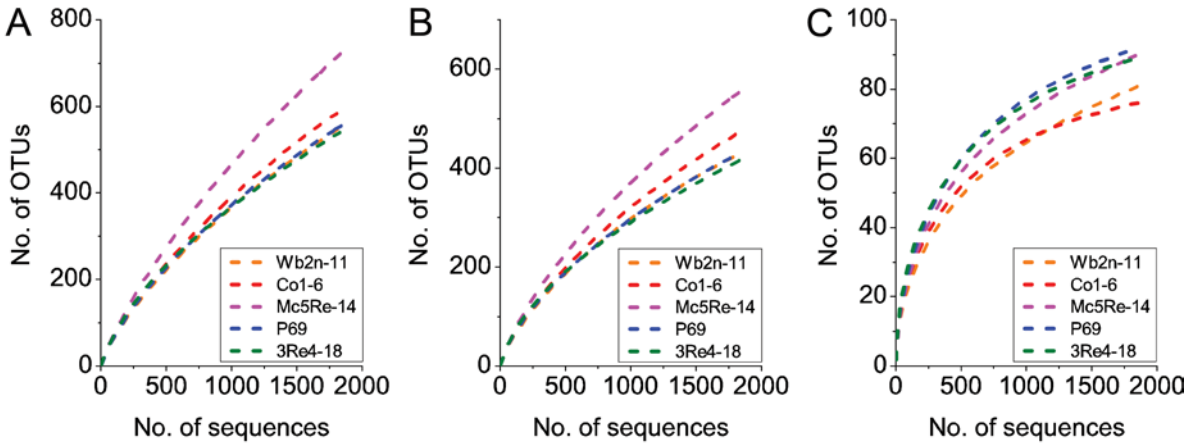

Fig. 27: Rarefaction analysis of the 16S rRNA gene amplicon libraries of rhizosphere samples of *Matricaria recutita* (L.) Rarefaction curves were calculated at (A) 3%, (B) 5% and (C) 20% genetic distance levels, corresponding to the taxonomic levels of species, genera and phyla, respectively. Coloured lines depict different treatments.

Table 12 Richness estimates and diversity indices for 16S rRNA gene amplicon libraries of rhizosphere samples of *Matricaria recutita* (L.) The number of sequences of each sample was normalised to 1,858. Genetic distances represent the taxonomic levels of species (97%), genera (95%) and phyla (80%).

Genetic distance	Treatment sample	No. of OTUs	Chao1	Coverage (%)	Shannon (H')
97%	Wb2n-11	557	1,443	38.6	5.14
	Co1-6	596	1,280	46.5	5.32
	Mc5Re-14	729	1,928	37.8	5.66
	P69	559	1,209	46.2	5.23
	3Re4-18	546	1,525	35.8	5.37
95%	Wb2n-11	433	871	49.7	4.80
	Co1-6	477	998	47.8	5.00
	Mc5Re-14	560	1,342	41.7	5.26
	P69	435	930	46.8	4.90
	3Re4-18	419	973	43.1	5.01
80%	Wb2n-11	81	143	56.6	2.85
	Co1-6	76	86	88.8	3.05
	Mc5Re-14	90	134	67.4	2.87
	P69	92	120	76.9	3.11
	3Re4-18	89	100	88.6	3.20

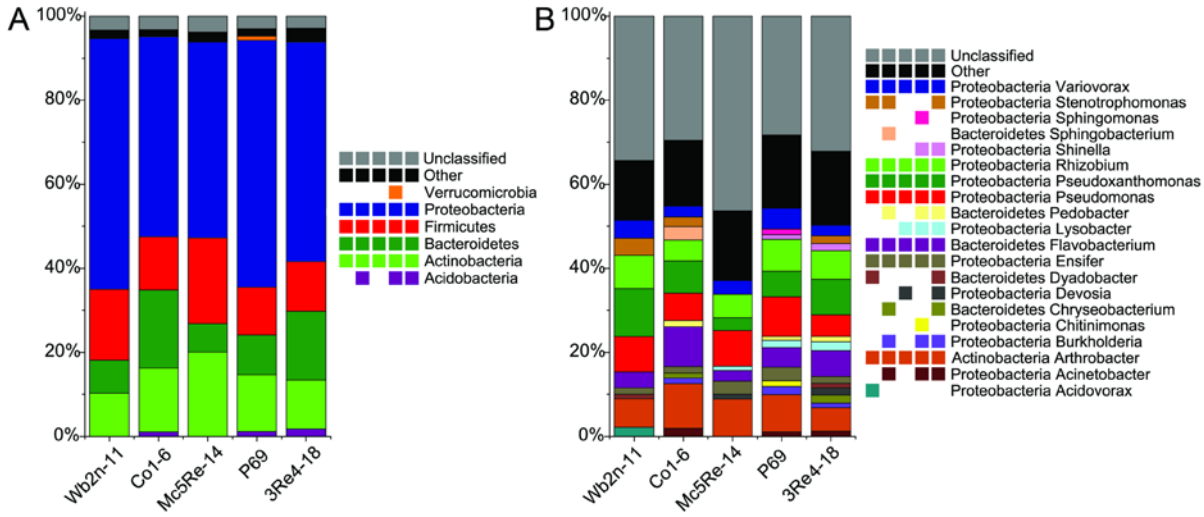

Fig. 28: classification of bacterial communities associated with *Matricaria recutita* (L.) Pyrosequencing reads were classified at phylum (A) and genus (B) level against RDP core set within QIIME pipeline with an 80% confidence threshold. Taxa below 1% of relative abundance are included in "Other". Multi-coloured charts at the legend are shown for each sample correspondingly.

Alpha-diversity of the amplicon libraries was characterised by Shannon index (H') for 97%, 95% and 80% similarity levels. Slight differences between treatments where revealed by the comparison of the index values (Table 12).

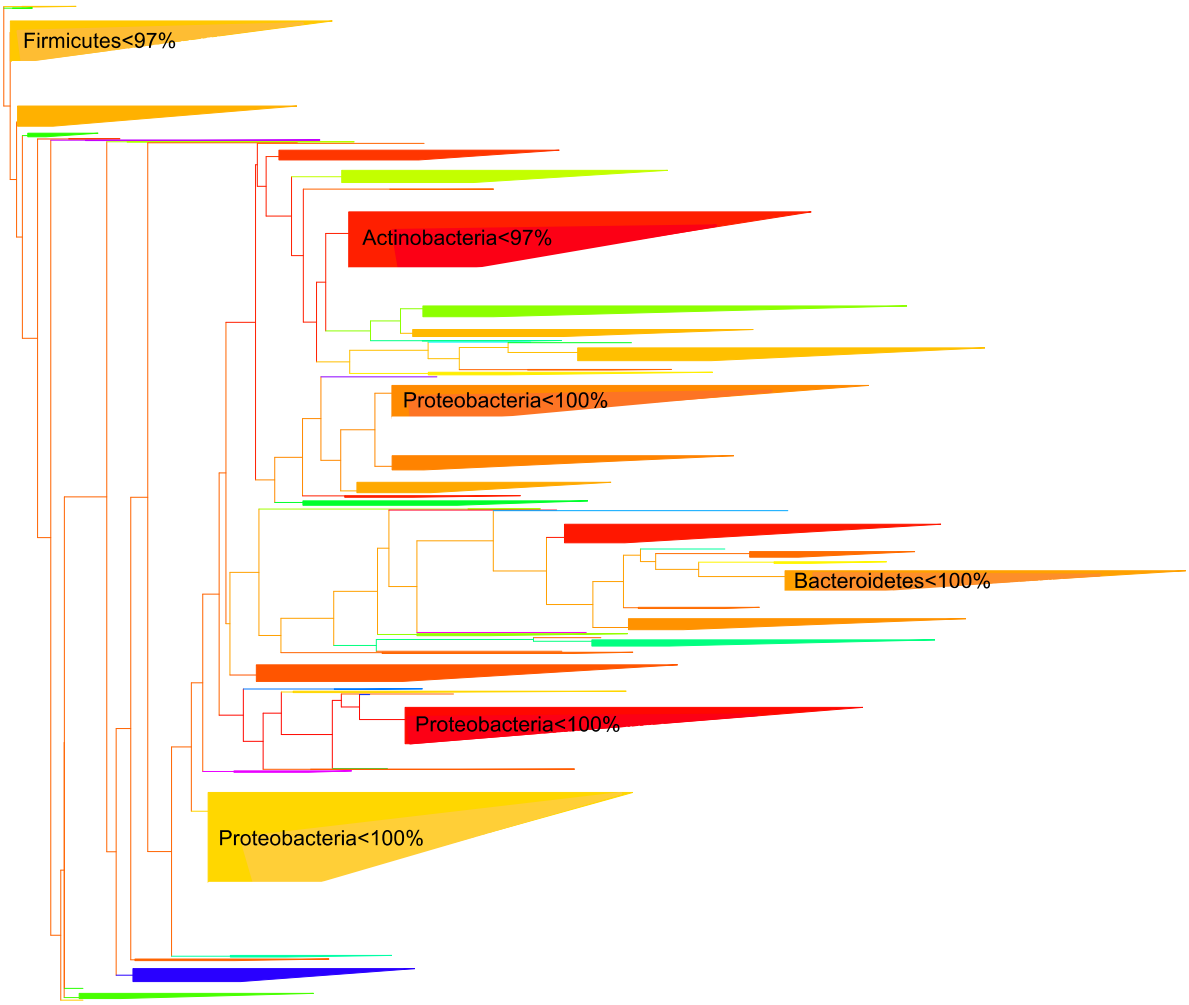

Fig. 29: Phylogenetic composition of the total bacterial community associated with *Matricaria recutita* (L.).

Jackknifed unweighted and weighted UniFrac two-dimensional (Fig. 30 and Fig. 32) and three-dimensional (Fig. 31 and Fig. 33) PCoA biplot were constructed in order to visualise relationships among samples based on differences in taxonomic diversity. Unweighted as well as weighted biplots show that the samples were clearly separated, implying a difference in bacterial community composition.

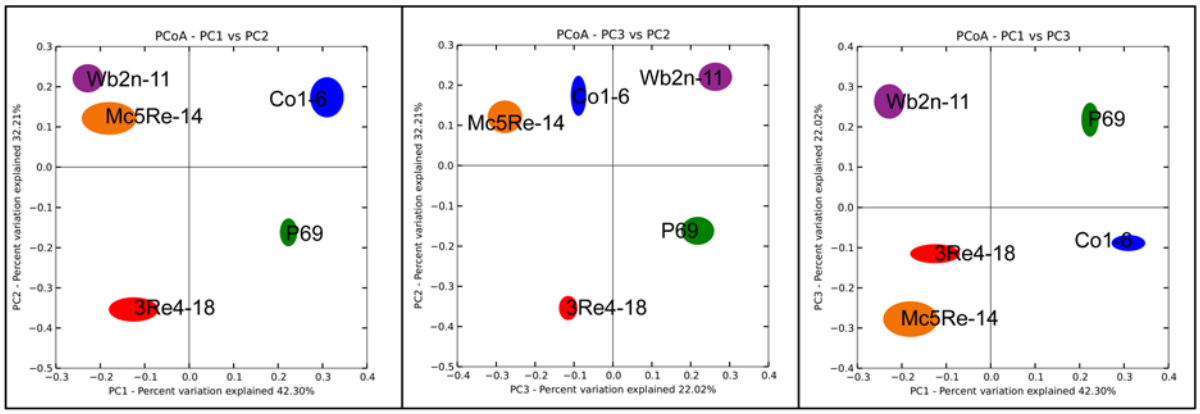

Fig. 30: Comparison of the microbial communities of *Matricaria recutita* (L.) rhizosphere by jackknifed principal coordinate analysis. The 2D-plot illustrates the compositional similarity between samples based on unweighted UniFrac. The positions of the points are the average for the jackknifed replicates generated by QIIME and are shown with ellipses representing the interquartile range (IQR) in each axis. Larger ellipses represent more diverse communities. Colours correspond to the different treatments.

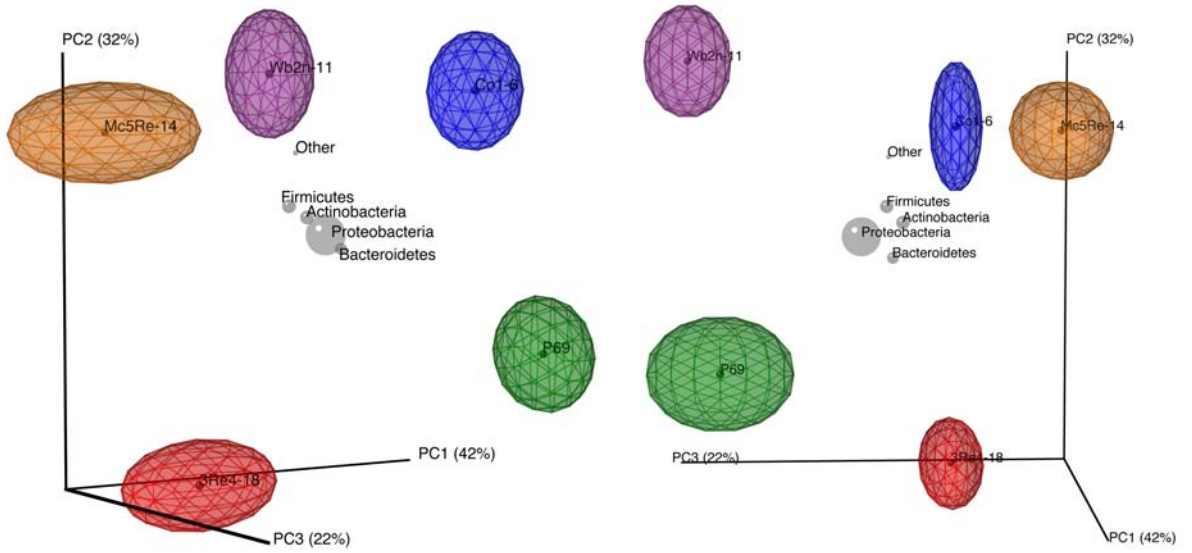

Fig. 31: Comparison of the microbial communities of *Matricaria recutita* (L.) rhizosphere by jackknifed principal coordinate analysis. The biplot illustrates the compositional similarity between samples based on unweighted UniFrac. Taxa coordinates are indicated by grey orbs with size, as a function of relative abundance. To confine the biplot, the number of the displayed taxa was restricted to 5. The positions of the points are the average for the jackknifed replicates generated by QIIME and are shown with ellipses representing the interquartile range (IQR) in each axis. Larger ellipses represent more diverse communities. Colours correspond to the different treatments.

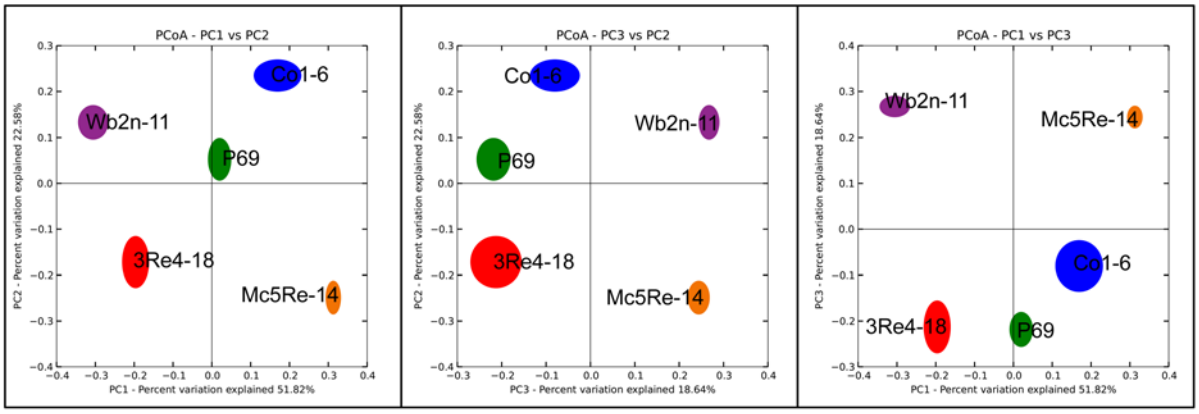

Fig. 32: Comparison of the microbial communities of *Matricaria recutita* (L.) rhizosphere by jackknifed principal coordinate analysis. The 2D-plot illustrates the compositional similarity between samples based on weighted UniFrac. The positions of the points are the average for the jackknifed replicates generated by QIIME and are shown with ellipses representing the interquartile range (IQR) in each axis. Larger ellipses represent more diverse communities. Colours correspond to the different treatments.

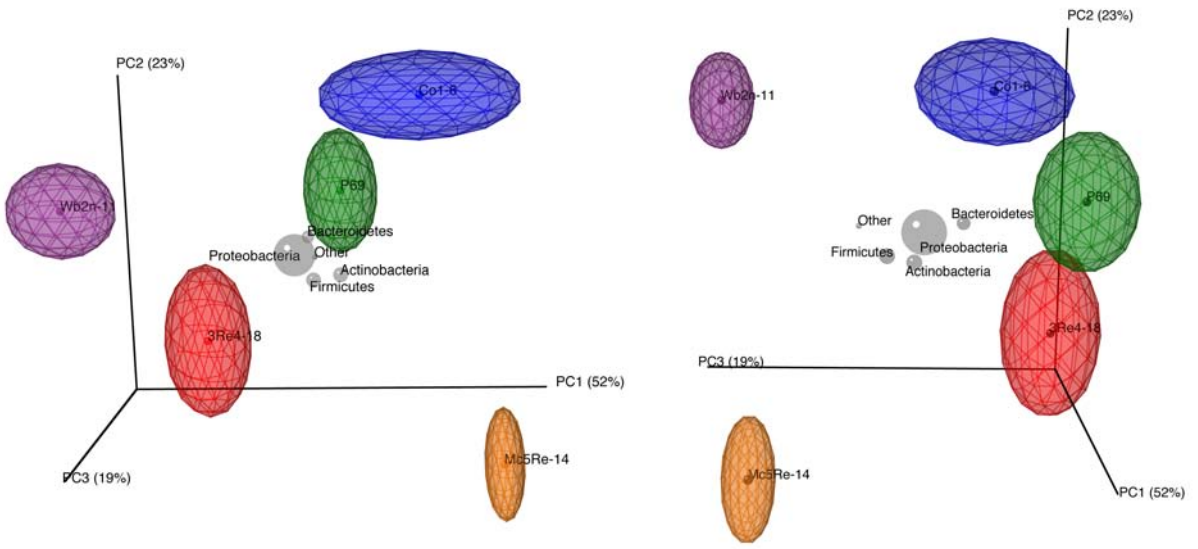

Fig. 33: Comparison of the microbial communities of *Matricaria recutita* (L.) rhizosphere by jackknifed principal coordinate analysis. The biplot illustrates the compositional similarity between samples based on weighted UniFrac. Taxa coordinates are indicated by grey orbs with size, as a function of relative abundance. To confine the biplot, the number of the displayed taxa was restricted to 5. The positions of the points are the average for the jackknifed replicates generated by QIIME and are shown with ellipses representing the interquartile range (IQR) in each axis. Larger ellipses represent more diverse communities. Colours correspond to the different treatments.

To get an overview about the co-occuring OTUs between the samples, a network analysis was carried out with 1685 OTUs of the data set (Fig. 34). Enhancing the viewing characteristics of the network and identify OTUs of interest a sub-network was created (Fig. 35). The resulting microbial network consisted of 168 nodes (OTUs) and 257 edges. The network analysis revealed the sample of *Bacillus subtilis*

Co1-6 treatment shared the most OTUs with samples treated with *Stenotrophomonas rhizophila* P69 and *Serratia plymuthica* 3Re4-18, comprising members of the phyla *Proteobacteria*, *Bacteroidetes* and *Firmicutes*. In general, the microbial network was composed of fewer connections between the samples, rather than of samples comprising their own, individual community.

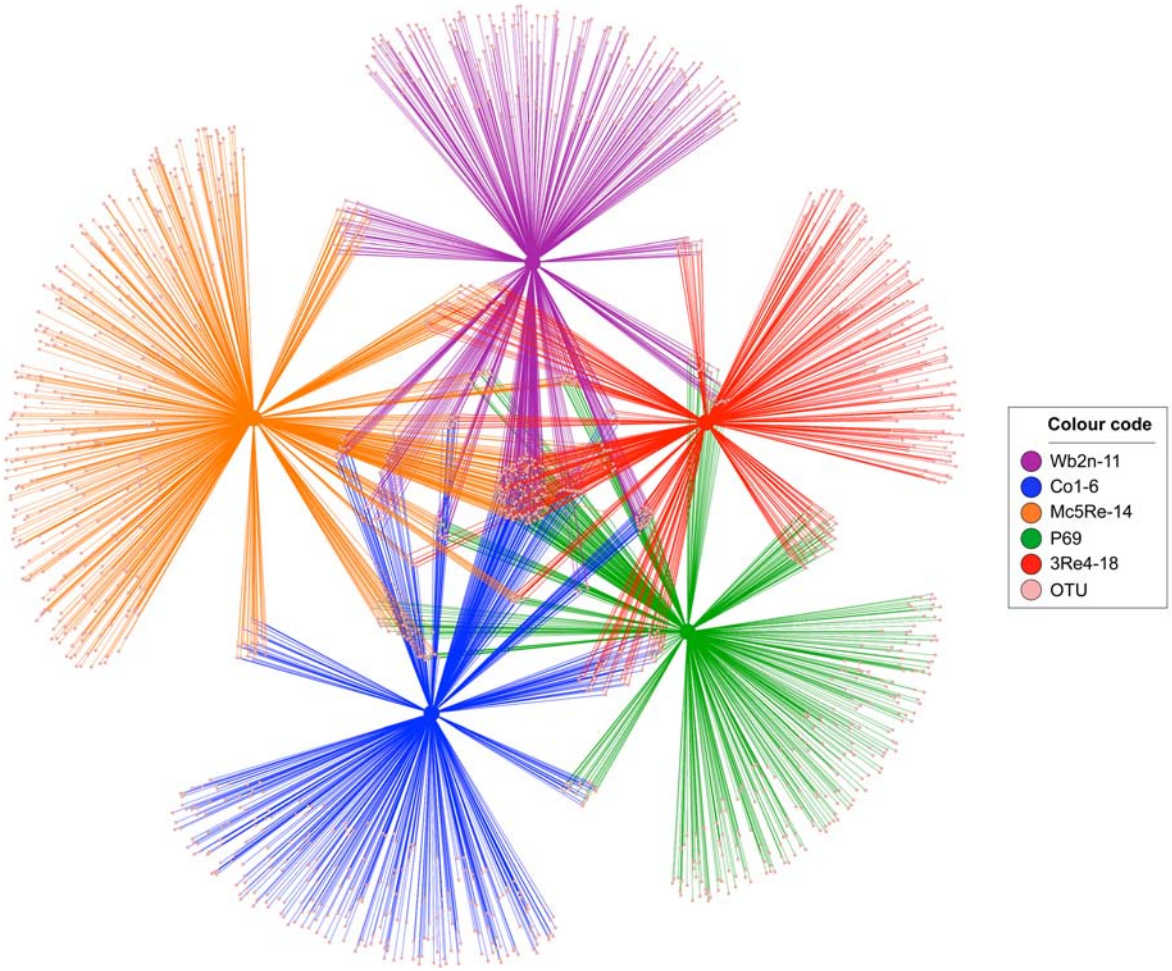

Fig. 34: Network of co-occurring 97% cutoff OTUs in the rhizosphere samples. Each OTU is connected to its corresponding sample in an edge-weighted spring embedded layout. Nodes are coloured by taxonomy.

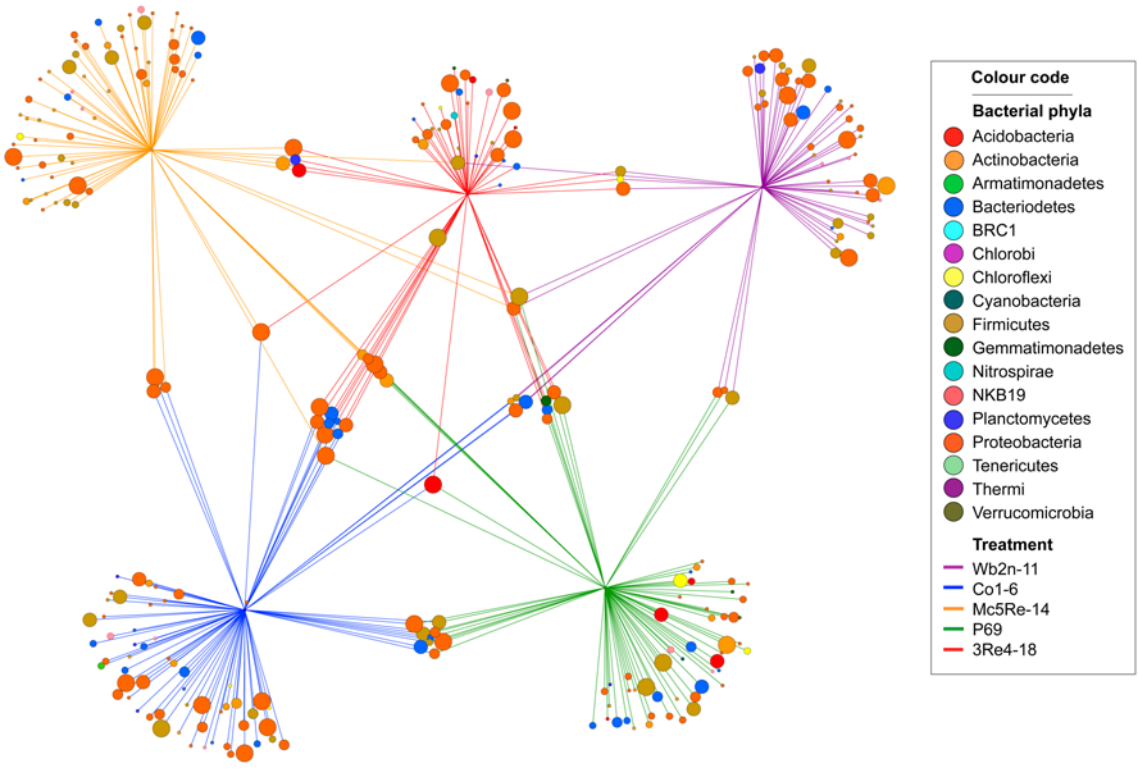

Fig. 35: Network of co-occurring OTUs in the rhizosphere samples. Edge weights <2 were filtered out. Each OTU is connected to its corresponding sample in an edge-weighted spring embedded layout. The size of each node is proportional to the number of connections (degree). Nodes are coloured by taxonomy.

3.4. qPCR estimates of bacterial abundances

The bacterial abundances of total bacteria and *Firmicutes* were determined by qPCR. 16S rRNA gene copy numbers per g rhizosphere were calculated and statistically evaluated (Fig. 36 and Fig. 37). For total bacteria, abundances ranged from 7.45 $\log_{10}$ copies per g rhizosphere for the treatment with *Streptomyces subrutilus* Wb2n-11 to 6.03 $\log_{10}$ copies per g rhizosphere for the treatment with *Paenibacillus polymyxa* Mc5Re-14. Abundances for *Firmicutes* ranged from 6.97 $\log_{10}$ copies per g rhizosphere for the treatment with *Streptomyces subrutilus* Wb2n-11 to 7.54 $\log_{10}$ copies per g rhizosphere for the treatment with *Paenibacillus polymyxa* Mc5Re-14. The treatment with *Paenibacillus polymyxa* Mc5Re-14 showed a slightly higher abundance of total bacteria as well as of *Firmicutes*. However, no significant differences between the treatments could be observed.

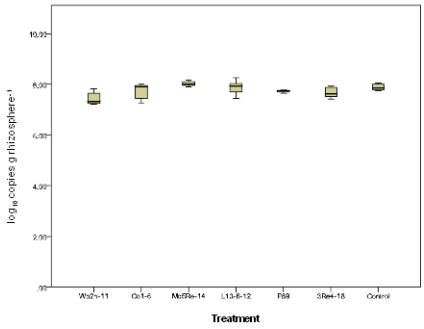

Fig. 36: Abundances of total bacteria obtained by qPCR of the 16S rRNA genes. Averages of 16S rRNA gene copy numbers per gram rhizosphere as log_{10} are shown.

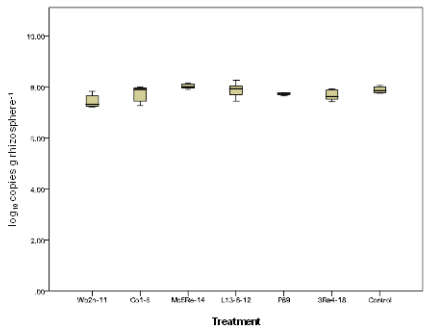

Fig. 37: Abundances of *Firmicutes* obtained by qPCR of the 16S rRNA genes. Averages of 16S rRNA gene copy numbers per gram rhizosphere as log_{10} are shown.

3.5. Confocal laser scanning microscopy

The colonisation pattern of the labelled bacterial (DsRed) strain *Serratia plymuthica* 3Re4-18 was monitored with CLSM. For chamomile seedlings cultivated in sterile soil, colonies of *Serratia plymuthica* 3Re4-18 were observed mainly on the upper parts of the roots (Fig. 38 A). Two different colonization patterns could be observed: Single cells, covering the root surface and forming a dense network. Furthermore, cells were often found as surrounding clouds (Fig. 38 B).

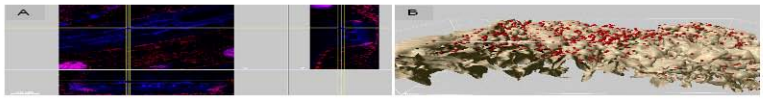

Fig. 38: Root epidermis of a chamomile seedling 14 days after inoculation. Visualisation of DsRed marked bacteria with confocal laser scanning microscopy. A) xy, xz and yz maximum projections showing a colonising of small colonies and single cells of *Serratia plymuthica* 3Re4-18 of the surrounding area of the root. Red: bacterial cells, blue: root B) Surface model of A shows the root-surface localisation of *Serratia plymuthica* 3Re4-18 in the three-dimensional space. Red: bacterial cells, brown: root.

3.6. Chemical analysis of *Matricaria recutita* (L.) secondary metabolites

3.6.1. Qualitative determination of chamomile extracts

HPTLC method was used for the qualitative analysis of the extracts. As stationery phase TLC on silica gel 60 F254 HPTLC plates with acetic acid:water:butanol (17:17:66 v/v/v) as mobile phase and derivatisation with diphenylboric acid-2-aminoethylester and PEG 400 was shown to be suitable for the analysis of the Matricaria *recutita* (L.) extracts, resulting in a good separation of flavonoids. Chromatograms obtained from the extracts and standards are shown in Fig. 39, Fig. 40, Fig. 41, Fig. 42 and Fig. 43. The applied standards, apigenin-7-*O*-glucoside and apigenin were present in all samples fluorescing in a green color. Altogether, 7 fluorescence bands could be observed. Among them, apigenin-7-*O*-glucoside and apigenin showed R_f values of 0.74 and 0.93, respectively. It could be shown that the

pattern of compounds was the same for all samples, however the compound content varied for the different treatments.

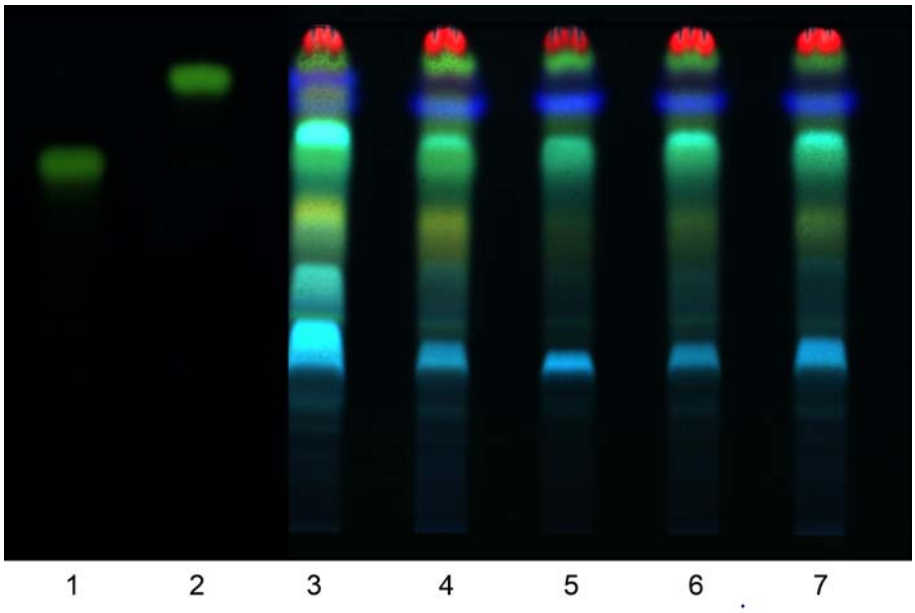

Fig. 39: HPTLC plate treated with diphenylboric acid-2-aminoethylester-PEG 400 reagent ($\lambda_{excitation}$ = 366 nm) of methanolic extracts from treatment with *Streptomyces subrutilus* Wb2n-11 and standards. Lane number, from left to right: 1: Apigenin-7-*O*-glucoside, 2: Apigenin, 3: Wb2n-11_1, 4: Wb2n-11_2; 5: Wb2n-11_3, 6: Wb2n-11_4, 7: Wb2n-11_5

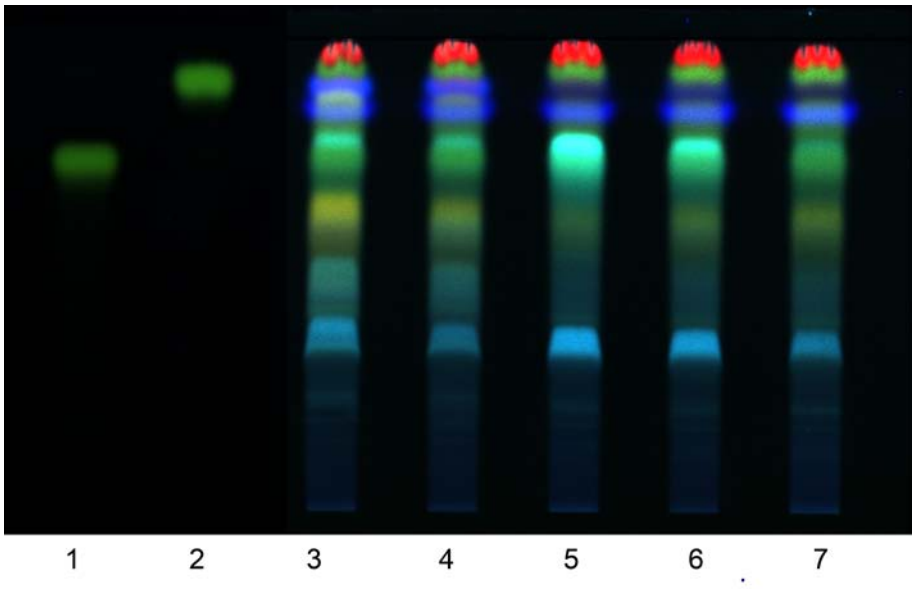

HPTLC plate treated with diphenylboric acid-2-aminoethylester-PEG 400 reagent ($\lambda_{excitation}$ = 366 nm) of methanolic extracts from treatment with *Bacillus subtilis* Co1-6 and standards. Lane number, from left to right: 1: Apigenin-7-*O*-glucoside, 2: Apigenin, 3: Mc5Re-14_1, 4: Mc5Re-14_2, 5: Mc5Re-14_3, 6: Mc5Re-14_4, 7: Mc5Re-14_5

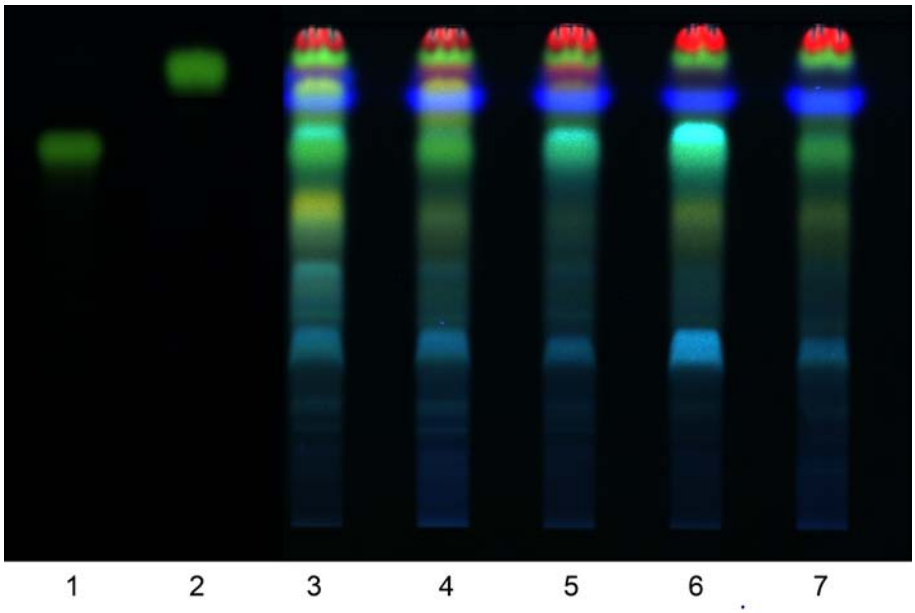

HPTLC plate treated with diphenylboric acid-2-aminoethylester-PEG 400 reagent ($\lambda_{excitation}$ = 366 nm) of methanolic extracts from treatment with *Paenibacillus polymyxa* Mc5Re-14 and standards. Lane number, from left to right: 1: Apigenin-7-*O*-glucoside, 2: Apigenin, 3: Mc5Re-14_1, 4: Mc5Re-14_2, 5: Mc5Re-14_3, 6: Mc5Re-14_4, 7: Mc5Re-14_5

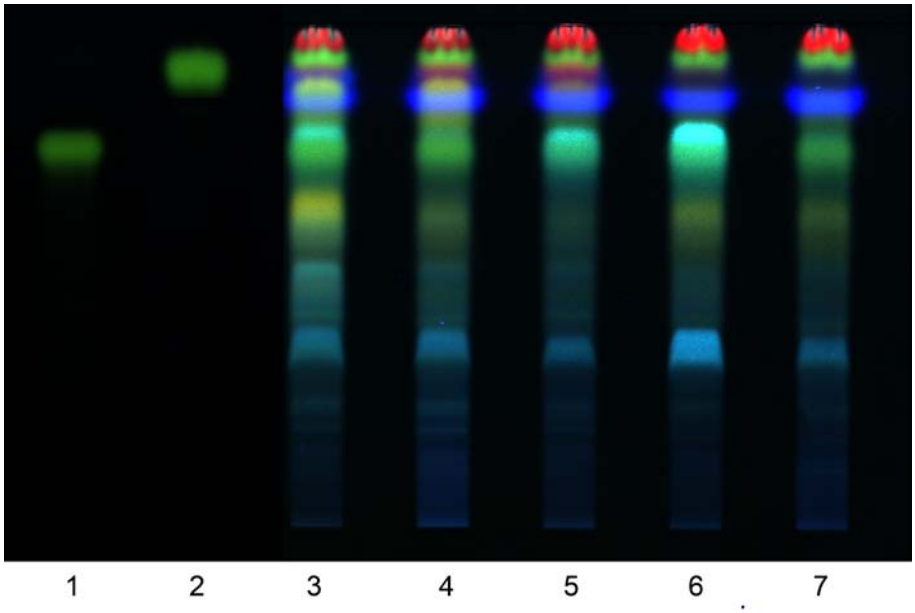

Fig. 40: HPTLC plate treated with diphenylboric acid-2-aminoethylester-PEG 400 reagent ($\lambda_{excitation}$ = 366 nm) of methanolic extracts from treatment with *Pseudomonas fluorescens* L13-6-12 and standards. Lane number, from left to right: 1: Apigenin-7-*O*-glucoside, 2: Apigenin, 3: L13_1, 4: L13_2, 5: L13_3, 6: L13_4, 7: L13_5

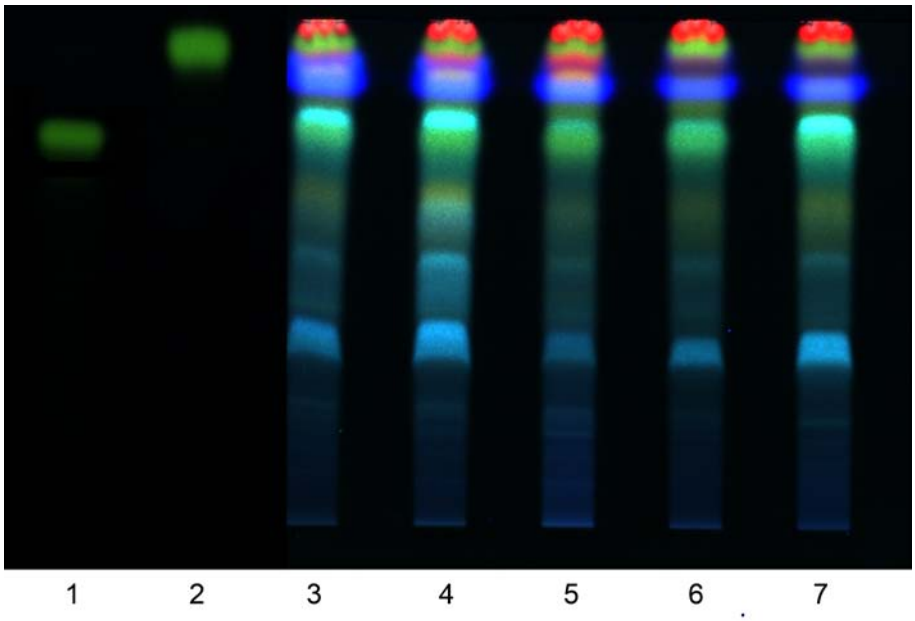

Fig. 41: HPTLC plate treated with diphenylboric acid-2-aminoethylester-PEG 400 reagent ($\lambda_{excitation}$ = 366 nm) of methanolic extracts from treatment with *Stenotrophomonas rhizophila* P69 and standards. Lane number, from left to right: 1: Apigenin-7-*O*-glucoside, 2: Apigenin, 3: P69_1, 4: P69_2, 5: P69_3, 6: P69_4, 7: P69_5

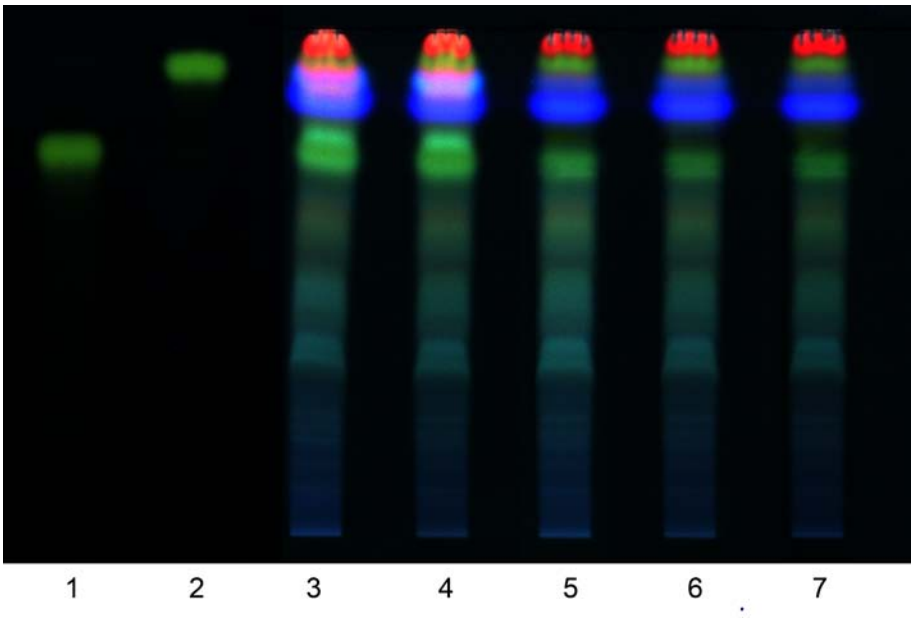

Fig. 42: HPTLC plate treated with diphenylboric acid-2-aminoethylester-PEG 400 reagent ($\lambda_{excitation}$ = 366 nm) of methanolic extracts from treatment with *Serratia plymuthica* 3Re4-18 and standards. Lane number, from left to right: 1: Apigenin-7-*O*-glucoside, 2: Apigenin, 3: 3Re_1, 4: 3Re_2, 5: 3Re_3, 6: 3Re_4, 7: 3Re_5

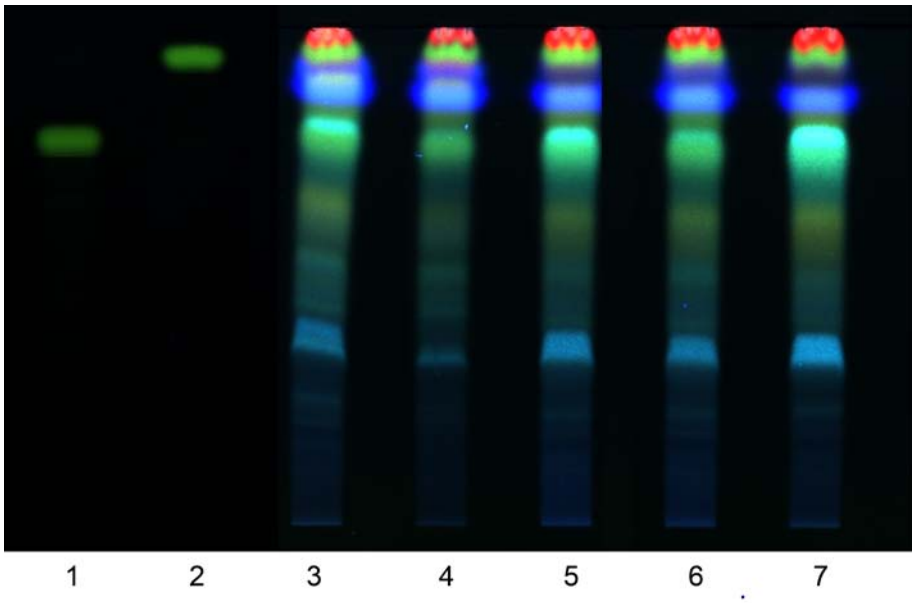

Fig. 43: HPTLC plate treated with diphenylboric acid-2-aminoethylester-PEG 400 reagent ($\lambda_{excitation}$ = 366 nm) of methanolic extracts from treatment with Control and standards. Lane number, from left to right: 1: Apigenin-7-O-glucoside, 2: Apigenin, 3: Control_1, 4: Control _2, 5: Control _3, 6: Control _4, 7: Control _5

3.6.2. Development of chromatographic conditions

A method coupling high-performance liquid chromatography (HPLC) with diode-array detector (DAD) was developed for the separation of flavonoid glycosides in the extract of *Matricaria recutita* (L.). Different mobile phase compositions were screened to obtain chromatograms with good resolution within an acceptable time of analysis. To avoid hydrolysis of glycosides a suitable mobile phase without any addition of acid had to be chosen. Therefore, water, as solvent A and acetonitrile, as solvent B were used for the gradient elution. A wavelength of 340 nm was chosen to monitor the absorption maxima of the analytes. The HPLC-DAD chromatograms of the methanol extracts at a wavelength of 340 nm are shown in Fig. 44, Fig. 45, Fig. 46, Fig. 47, Fig. 48, Fig. 49 and Fig. 50.

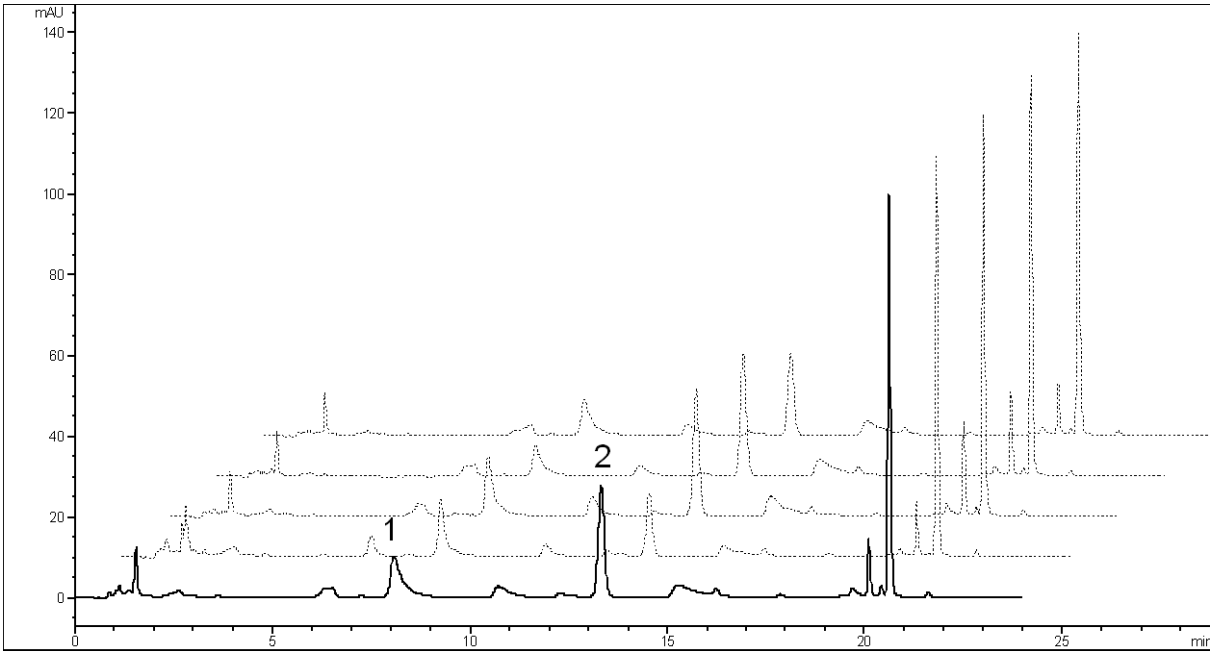

Fig. 44: HPLC chromatogram of the methanolic extracts from the treatment with *Streptomyces subrutilus* Wb2n-11 at 340 nm. 1: Apigenin-7-*O*-glucoside, 2: Apigenin

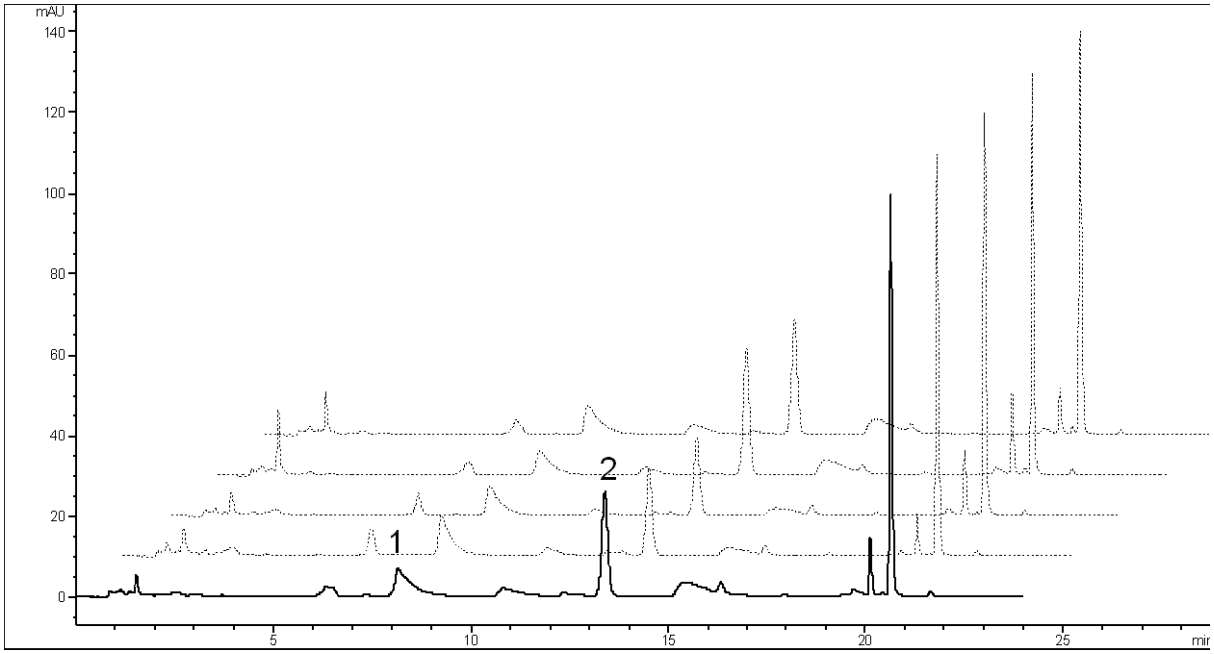

Fig. 45: HPLC chromatogram of the methanolic extracts from the treatment with *Bacillus subtilis* Co1-6 at 340 nm. 1: Apigenin-7-*O*-glucoside, 2: Apigenin

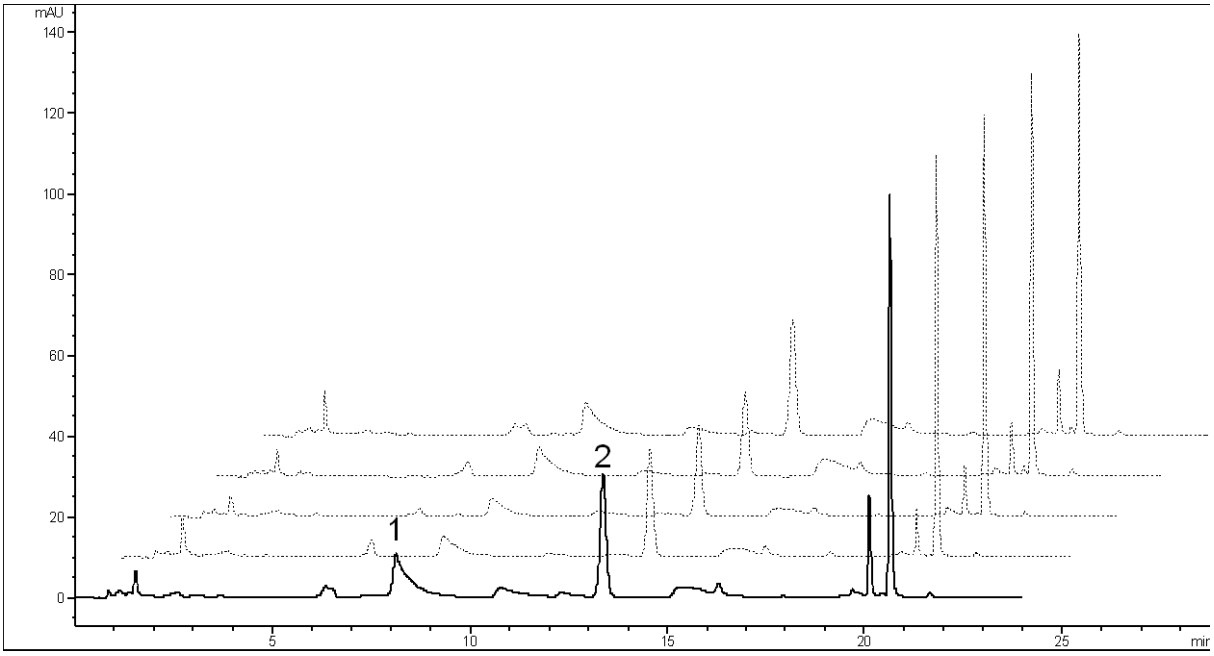

Fig. 46: HPLC chromatogram of the methanolic extracts from the treatment with *Panibacillus polymxa* Mc5Re-14 at 340 nm. 1: Apigenin-7-*O*-glucoside, 2: Apigenin

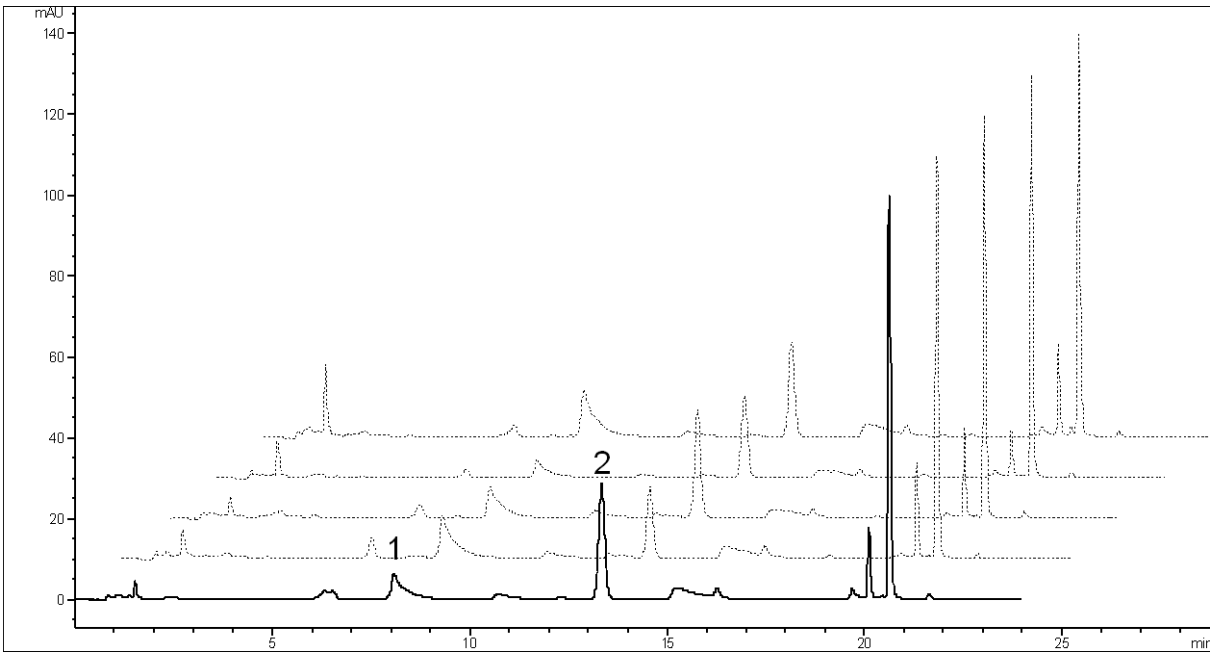

Fig. 47: HPLC chromatogram of the methanolic extracts from the treatment with *Pseudomonas fluorescens* L13-6-12 at 340 nm. 1: Apigenin-7-*O*-glucoside, 2: Apigenin

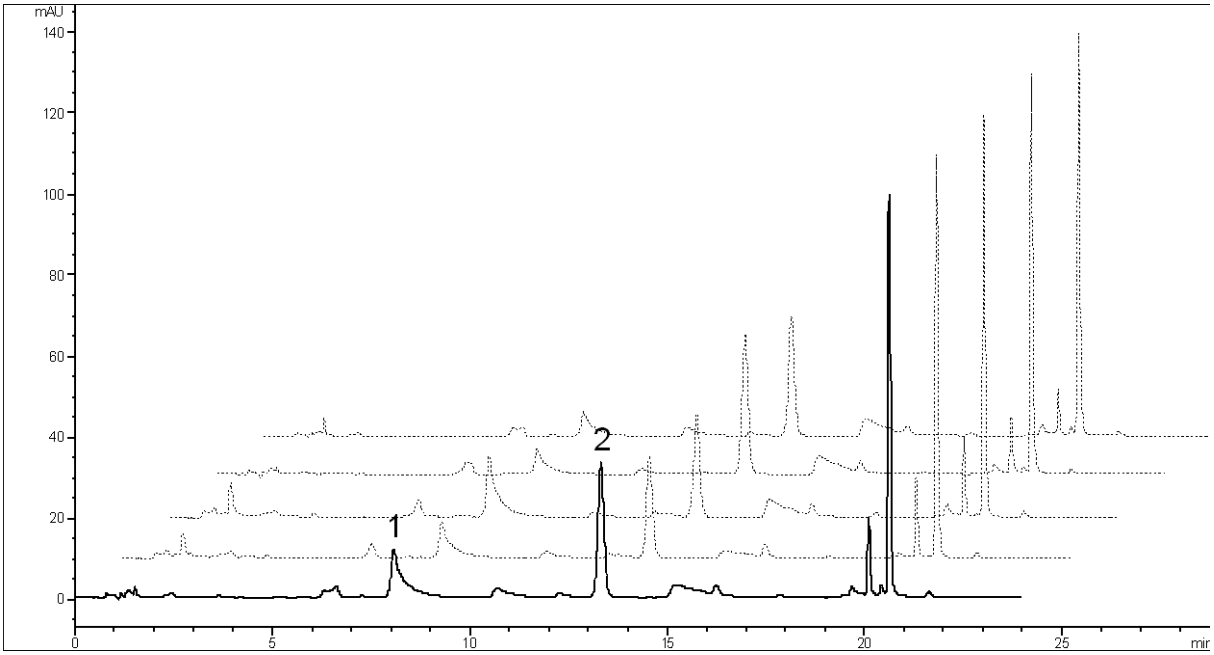

Fig. 48: HPLC chromatogram of the methanolic extracts from the treatment with *Stenotrophomonas rhizophila* P69 at 340 nm. 1: Apigenin-7-*O*-glucoside, 2: Apigenin

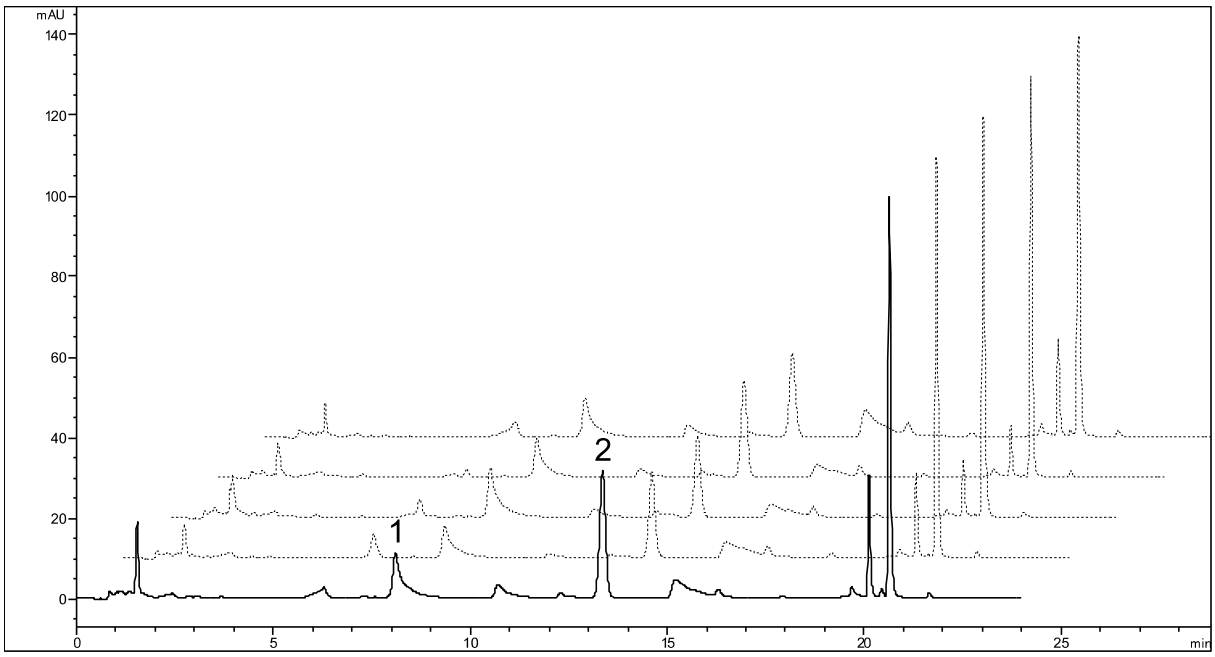

Fig. 49: HPLC chromatogram of the methanolic extracts from the treatment with *Serratia plymuthica* 3Re4-18 at 340 nm. 1: Apigenin-7-*O*-glucoside, 2: Apigenin

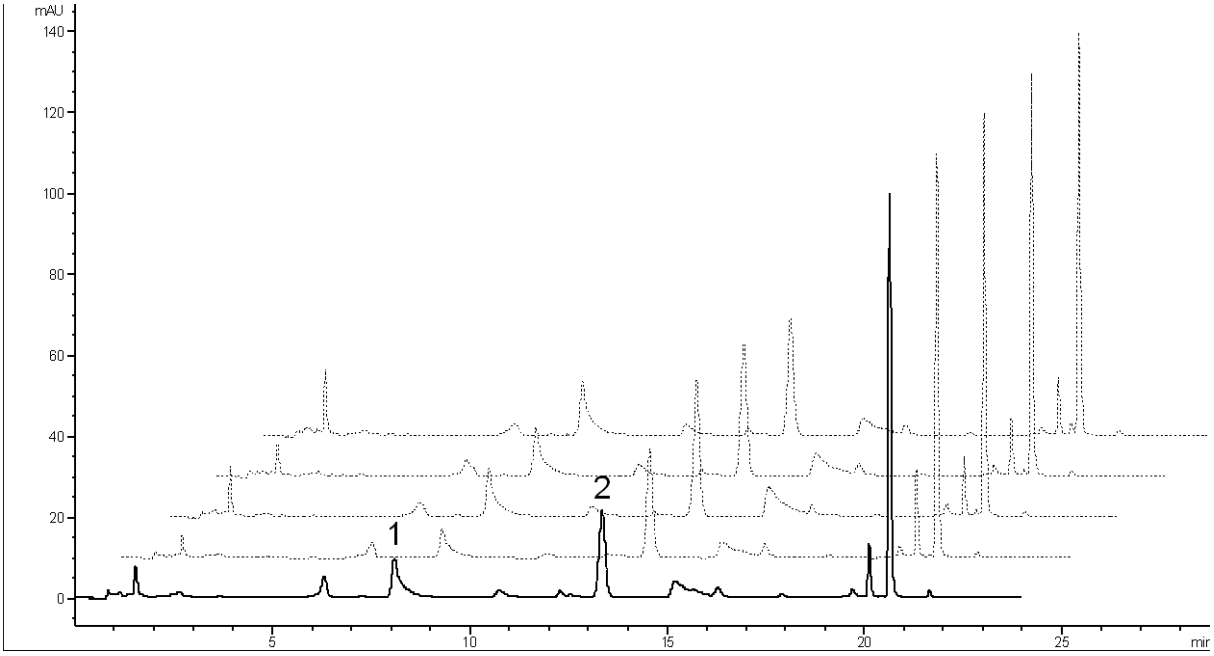

Fig. 50: HPLC chromatogram of the methanolic extracts from the Control at 340 nm. 1: Apigenin-7-*O*-glucoside, 2: Apigenin

3.6.3. LC-MS analysis and identification

Under the described chromatographic conditions, the retention times for apigenin-7-*O*-glucoside and apigenin were 7.73 min (Fig. 51 A) and 14.53 min (Fig. 52 A)

respectively; the total run time was 30 min. Using the ESI negative full-scan mode between 50 to 2000 m/z, major mass spectral ion peaks were observed corresponding to apigenin-7-*O*-glucoside [m/z 431.31 $(M-H)^-$] (Fig. 51 C) and apigenin [m/z 269.15 $(M-H)^-$] (Fig. 52 C).

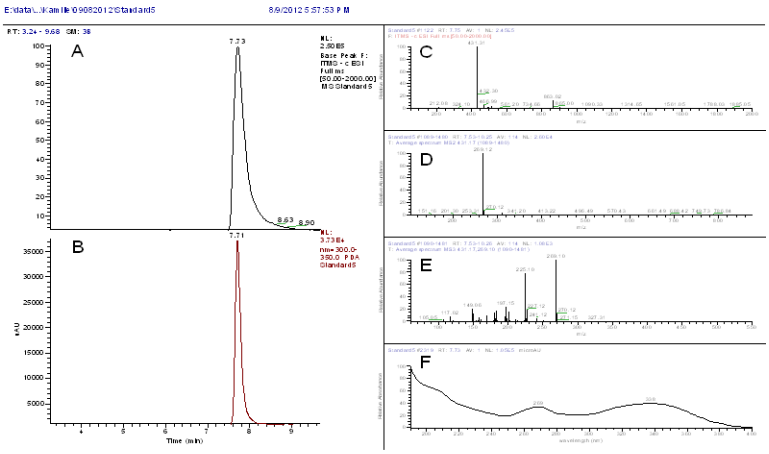

Fig. 51: A-B: LC/MS chromatogram of standard apigenin-7-*O*-glucoside. A: base peak chromatogram ESI negative ion mode (50-2000 m/z), B: UV-chromatogram (350 nm); C-E: Mass spectra of apigenin-7-*O*-glucoside (200-5000 m/z), C: ESI-MS negative mode, D: MS^2, E: MS^3, F: Absorption spectrum of apigenin-7-*O*-glucoside (200-400 nm).

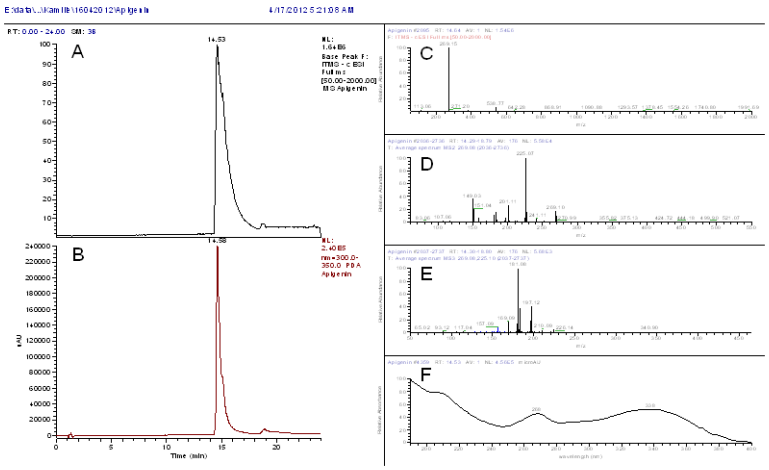

Fig. 52: A-B: LC/MS chromatogram of standard apigenin. A: base peak chromatogram ESI negative ion mode (50-2000 m/z), B: UV-chromatogram (350 nm); C-E: Mass spectra of apigenin (200-5000 m/z), C: ESI-MS negative mode, D: MS^2, E: MS^3, F: Absorption spectrum of apigenin (200-400 nm).

Apigenin-7-*O*-glucoside and apigenin were identified in all chromatograms by comparing retention times (T_R), UV and MS data with those of the reference standards. An example LC/MS chromatogram, UV-chromatogram and ion chromatogram in negative mode of the extract of *Matricaria recutita* (L.) treated with *Stenotrophomonas subrutilus* Wb2n-11 are shown in Fig. 53.

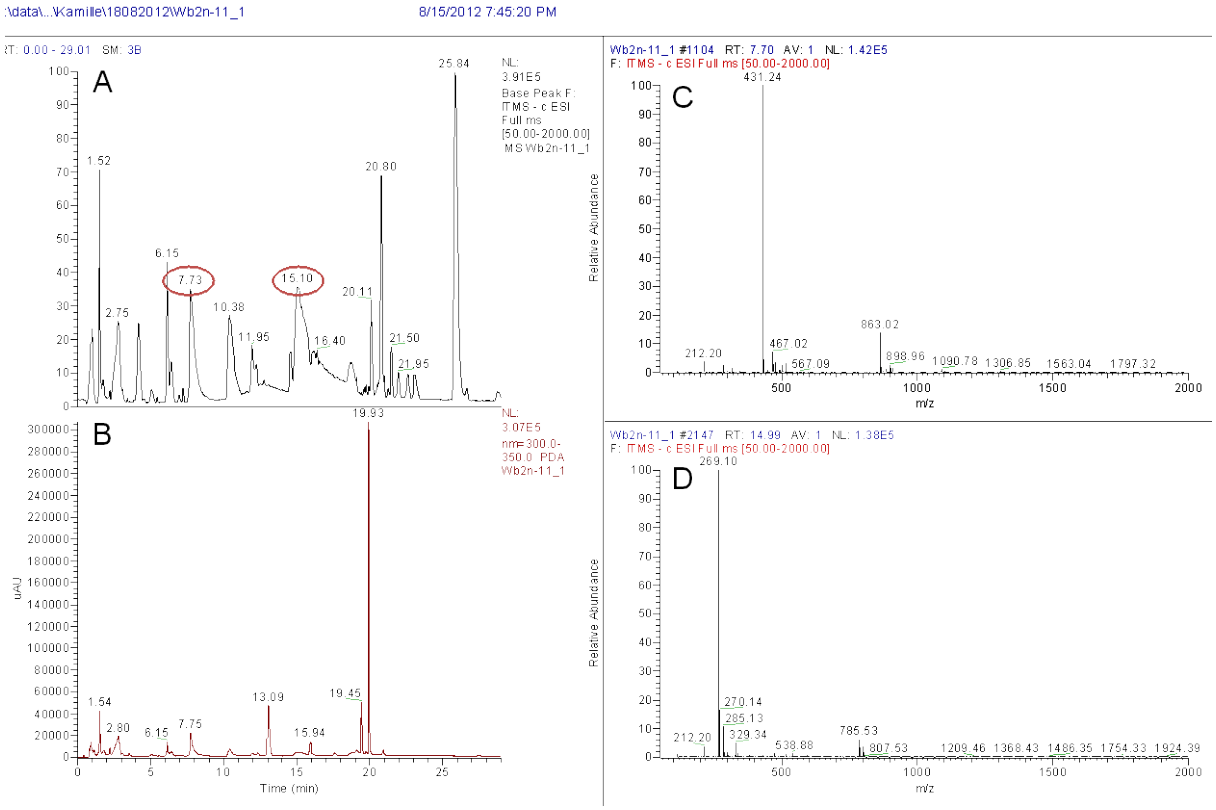

Fig. 53: A: LC/MS chromatogram of one sample (Wb2n-11_1). Peaks of apigenin7-*O*-glucoside and apigenin are marked red. B: UV-chromatogram (350 nm). C: Mass spectra of apigenin7-*O*-glucoside and apigenin (200-5000 m/z).

3.6.4. Quantification of apigenin-7-*O*-glucoside and apigenin

For quantification of apigenin-7-*O*-glucoside and apigenin, calibration curves were obtained by the external standard method. Therefore, eight concentrations (8.515 ng, 17.031 ng, 34.062 ng, 68.125 ng and 136.25 ng 272.5 ng, 544.8 ng and 1090 ng of apigenin-7-*O*-glucoside in 1 µl methanol 80% and 4.609 ng, 9.218 ng, 18.437 ng, 36.875 ng, 73.75 ng, 147.5 ng, 295 ng and 590 ng of apigenin in 1 µl methanol 80%) were injected two times per level and measured at a wavelength of 340 nm. Chromatogram peak areas on 340 nm for apigenin-7-*O*-glusocide and apigenin were plotted against the known concentrations of the standard solutions to establish the calibration equations. A quadratic regression equation was calculated by the least squares method. The regression equation and correlation coefficient of each analytes are summarized in Table 13.

Table 13: Detection wavelength (λ), retention time (T_R) and regression equation of analytes

Compounds	λ (nm)	T_R (min)	Regression equation[1]	R^2
Apigenin-7-*O*-glucoside	340	7.82 ± 0.02426	$y = 434109+4116.59*x-0.789087*x^2$	0.9888
Apigenin	340	15.18 ± 0.109514	$y = 698511+11201.6*x+0.247327*x^2$	0.9988

[1] $y = ax^2+bx+c$; where x is concentration in ng/µl, and y is area under curve at the selected wavelength.
[2] AUC = area under curve.

Peaks of apigenin-7-*O*-glucoside and apigenin were assigned based on the retention time, UV spectra of the standard compound and HPLC-ESI-MS^n (n = up to 3). The two phenolic components apigenin-7-*O*-glucoside and apigenin were simultaneously determined by the proposed LC-MS method by means of external standard method using Xcalibur Quan Browser. Data of quantitative analyses are expressed as mean ± standard deviation and are listed in Table 14 and Table 15. Results showed that the percentages of apigenin-7-*O*-glucoside and apigenin differed significantly between the different treatments (Fig. 54 and Fig. 55). For apigenin-7-*O*-glucoside the highest content could be observed for the treatments with the Gram-positive strains *Streptomyces subrutilus* Wb2n-11 (0.87% ± 0.16), *Bacillus subtilis* Co1-6 (1.06% ± 0.12), *Paenibacillus polymyxa* Mc5Re-14 (1.04% ± 0.09), followed by the control (0.86% ± 0.07). All three Gram-negative strains *Pseudomonas fluorescens* L13-6-12 (0.79% ± 0.09), *Stenotrophomonas rhizophila* P69 (0.78% ± 0.25) and *Serratia plymuthica* 3Re4-18 (0.82% ± 0.16) showed lower content of apigenin-7-*O*-glucoside. The same trend, however without statistical significance, could be observed for the content of apigenin. The treatments with Gram-positive strains *Bacillus subtilis* Co1-6 (0.95% ± 0.23), *Paenibacillus polymyxa* Mc5Re-14 (0.95% ± 0.18) showed the highest content of apigenin, followed by the control (0.94% ± 0.17). The Gram-negative strains *Pseudomonas fluorescens* L13-6-12 (0.83% ± 0.12), *Stenotrophomonas rhizophila* P69 (0.77% ± 0.20) and *Serratia plymuthica* 3Re4-18 (0.91% ± 0.16) showed a lower content compared to the control. In case of apigenin, the Gram-negative strain *Streptomyces subrutilus* Wb2n-11 (0.79% ± 1.40) did not show an alteration of the content of apigenin. The results state a clear indication that the Gram-positive strains *Bacillus subtilis* Co1-6, *Paenibacillus polymyxa* Mc5Re-14 had a higher impact on the content of apigenin-7-*O*-glucoside apigenin.

Table 14: Content (%) of apigenin-7-*O*-glucside in *Matricaria recutita* (L.) samples

Sample	Percentage (%)	SD
Wb2n-11 (n=10)	0.87	± 0.16 a
Co1-6 (n=10)	1.06	± 0.12 a
Mc5Re-14 (n=8)	1.04	± 0.09 a
L13-6-12 (n=7)	0.79	± 0.09 b
P69 (n=10)	0.78	± 0.25 b
3Re4-18 (n=10)	0.82	± 0.16 b
Control (n=10)	0.86	± 0.07 b

Statistically significant differences are marked with different letters. Level of significance is p ≤ 0.74.
n = number of samples

Table 15: Content (%) of apigenin in *Matricaria recutita* (L.) samples

Sample	Percentage (%)	SD
Wb2n-11 (n=10)	0.79	± 1.40 a
Co1-6 (n=10)	0.95	± 0.23 a
Mc5Re-14 (n=10)	0.95	± 0.18 a
L13-6-12 (n=10)	0.83	± 0.12 a
P69 (n=10)	0.77	± 0.20 a
3Re4-18 (n=10)	0.91	± 0.16 a
Control (n=10)	0.94	± 0.17 a

Level of significance is p ≤ 0.231.
n = number of samples

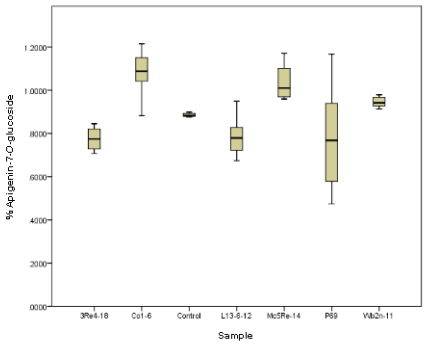

Fig. 54: Content (%) of apigenin-7-O-gucoside in the samples according to their treatment.

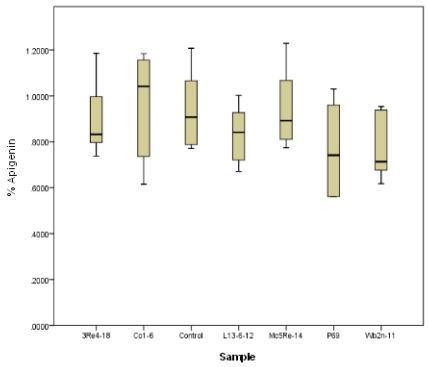

Fig. 55: Content (%) of apigenin in the samples according to their treatment.

For the identification of new peaks that arise from the microbial inoculants, all five spectra from one treatment were overlaid with the control and peaks showing differences were pictured (Fig. 56, Fig. 57, Fig. 58, Fig. 59, Fig. 60 and Fig. 61). Furthermore, the fragmentation patterns of new peaks were investigated (Table 16). However, the peaks could not been identified as flavonoid compounds.

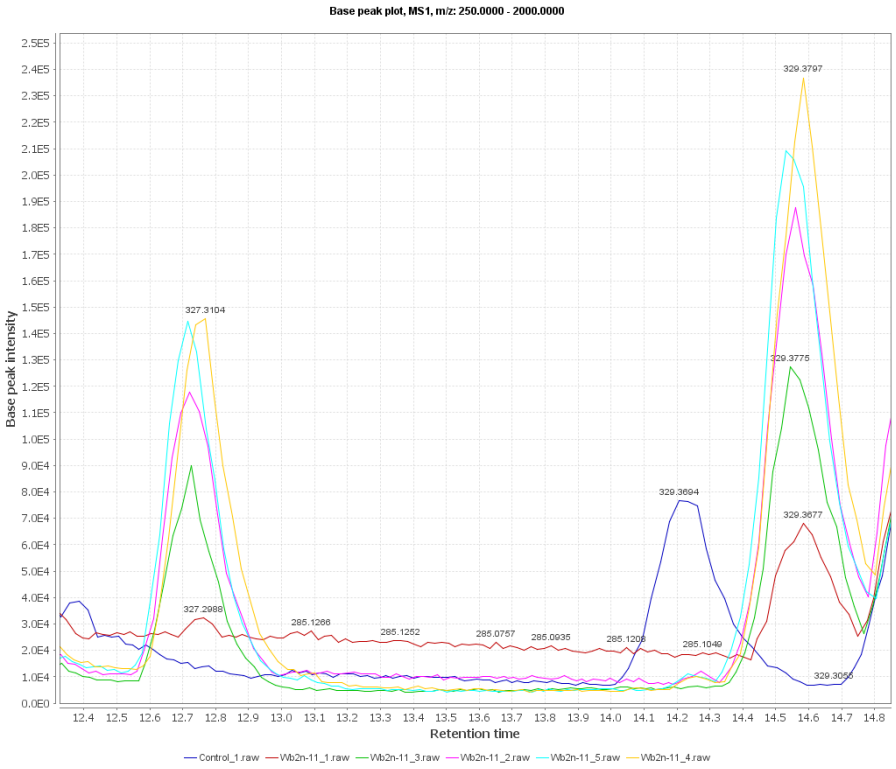

Fig. 56: Chromatogram of the treatment with *Streptomyces subrutilus* Wb2n-11 in comparison to the control.

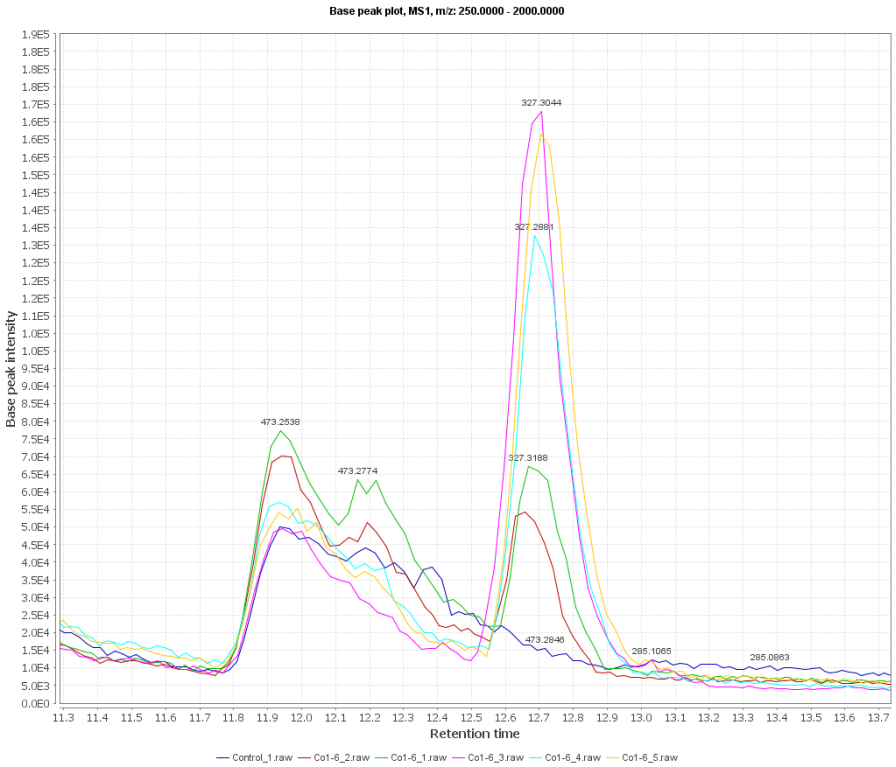

Fig. 57: Chromatograms from the treatment with *Bacillus subtilis* Co1-6 in comparison to the control.

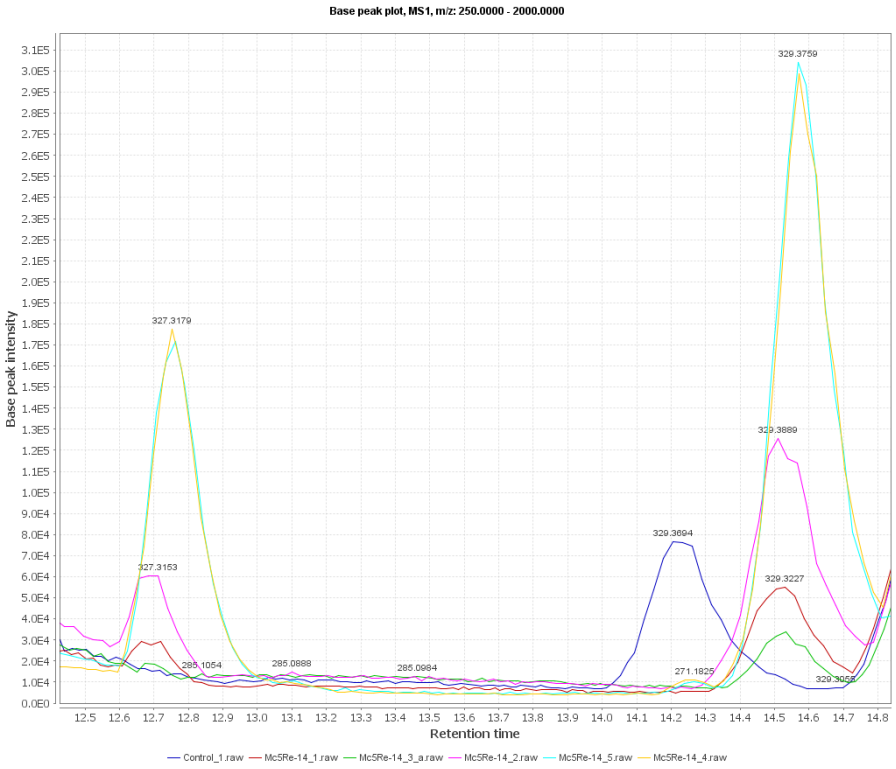

Fig. 58: Chromatograms from the treatment with *Paenibacillus polymyxa* Mc5Re-14 in comparison to the control.

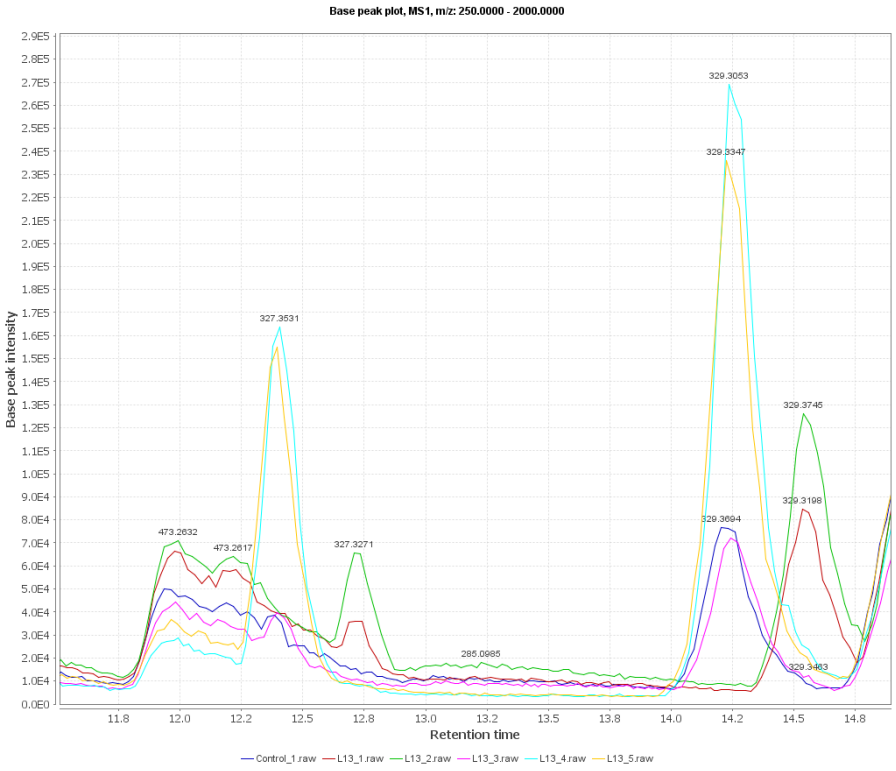

Fig. 59: Chromatograms from the treatment with *Pseudomonas fluorescens* L13-6-12 in comparison to the control.

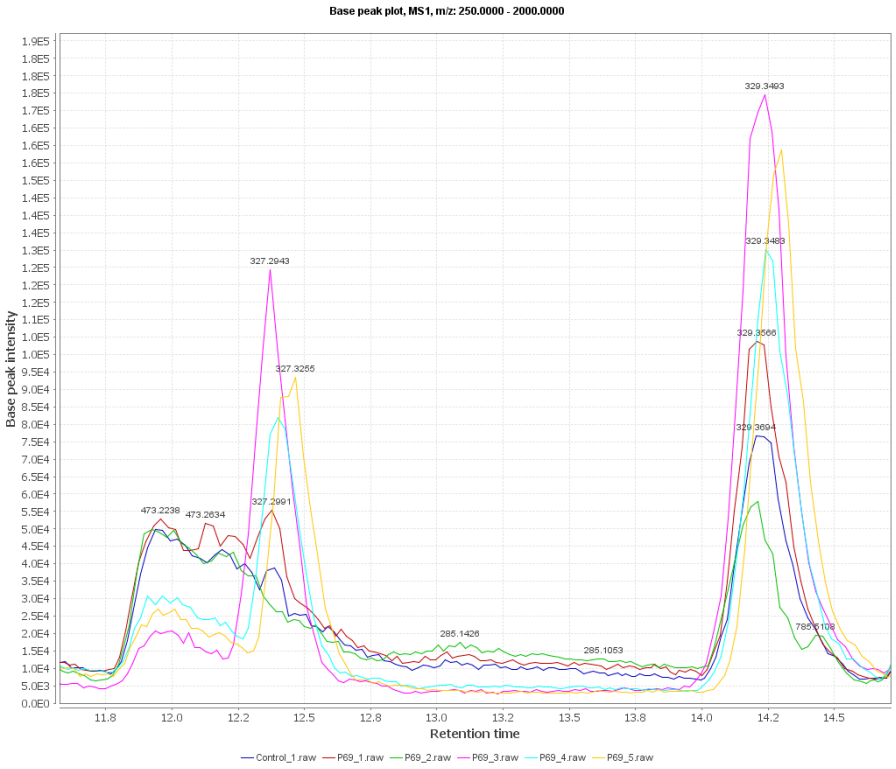

Fig. 60: Chromatograms from the treatment with *Stenotrophomonas rhizophila* P69 in comparison to the control.

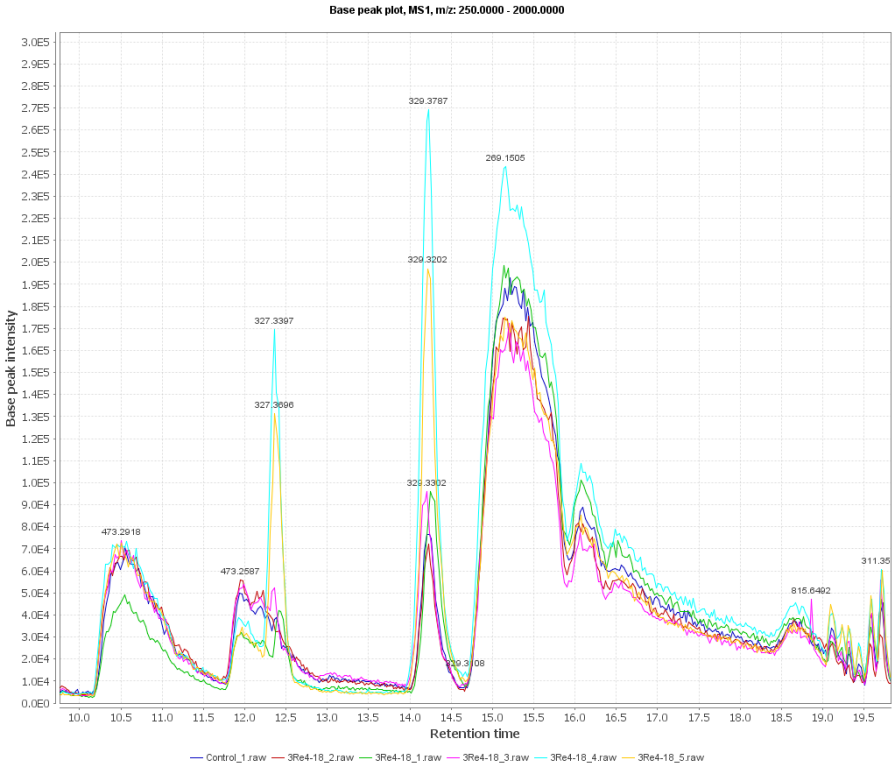

Fig. 61: Chromatograms of the treatment with *Serratia plymuthica* 3Re4-18 in comparison to the control.

Table 16: Fragmentation patterns of new peaks

T_R (min)	$[M+H]^+$ (*m/z*)	MS^2	MS^3	MS^4	Supp. MW	Supposed ID
12.74	327	229	211	183, 167, 193	328	n.i.
14.58	329	229, 211	211, 209	183, 167, 193	330	n.i.

n.i. = not identified

4. Discussion

Biological control plays an important role in sustainable agriculture as an alternative to the use of chemical pesticides. Within this work, the plant-growth promoting effect of six antagonistic bacterial strains on *Matricaria recutita* (L.) at a field site in Egypt was demonstrated. As risk assessment represents an important part of the evaluation of potential BCAs, the influence of the introduced strains on the native bacterial community inhabiting the soil was investigated by using cultivation-independent approaches. Furthermore, the effect of biological control agents on the flavonoid production of plants was examined by several analytical techniques.

4.1. Composition of the microbial communities of *Matricaria recutita* (L.)

All SSCP patterns obtained with universal and group-specific primers revealed high similarity of microbial community composition and were strongly related to the sampling times, showing about 10% similarity for rhizosphere and 3% to 40% for endorhiza samples. In both sampling times, the bacterial abundances did not differ between the treatments and the control.

The rhizosphere of the young chamomile plant was shown to be colonized mainly by *Bacillus sp. and Pseudomonas sp.* The high abundance of *Bacillus* species in the field soil at Sekem farms had been already described by Köberl et al. (2011). Pseudomonads represent important members of the rhizosphere microbial community due to their aggressive colonization (Scherwinski et al., 2006). Their plant growth promoting ability was described in several studies (Bloemberg & Lugtenberg, 2001; Weller, 2007). Moreover, bands corresponded to the genera *Serratia*, *Flavobacterium*, *Klebsiella* and *Pantoea*. The species *Pantoea dispersa* was already described as biocontrol agent of sugar cane leaf scald disease (Zangh & Birch, 1997). Furthermore, *Klebsiella pneumoniae* was identified, which is a commensal bacterium that colonizes the skin and mucosa surfaces (French et al., 1996). However, one band showed the identification of *Serratia marcescens*, an opportunistic pathogen of humans (Colombo et al., 2011). As described by Berg et al., (2005), the rhizosphere represents a natural reservoir of opportunistic pathogens due to a high content of nutrients, especially enhancing bacteria with a strong

antagonistic ability. Generally, the species composition differed slightly between the two sampling times. However, due to the limited number of identified strains, these results should be interpreted carefully. The SSCP analysis showed that there was no clear influence by the bacterial inoculants on the diversity of the naturally occurring bacterial populations in the rhizosphere of *Matricaria recutita* (L.).

4.2. Deeper insights into the microbial community structure in the rhizosphere of *Matricaria recutita* (L.)

Next-Generation sequencing allows a deeper insight into microbial community composition and therefore answers to the following questions can be provided: (i) how are microbial communities composed on different taxonomic levels?; (ii) how does the structure of communities look like between different samples?; (iii) how communities change across treatments?; (iv) what are the benefits and limitations of the pyrosequencing method comparable to a conventional one? To address these questions, samples from different treatments with bacterial inoculants were investigated and compared to one another. At first, the pyrosequencing approach showed similar patterns of bacterial diversity between the different treatments, whereas *Proteobacteria*, *Actinobacteria*, *Acidobacteria*, *Chloroflexi*, *Verrucomicrobia*, *Bacteroidetes*, *Planctomycetes*, *Gemmatimonadetes* and *Firmicutes* represented the most abundant phyla in all analysed samples (>1% of all sequences). Janssen (2006) already described members of these identified phyla as the most abundant soil bacteria. The phylum *Verrucomicrobia* was only present in the sample from the treatment with *Stenotrophomonas rhizophila* P69 (= DSM14405^T). In other *ad planta* studies, this strain was found to have an indirect positive interaction with their host plants by altering fungal communities (Schmidt et al., 2012). When bacteria were analysed at the genus level, the relative abundances of different genera belonging to phyla *Proteobacteria*, *Bacteroidetes* and *Actinobacteria* varied among the samples under different treatments. These results showed that it is of crucial importance to be aware of using the appropriate levels of taxonomy for different investigations. Therefore, this study suggests that for the detection of differences within microbial communities deriving from bacterial inoculants the use of genus or even lower levels of taxonomy yield the greatest benefits.

Unlike alpha diversity measurements, such as species richness and rarefaction curves, beta diversity measures the degree of similarity, e.g. phylogenetic relatedness between pairs of communities (Caporaso et al., 2010). Therefore, phylogenetic beta diversity metrics were used to investigate the structure of communities between the samples. Principal coordinates analysis (PCoA) plots showed that samples differed according to the treatments. Despite the SSCP results, pyrosequencing results suggest that the introduction of antagonistic bacterial strains leads to changes in the native bacterial community structure. Further, to describe the composition of microbial communities, their diversity and how communities may change across treatments, a network analysis of co-occurrence patterns helps to elucidate a structure of complex microbial communities (Barberán et al., 2012). Fig. 35 gives an overview of how such a network is composed and which taxa are shared between different samples. However, further analysis to species level will provide more detailed information about the co-occurrence and interaction of microbial communities.

Comparing the two methods, SSCP and pyrosequencing, each has its own benefits and limitations. SSCP represents a suitable technique for the analysis of multiple, replicated samples due to lower costs and automation of electrophoresis. However, detection limits of this technique prevent the coverage of the overall microbial diversity within one habitat, e.g. the rhizosphere. Pyrosequencing is a high-throughput parallel DNA sequencing technique that has revolutionised microbial detection (Edwards et al., 2006; Hudson, 2008; Roesch et al., 2007) due to its greater sample coverage and the detection of low abundant and rare species (Hudson, 2008). However, due to higher costs and the generation of a large amount of data, replication is more difficult to achieve. Within this experiment, the results show that pyrosequencing is an attractive alternative to SSCP analysis for finding the needles in the haystack (Dohrmann et al., 2012).

4.3. Abundances of bacterial communities in the rhizosphere of *Matricaria recutita* (L.)

To get a quantitative insight into the microbial communities in the rhizosphere, a real time PCR was performed. Total bacteria (up to 7.45 $\log_{10}$ copies per g rhizosphere for the treatment with *Streptomyces subrutilus* Wb2n-11) as well as *Firmicutes* (up to

7.54 $\log_{10}$ copies per g rhizosphere for the treatment with *Streptomyces subrutilus* Wb2n-11) resulted in a high abundance in the rhizosphere. The phenomenon that the number of microorganisms in the rhizosphere is enhanced as a result of exudation of compounds by the root, was described as the rhizosphere effect by Lynch (1990) and Sørensen (1997). However, no clear influence on the abundance of microorganisms by bacterial inoculants could be detected even though, results give a hint that Gram-positive bacteria are more dominant in the rhizosphere than introduced Gram-negative strains. The high abundance of Gram-positive bacteria in bulk soil was already described by (Smalla et al., 2001).

4.4. Colonization pattern of *Serratia plymuthica* 3Re4-18 in the root system of *Matricaria recutita* (L.)

As effective root colonization is a major factor for successful biocontrol approaches (Lugtenberg & Kamilova, 2009), the colonization pattern of *Serratia plymuthica* 3Re4-18 as a model bacterium for the colonization of chamomile roots was investigated. For this experiment the vector pME6031-DsRed2 was used, which is suitable for the monitoring of rhizosphere gram-negative bacteria (Zachow, 2010). *Serratia plymuthica* 3Re4-18 was able to colonize the roots of chamomile. Bacterial cells formed a dense network on the root epidermis colonizing the rhizoplane. Furthermore, single cells were arranged in clouds. In contrast to Zachow et al. (2010), no endophytic life style was observed.

4.5. Influence of biological control agents on the secondary metabolism of *Matricaria recutita* (L.)

To investigate the influence of the bacterial inoculums on the secondary metabolism of chamomile plants, apigenin-7-*O*-glucoside and apigenin were quantified, as they represent the major flavonoids of chamomile florets (Srivastava & Gupta, 2009; Kato et al., 2008). However, previous studies have isolated and identified the presence of both mono- and di- acetylated apigenin-7-*O*-glucoside, which are known to undergo rapid ester hydrolysis leading to the formation of apigenin-7-*O*-glucoside (
et al., 2004; Redaelli et al., 1981). Moreover, apigenin-7-*O*-glucoside is highly susceptible for the hydrolysis to its corresponding aglycone in presence of acid or hydrolytic enzymes. As a result, the formation or degradation of apigenin-7-*O*-glucoside leads to a falsification of quantification. The degradation products formed

are dependent on the extraction and storage conditions

.,

2004). Therefore, chamomile flowers were dried at a low temperature of 40°C, as this method was reported as the most effective one (Harbourne et al., 2009). Extraction of chamomile flowers was carried out with an accelerated solvent extractor using pure methanol as extraction solvent. This technique combines elevated temperatures and pressures greatly decreasing the time of extraction and therefore represents an alternative method for the extraction of temperature-sensitive compounds (Richter et al. 1997). As a minimal presence of acid in the mobile phase leads to the hydrolysis of acetyl derivates, a suitable mobile phase without the addition of acid had to be developed. A mobile phase for the assessment of apigenin-7-*O*-glucoside and apigenin in different chamomile flowers was already described by Srivastava et al. (2010). The developed HPLC system with a binary mobile phase consisting of acetonitrile and water resulted in a good separation within a relatively short time. For identification and quantification of apigenin-7-*O*-glucoside and apigenin, the same conditions were used. Quantification resulted in a statistically higher content of apigenin-7-*O*-glucoside for the treatments with the two Gram-positive strains *Bacillus subtilis* Co1-6 and *Paenibacillus polymyxa* 3Re4-18 compared to the treatments with Gram-positive strains. *Streptomyces subrutilus* Wb2n-11 showed a slightly higher content compared to the control. The same trend, however, without statistical significance, was observed for the content of apigenin. Treatments with *Bacillus subtilis* Co1-6 and *Paenibacillus polymyxa* 3Re4-18 showed higher contents compared to the other treatments and the control. The results suggest that particularly the two Gram-positive strains *Bacillus subtilis* Co-6 and *Paenibacillus polymyxa* 3Re4-18 have an influence on the production of secondary metabolites of *Matricaria recutita* (L.). Moreover, new substances could arise as a respond to microbial inoculants. However, only very few studies have considered such effects. Schmidt et al., 1994 and Zuanazzi et al., 1998 reported that the concentrations of flavonoids increased significantly in the presence of compatible rhizobial strains. Furthermore, a study investigating the induction of plant-growth promoting bacteria on the phenolic compounds in *Pisum sativum* (Singh et al., 2002) under pathogenic stress, described an enhancement of these compounds. Furthermore, (Orhan et al., 2006) reported that the plant nutrient elements (PNE) content of leaves were elevated by applying several *Bacillus* strains.

One possible explanation for the elevated production of flavonoids could be the mechanism of induced systemic resistance (IRS). ISR was first described by Van Peer et al. (1991) and by Wei et al. (1991), which confers the plant as an enhanced defence against pathogenic microorganisms. However, ISR can also be induced by various non-pathogenic microorganisms that may activate inducible defense mechanisms in the plant in a similar way to pathogenic microorganisms (Loon et al., 2007). Activation of defence mechanisms by plants suggests that even a beneficial rhizobacterium may be recognized as a potential threat, leading to the production of resistance compounds. Over the past decade, numerous of bacterial traits operative in triggering ISR have been identified, including flagella, cell envelope components such as lipopolysaccharides, and secreted metabolites like siderophores, cyclic lipopeptides, volatiles, antibiotics, phenolic compounds, and quorum sensing molecules (Vleesschauwer and Höfte, 2009). Several studies addressed the reaction of plants to rhizobacteria at the transcriptional level by analysing different gene expressions. Ongena et al. (2005) describe the upregulation and downreagulation of all genes in cucumber and tomato plants in response to root colonization by *Bacillus subtilis* M4. Analysis of the reaction of tomato to the ISR-eliciting strain *Serratia liquefaciens* MG1 revealed enhanced expression of 12 genes, whereas several of those genes were involved in oxidative stress, ethylene signalling, or metabolism (Shuhegger et al. 2006). Similarly, inoculation of lettuce plants with cytokinin-producing *Bacillus subtilis* was shown to have a beneficial effect on plant growth under moderate drought stress and leads to accumulation of this hormone in the plant tissues and to an increased biomass (Arkhipova et al., 2007). Likewise, the impact of *Paenibacillus polymyxa* on plant growth is strong through the production of cytokinin and auxin (Lal & Tabacchioni, 2009). The best-known Gram-positive ISR-activating species belongs to the genera *Bacillus* (Kloepper et al., 2004) and *Streptomyces* (Lehr et al., 2008). A possible model for the nonpathogenic rhizobacteria-mediated ISR signaling pathway is depicted in Fig. 56.

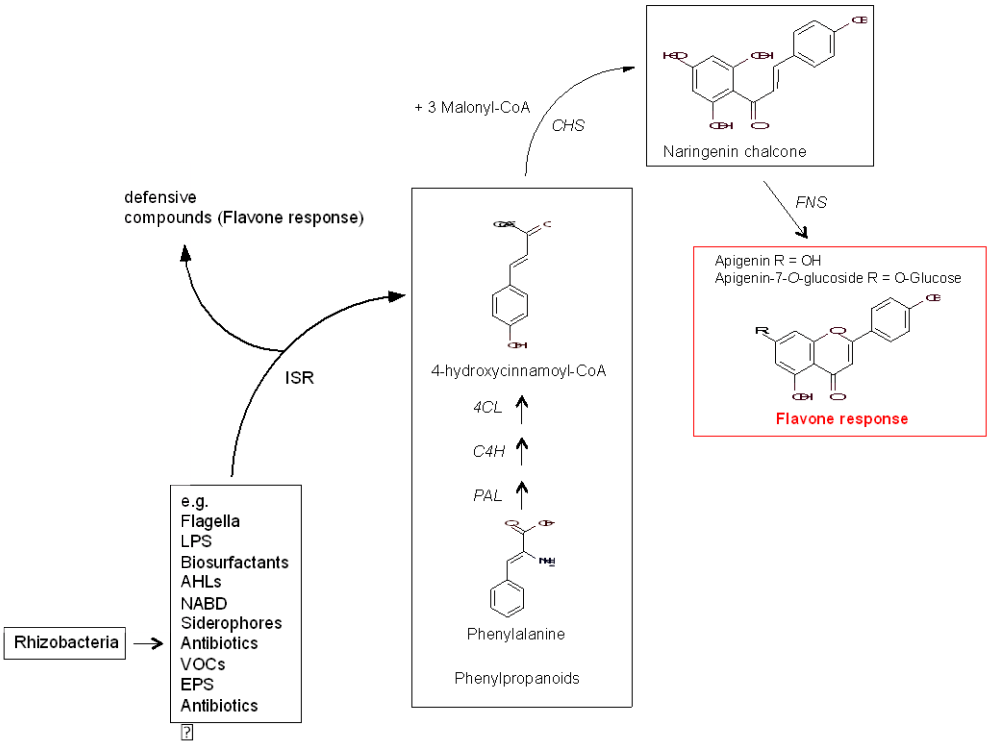

Fig. 62: Proposed model for the nonpathogenic rhizobacteria-mediated ISR signaling pathway. The production of several bacterial traits by rhizobacteria trigger ISR, resulting in the enrichment of defensive compounds, e.g. Flavones through the phenylpropanoid biosynthesis. The enzymes catalysing some key reactions are indicated by the following abbreviations: PAL, phenylalanine ammonia-lyase; C4H, cinnamate-4-hydroxylase; 4CL, 4-coumaroyl:CoA-ligase; CHS, chalcone synthase; FNS, flavone synthase.

5. Conclusions

Within this study, the influence of the BCAs on the native microbial community structure of *Matricaria recutita* (L.) as well as on the production of flavonoids was successfully investigated. While SSCP analysis did not show any influence of the bacterial inoculants, a pyrosequencing resulted in differences between the different treatments. The better understanding of the microbial community composition of the target habitat as well as the interactions and effects of BCAs will lead to more consistent effects of BCAs in the field and to overcome this main hurdle for commercialisation. However, to obtain definite information it is of essential importance to include independent replicates in such studies, as in SSCP analyses. The two Gram-positive strains *Bacillus subtilis* Co1-6 and *Paenibacillus polymyxa* Mc5Re-14 showed an increase in the flavonoid production of the plant. In future studies the analysis of expressions patterns of different genes belonging to the phenylpropanoidbiosynthesis pathway in response to bacterial inoculants should be implemented. For structure elucidation NMR analyses of unknown compounds should be integrated. Moreover, additional field experiments with the same conditions are planned in order to evaluate the results obtained from this first field experiment.

References

Abdoul-Latif, F.M., Nabil, M. Edou, P., Ali, A.A., Djama, S.O., Obamé, L.C., Bassolé, I. & Dicko H.M. (2011). Antimicrobial and antioxidant activities of essential oil and methanol extract of Matricaria chamomilla L. from Djibouti. *Journal of Medicinal Plants Research, 5*(9),1512-1517.

Alstrom, S. (2001). Characteristics of Bacteria from Oilseed Rape in Relation to their Biocontrol Activity against Verticillium dahliae. *Journal of Phytopathology*, *149*(2), 57–64.

Altschul, S. F., Madden, T. L., Schäffer, A., Zhang, J., Zhang, Z., Miller, W., & Lipman, D. J. (1997). Gapped BLAST and PSI-BLAST: a new generation of protein database search programs. *Nucleic acids research*, *25*(17), 3389–402.

Arkhipova, T.N., Prinsen, E., Veselov, S.U., Martinenko, E.V., Melentiev, A.I., and Kudoyarova, G.R. (2007). Cytokinin producing bacteria enhance plant growth in drying soil. *Plant Soil, 292*, 305–315.

Bais, H. P., Weir, T. L., Perry, L. G., Gilroy, S., & Vivanco, J. M. (2006). The role of root exudates in rhizosphere interactions with plants and other organisms. *Annual review of plant biology*, *57*, 233–66.

Bakker, P. a H. M., Pieterse, C. M. J., & van Loon, L. C. (2007). Induced Systemic Resistance by Fluorescent Pseudomonas spp. *Phytopathology*, *97*(2), 239–43.

Barberán, A., Bates, S. T., Casamayor, E. O., & Fierer, N. (2012). Using network analysis to explore co-occurrence patterns in soil microbial communities. *The ISME journal*, *6*(2), 343–51.

Bassam, B. J., Caetano-Anollés, G., & Gresshoff, P. M. (1991). Fast and sensitive silver staining of DNA in polyacrylamide gels. *Analytical biochemistry*, *196*(1), 80–3.

Berg, G, Fritze, A., Roskot, N., & Smalla, K. (2001). Evaluation of potential biocontrol rhizobacteria from different host plants of Verticillium dahliae Kleb. *Journal of Applied Microbiology*, 91(6), 963–971.

Berg, G. (2009). Plant-microbe interactions promoting plant growth and health: perspectives for controlled use of microorganisms in agriculture. *Applied microbiology and biotechnology*, *84*(1), 11–8.

Berg, G., Eberl, L., & Hartmann, A. (2005). Minireview The rhizosphere as a reservoir for opportunistic human pathogenic bacteria. *Environmental Micorbiology*, *7*(11), 1673–1685.

Blackwood, C. B., Oaks, A., & Buyer, J. S. (2005). Phylum- and class-specific PCR primers for general microbial community analysis. *Applied and environmental microbiology*, *71*(10), 6193–8.

Blackwood, C. B.,Adam,O., and Buyer, J. S. (2005). Phylum- and class- specific PCR primers for general microbial community analysis, *Applied and Environmental Microbiology, 71*, 6193–6198.

Bloemberg, G. V., & Lugtenberg, B. J. (2001). Molecular basis of plant growth promotion and biocontrol by rhizobacteria. *Current opinion in plant biology*, *4*(4), 343–50.

Caporaso, J. G., Kuczynski, J., Stombaugh, J., Bittinger, K., Bushman, F. D., Costello, E. K., Fierer, N. (2010). QIIME allows analysis of high-throughput community sequencing data. *Nature methods*, *7*(5), 335–6.

Caporaso, J. G., Lauber, C. L., Walters, W. A., Berg-lyons, D., Lozupone, C. A., Turnbaugh, P. J., Fierer, N. (2010). Global patterns of 16S rRNA diversity at a depth of millions of sequences per sample. *Proceedings of the National Academy of Science of the United States of America, 108*(1), 4516-22.

Chao, A., & Bunge, J. (2002). Estimating the Number of Species in a Stochastic Abundance Model. *Biometrics*, *58*(3), 531–539.

Chin-A-Woeng, T. F., Bloemberg, G. V., Mulders, I. H., Dekkers, L. C., & Lugtenberg, B. J. (2000). Root colonization by phenazine-1-carboxamide-producing bacterium Pseudomonas chlororaphis PCL1391 is essential for biocontrol of tomato foot and root rot. *Molecular plant-microbe interactions□: MPMI*, *13*(12), 1340–5.

Cole, J. R., Chai, B., Farris, R. J., Wang, Q., Kulam-Syed-Mohideen, a S., McGarrell, D. M., Bandela, a M. (2007). The ribosomal database project (RDP-II): introducing myRDP space and quality controlled public data. *Nucleic acids research*, *35*, 169–72.

Cole, J. R., Wang, Q., Cardenas, E., Fish, J., Chai, B., Farris, R. J., Kulam-Syed-Mohideen, a S. (2009). The Ribosomal Database Project: improved alignments and new tools for rRNA analysis. *Nucleic acids research*, *37*(Database issue).

Colombo, I., Fedrigo, G. V., Campoy, E. M., & Venanzio, G. D. (2011). Serratia marcescens Is Able to Survive and Proliferate in Autophagic-Like Vacuoles inside Non-Phagocytic Cells. *PLoS One, 6*(8).

Compant, S., Duffy, B., Nowak, J., & Cle, C. (2005). Use of Plant Growth-Promoting Bacteria for Biocontrol of Plant Diseases□: Principles , Mechanisms of Action , and Future Prospects MINIREVIEW Use of Plant Growth-Promoting Bacteria for Biocontrol of Plant Diseases□: Principles , Mechanisms of Action , and future prospects. *Applied and environmental microbiology, 71*(9), 4951-9.

Dobbelaere, S., Vanderleyden, J., & Okon, Y. (2003). Plant Growth-Promoting Effects of Diazotrophs in the Rhizosphere. *Critical Reviews in Plant Sciences*, *22*(2), 107–149.

Dohrmann, A. B., Küting, M, Jünemann, S., Jaenicke, S., Schlüter, A. and Tebbe, C. C. (2012). Importance of rare taxa for bacterial diversity in the rhizosphere of Bt- and conventional maize varieties, *The ISME journal*, In press.

Edgar, R. C. (2010). Search and clustering orders of magnitude faster than BLAST. *Bioinformatics (Oxford, England)*, *26*(19), 2460–1.

Edwards, R. A., Rodriguez-brito, B., Wegley, L., Haynes, M., Breitbart, M., Peterson, D. M., Saar, M. O. (2006). Using pyrosequencing to shed light on deep mine microbial ecology, *BMC Genomics, 13*, 1–13.

Emmert, E. a, & Handelsman, J. (1999). Biocontrol of plant disease: a (gram-) positive perspective. *FEMS microbiology letters*, *171*(1), 1–9.

Falcone Ferreyra, M. L., Rius, S. P., & Casati, P. (2012). Flavonoids: biosynthesis, biological functions, and biotechnological applications. *Frontiers in plant science*, *3*, 222.

Faure, D., Vereecke, D., & Leveau, J. H. J. (2008). Molecular communication in the rhizosphere. *Plant and Soil*, *321*(1-2), 279–303.

Fernández-Ruvalcaba, M., Peña-Chora, G., Romo-Martínez, A., Hernández-Velázquez, V., de la Parra, A. B., & De La Rosa, D. P. (2010). Evaluation of Bacillus thuringiensis pathogenicity for a strain of the tick, Rhipicephalus microplus, resistant to chemical pesticides. *Journal of insect science*, *10*, 186.

Ferrer, J.-L., Austin, M. B., Stewart, C., & Noel, J. P. (2008). Structure and function of enzymes involved in the biosynthesis of phenylpropanoids. *Plant physiology and biochemistry : PPB / Société française de physiologie végétale*, *46*(3), 356–70.

Fischer, R., Budde, I., & Hain, R. (1997). Stilbene synthase gene expression causes changes in flower colour and male sterility in tobacco. *The Plant Journal*, *11*(3), 489–498.

Francis, I., Holsters, M., & Vereecke, D. (2010). Minireview The Gram-positive side of plant – microbe interactions. *Environmental microbiology, 12*(1), 1–12.

Fravel, D. R. (2005). Commercialization and implementation of biocontrol. *Annual review of phytopathology*, *43*, 337–59.

French, G. L., Shannon, K. P., & Simmons, N. (1996). Hospital Outbreak of Klebsiella pneumoniae Resistant to Broad- Spectrum Cephalosporins and Beta-Lactam-Beta-Lactamase Inhibitor Combinations by Hyperproduction of SHV-5 Beta-Lactamase, *Journal of clinical microbiology, 34*(2), 358–363.

Fürnkranz, M., Adam, E., Müller, H., Grube, M., Huss, H., Winkler, J., & Berg, G. (2012). Promotion of growth, health and stress tolerance of Styrian oil pumpkins by bacterial endophytes. *European Journal of Plant Pathology*, *134*(3), 509–519.

Ganzera, M., Schneider, P., & Stuppner, H. (2006). Inhibitory effects of the essential oil of chamomile (Matricaria recutita L.) and its major constituents on human cytochrome P450 enzymes. *Life sciences*, *78*(8), 856–61.

Garcia, O., Saveanu, C., Cline, M., Fromont-Racine, M., Jacquier, A., Schwikowski, B., & Aittokallio, T. (2007). GOlorize: a Cytoscape plug-in for network visualization with Gene Ontology-based layout and coloring. *Bioinformatics*, *23*(3), 394–6.

Hagemann, M., Ribbeck-Busch, K., Klähn, S., Hasse, D., Steinbruch, R., & Berg, G. (2008). The plant-associated bacterium Stenotrophomonas rhizophila expresses a new enzyme for the synthesis of the compatible solute glucosylglycerol. *Journal of bacteriology*, *190*(17), 5898–906. doi:10.1128/JB.00643-08

Harbourne, N., Jacquier, J. C., O&rsquo, & Riordan, D. (2009). Optimisation of the extraction and processing conditions of chamomile (*Matricaria chamomilla* L.) for incorporation into a beverage. *Food Chemistry*, *115*(1), 15–19.

Hardoim, P. R., van Overbeek, L. S., & Elsas, J. D. V. (2008). Properties of bacterial endophytes and their proposed role in plant growth. *Trends in microbiology*, *16*(10), 463–71.

Hashidoko Y., Nakayama T., Homma Y., & Tahara S. (1999). Structure Elucidation of Xanthobaccin A, a New Antibiotic Produced from Stenotrophomonas sp. Strain SB-K88. *Tetrahedron Letters*, *40*(15), 4.

Hudson, M. E. (2008). Sequencing breakthroughs for genomic ecology and evolutionary biology. *Molecular ecology resources*, *8*(1), 3–17.

Insam, H., & Seewald, M. S. (2010). Volatile organic compounds (VOCs) in soils. *Biology and Fertility of Soils*, *46*(3), 199–213.

Janssen, P. H. (2006). Identifying the dominant soil bacterial taxa in libraries of 16S rRNA and 16S rRNA genes. *Applied Environmental Microbiology, 72*,1719–1728.

Jaleel, C. A., Manivannan, P., Sankar, B., Kishorekumar, A., Gopi, R., Somasundaram, R., & Panneerselvam, R. (2007). Pseudomonas fluorescens enhances biomass yield and ajmalicine production in Catharanthus roseus under water deficit stress. *Colloids and surfaces. B, Biointerfaces*, *60*(1), 7–11.

Janssen, P. H. (2006). Identifying the Dominant Soil Bacterial Taxa in Libraries of 16S rRNA and 16S rRNA Genes, *Applied and environmental microbiology, 72*(3), 1719–1728.

Jeandet, P., Douillet-Breuil, A.-C., Bessis, R., Debord, S., Sbaghi, M., Adrian, M. (2002). Phytoalexins from the Vitaceae: biosynthesis, phytoalexins gene expression in transgenic plants, antifungal activity and metabolism. *Journal of Agricultural and Food Chemistry, 50*(10), 2731–2741.

Kai, M., Effmert, U., Berg, G., & Piechulla, B. (2007). Volatiles of bacterial antagonists inhibit mycelial growth of the plant pathogen Rhizoctonia solani. *Archives of microbiology*, *187*(5), 351–60.

Kalbe, C., Marten, P., & Berg, G. (1996). Strains of the genus Serratia as beneficial rhizobacteria of oilseed rape with antifungal properties. *Microbiological Research*, *151*(4), 433–439.

Katajamaa, M., Miettinen, J., & Oresic, M. (2006). MZmine: toolbox for processing and visualization of mass spectrometry based molecular profile data. *Bioinformatics, 22*(5), 634–6.

Kilian, M., Steiner, U., Krebs, B., Junge, H., Schmiedeknecht, G., Hain, R. (2000). FZB24® Bacillus subtilis - mode of action of a microbial agent enhancing plant vitality. *Pflanzenschutz-Nachrichten Bayer, 53* (1), 72–93.

Kato, A., Minoshima, Y., Yamamoto, J., Adachi, I. Watson, A.A., & Robert J.N. (2008), Protective Effects of Dietary Chamomile Tea on Diabetic Complications, *Journal of Agricultural and Food Chemistry, 56*(17), 8206-8211.

Kloepper, J.W., Ryu, C. & Zhang, S., 2004. Induced Systemic Resistance and Promotion of Plant Growth by Bacillus spp., *Phytopathology, 94*(11),1259–1266.

Kloepper, S. (1981). Plant growth-promoting rhizobacteria and plant growth under gnotobiotic conditions. *Phytopathology, 71*, 642-644.

Köberl, M. (2010). Analyse von Arzneipflanzen-assoziierten Mikroorganismen: Biodiversität und antagonistisches Potenzial gegen bodenbürtige Phytopathogene. *Master thesis*, Graz University of Technology, Institute for Environmental Biotechnology, Austria.

Köberl, M., Müller, H., Ramadan, E.M., and Berg, G. (2011). Desert farming benefits from microbial potential in arid soils and promotes diversity and plant health. *PloS one*, *6*(9).

Lal, S. and Tabacchioni, S., 2009. Ecology and biotechnological potential of Paenibacillus polymyxa: a minireview. *Indian Journal of Microbiology, 49*(1), 2–10.

Lane, D.J. (1991). 16S/23S rRNA sequencing. In: E. Stackebrandt and M. Goodfellow (eds), Nucleic Acid Techniques in Bacterial Systematics. Wiley, New York. 115–175.

Lehr, N.A., Schrey, S.D., Hampp, R., and Tarkka, M.T. (2008) Root inoculation with a forest soil streptomycete leads to locally and systemically increased resistance against phytopathogens in Norway spruce. *New Phytologist, 177*(4), 965–976.

Lieber, A., Kiesel, B., & Babel, W. (2002). Microbial diversity analysis of soil by SSCP fingerprinting technique using TGGE Maxi System. 13. Borkheider Seminar zur Ökophysiologie des Wurzelraumes, 61–65. Teubner, Leipzig.

Loon, L.C. (2007). Plant responses to plant growth-promoting rhizobacteria. *European Journal of Plant Pathology*, *119*(3), 243–254.

Lugtenberg, B., & Kamilova, F. (2009). Plant-growth-promoting rhizobacteria. *Annual review of microbiology*, *63*, 541–56.

Lynch, J. M. (1990). Introduction: some consequences of microbial rhizosphere competence for plant and soil. The Rhizosphere, 1–10. Wiley & Sons, Chichester.

Mandal, S. M., Chakraborty, D., & Dey, S. (2010). Phenolic acids act as signaling molecules in plant-microbe symbioses. *Plant signaling & behavior*, *5*(4), 359–68.

McKay, D. L., & Blumberg, J. B. (2006). A review of the bioactivity and potential health benefits of chamomile tea (Matricaria recutita L.). *Phytotherapy research : PTR*, *20*(7), 519–30.

Merav Kamensky, M. O., Ilan Chet,Leonid Chernin,. (2003). Soil-borne strain IC14 of Serratia plymuthica with multiple mechanisms of antifungal activity provides biocontrol of Botrytis cinerea and Sclerotinia sclerotiorum diseases. *Soil Biology and Biochemistry*, *35*, 323–331.

Milling, A., Smalla, K., Maidl, F. X., Schloter M. and Munch, J.C. (2004). Effects of transgenic potatoes with an altered starch composition on the diversity of soil and rhizosphere bacteria and fungi. *Plant Soil, 266*, 23–39.

Mulinacci, N., Romani, A., Pinelli, P., Vincieri, F. F., & Prucher, D. (2000). Characterization of Matricaria recutita L. Flower Extracts by HPLC-MS and HPLC-DAD Analysis, *Chromatographia 51*(5), 301–307.

Müller, H., Westendorf, C., Leitner, E., Chernin, L., Riedel, K., Schmidt, S., Eberl, L. (2009). Quorum-sensing effects in the antagonistic rhizosphere bacterium Serratia plymuthica HRO-C48. *FEMS microbiology ecology*, *67*(3), 468–78.

Ongena, M., Duby, F., Jourdan, E., Beaudry, T., Jadin, V., Dommes, J. and Thonart, P. (2005). Bacillus subtilis M4 decreases plant susceptibility towards fungal pathogens by increasing host resistance associated with differential gene expression. *Applied Microbiology and Biotechnology, 67*(5), 692–698.

Opelt, K. and Berg, G. (2004). Diversity and antagonistic potential of bacteria associated with bryophytes from nutrient-poor habitats of the Baltic Sea Coast. *Applied and environmental microbiology*, *70*(11), 6569–79.

Opelt, K., Berg, C., Schönmann, S., Eberl, L., & Berg, G. (2007). High specificity but contrasting biodiversity of Sphagnum-associated bacterial and plant communities in bog ecosystems independent of the geographical region. *The ISME Journal,* 1,502-506.

Orhan, E., Esitken, A., Ercisli, S., Turan, M. and Sahin, F. (2006). Effects of plant growth promoting rhizobacteria (PGPR) on yield, growth and nutrient contents in organically growing raspberry. *Scientia Horticulturae*, *111*(1), 38–43.

Pirrung, M., Kennedy, R., Caporaso, J. G., Stombaugh, J., Wendel, D., & Knight, R. (2011). TopiaryExplorer: visualizing large phylogenetic trees with environmental metadata. *Bioinformatics*, *27*(21), 3067–9.

Podile, A. R. and Laxmi, V. D. V. (1998). Seed Bacterization with Bacillus subtilis AF 1 Increases Phenylalanine Ammonia-lyase and Reduces the Incidence of Fusarial Wilt in Pigeonpea. *Journal of Phytopathology*, *146*(5-6), 255–259.

Redaelli, C., Formentini, L., Santaniello, E., (1981). Reversed-phase high-performance liquid chromatography analysis of apigenin and its glucosides in flowers of Matricaria chamomilla and chamomile extracts. *Planta medica, 42*(7), 288-92.

Richter, B.E., Brian, A. ,Jones, J., Ezzell, L., Porter, N.L., Avdalovic, N., & Pohl, C. (1996). Accelerated Solvent Extraction: A Technique for Sample Preparatio n. *Analytical Chemistry*, *68*(6), 1033-1039.

Rigby, D., & Ca, D. (2001). Organic farming and the sustainability of agricultural systems. *Agricultural systems, 68*, 21–40.

Roesch, L. F. W., Fulthorpe, R. R., Riva, A., Casella, G., Hadwin, A. K. M., Kent, A. D., Daroub, S. H., et al. (2007). Pyrosequencing enumerates and contrasts soil microbial diversity. *The ISME journal*, *1*(4), 283–90.

Ryan, R. P., Monchy, S., Cardinale, M., Taghavi, S., Crossman, L., Avison, M. B., Berg, G., et al. (2009). The versatility and adaptation of bacteria from the genus Stenotrophomonas. *Nature reviews. Microbiology*, *7*(7), 514–25.

Ryu, C.-M., Farag, M. a, Hu, C.-H., Reddy, M. S., Wei, H.-X., Paré, P. W., & Kloepper, J. W. (2003). Bacterial volatiles promote growth in Arabidopsis. *Proceedings of the National Academy of Sciences of the United States of America*, *100*(8), 4927–32.

Sabaratnam, S., & Traquair, J. a. (2002). Formulation of a Streptomyces Biocontrol Agent for the Suppression of Rhizoctonia Damping-off in Tomato Transplants. *Biological Control*, *23*(3), 245–253.

Salamon, I. (1992). Effect of the Internal and External Factors on Yield and Qualitative-Quantitative Characteristics of Chamomile Essential Oil. *Acta Horticulturae, 749* 65-74.

Sarker, N. and Mahbub, K R. (2011). Bacillus thuringiensis: An Environment Friendly Microbial Control Agent. *Research Journal of Biological Sciences*, 6: 615-626.

Scherwinski, K., Grosch, R., & Berg, G. (2008). Effect of bacterial antagonists on lettuce: active biocontrol of Rhizoctonia solani and negligible, short-term effects on nontarget microorganisms. *FEMS microbiology ecology*, *64*(1), 106–16.

Scherwinski, K., Wolf, A., & Berg, G. (2006). Assessing the Risk of Biological Control Agents on the Indigenous Microbial Communities: Serratia plymuthica HRO-C48 and Streptomyces sp. HRO-71 as Model Bacteria. *BioControl*, *52*(1), 87–112.

Schijlen, E. G. W. M., Ric de Vos, C. H., van Tunen, A. J., & Bovy, A. G. (2004). Modification of flavonoid biosynthesis in crop plants. *Phytochemistry*, *65*(19), 2631–48.

Schmidt, C. S., Cardinale, M., Zachow, C., Müller, H., & Berg, G. (2012). Indirect, plant-specific plant growth promotion by *Stenotrophomonas rhizophila* DSM14405^T by altering fungal communities in the rhizosphere. *Plant and Soil*, In press.

Schmidt, P.E., Broughton, W.J., and Werner, D. (1994) Nod factors of Bradyrhizobium Japonicum and Rhizobium Sp NGR234 induce flavonoid accumulation in soybean root exudate. Mol Plant Microbe In 7: 384–390.

Schöller, C. E. G., Gürtler, H., Pedersen, R., Molin, S., & Wilkins, K. (2002). Volatile Metabolites from Actinomycetes. *Journal of Agricultural and Food Chemistry*, *50*(9), 2615–2621.

Schroth, M. N., & Hancock, J. G. (1982). Disease-suppressive soil and root-colonizing bacteria. *Science*, *216*(4553), 1376–81.

Schwieger, F., & Tebbe, C. C. (1998). A new approach to utilize PCR-single-strand-conformation polymorphism for 16S rRNA gene-based microbial community analysis. *Applied and environmental microbiology*, *64*(12), 4870–6.

Selim, S., Negrel, J., Wendehenne, D., Ochatt, S., Gianinazzi, S., & van Tuinen, D. (2010). Stimulation of defense reactions in Medicago truncatula by antagonistic lipopeptides from Paenibacillus sp. strain B2. *Applied and environmental microbiology*, *76*(22), 7420–8.

Shannon, C. E. (1963). The mathematical theory of communication. *M.D. computing : computers in medical practice*, *14*(4), 306–17.

Shannon, P., Markiel, A., Ozier, O., Baliga, N. S., Wang, J. T., Ramage, D., Amin, N., et al. (2003). Cytoscape: a software environment for integrated models of biomolecular interaction networks. *Genome research*, *13*(11), 2498–504.

Shaw, L. J., Morris, P., & Hooker, J. E. (2006). Perception and modification of plant flavonoid signals by rhizosphere microorganisms. *Environmental microbiology*, *8*(11), 1867–80.

Shuhegger, R., Ihring, A., Gantner, S., Bahnweg, G., Knappe, C., Vogg, G., Hutzler, P., Schmid, M., Van Breusegem, F., Eberl, L., Hartmann, A., & Langebartels, C. (2006). Induction of systemic resistance in tomato by N-acyl-L- homoserine lactone-producing rhizosphere bacteria. *Plant, Cell and Environment, 29*, 909–918.

Singh, U. P., Sarma, B. K., Singh, D. P., & Bahadur, A. (2002). Plant growth-promoting rhizobacteria-mediated induction of phenolics in pea (Pisum sativum) after infection with Erysiphe pisi. *Current microbiology*, *44*(6), 396–400.

Smalla, K, Wieland, G., Buchner, A., Zock, A., Parzy, J., Kaiser, S., & Roskot, N. (2001). Bulk and Rhizosphere Soil Bacterial Communities Studied by Denaturing Gradient Gel Electrophoresis: Plant -Dependent Enrichment and Seasonal Shifts Revealed, Applied and environmental microbiology *67*(10), 4742–4751.

Smalla, Kornelia, Sessitsch, A., & Hartmann, A. (2006). The rhizosphere: "soil compartment influenced by the root". *FEMS microbiology ecology*, *56*(2), 165.

Sokal, R., & Sneath, P.H.A. (1963). Principles of numerical taxonomy. Freeman, San Francisco.

Sørensen, J. (1997) The rhizosphere as a habitat for soil microorganisms. *Modern Soil Microbiology*, 21-45.

Sorenson, T. (1948). A method of establishing groups of equal amplitude in a plant based on similarity of species content and its applications to analysis of vegetation on Danish commons. *Biologiske Skrifter, 5*, 1–34.

Spaepen, S., Vanderleyden, J., & Remans, R. (2007). Indole-3-acetic acid in microbial and microorganism-plant signaling. *FEMS microbiology reviews*, *31*(4), 425–48.

Srivastava, J. K., & Gupta, S. (2009). Extraction, Characterization, Stability and Biological Activity of Flavonoids Isolated from Chamomile Flowers. *Molecular and cellular pharmacology*, *1*(3), 138.

Stafford, H. A. (1991). Flavonoid evolution: an enzymic approach. *Plant physiology*, *96*(3), 680–5.

Svehlikova V, Bennett RN, Mellon FA, Needs PW, Piacente S, Kroon PA, Bao Y. (2004). Isolation, identification and stability of acylated derivatives of apigenin 7-O-glucoside from chamomile (Chamomilla recutita [L.] Rauschert) *Phytochemistry, 65*, 2323–2332.

Timmusk, S, & Wagner, E. G. (1999). The plant-growth-promoting rhizobacterium Paenibacillus polymyxa induces changes in Arabidopsis thaliana gene expression: a possible connection between biotic and abiotic stress responses. *Molecular plant-microbe interactions : MPMI*, *12*(11), 951–9.

Timmusk, Salme, Grantcharova, N., Gerhart, E. H., & Wagner, E. G. H. (2005). Paenibacillus polymyxa Invades Plant Roots and Forms Biofilms Paenibacillus polymyxa Invades Plant Roots and Forms Biofilms, *71*(11).

Treutter, D. (2006). Significance of flavonoids in plant resistance: a review. *Environmental Chemistry Letters*, *4*(3), 147–157.

Tsavkelova, E. A., Klimova, S. Y., Cherdyntseva, T. A., & Netrusov, A. I. (2006). Microbial producers of plant growth stimulators and their practical use: A review. *Applied Biochemistry and Microbiology*, *42*(2), 117–126.

Van Peer R, Nieman GJ, Schippers B (1991) Induced resistance and phytoalexin accumulation in biological control of Fusarium wilt of carnation by Pseudomonas WCS417r. *Phytopathology, 81,* 728–734.

Verginer, M., Leitner, E., & Berg, G. (2010). Production of volatile metabolites by grape-associated microorganisms. *Journal of agricultural and food chemistry*, *58*(14), 8344–50. doi:10.1021/jf100393w

Viebahn, M., Glandorf, D. C. M., Ouwens, T. W. M., Smit, E., Leeflang, P., Wernars, K., Thomashow, L. S., et al. (2003). Repeated Introduction of Genetically Modified Pseudomonas putida WCS358r without Intensified Effects on the Indigenous Microflora of Field-Grown Wheat, *69*(6), 3110–3118.

Vleesschauwer, D. D. and Höfte, M. (2009). Rhizobacteria-Induced Systemic Resistance, *Advances in Botanical Research*, *Academic Press, 51*(6), 223-281.

Wang, Q., Garrity, G. M., Tiedje, J. M., & Cole, J. R. (2007). Naive Bayesian classifier for rapid assignment of rRNA sequences into the new bacterial taxonomy. *Applied and environmental microbiology*, *73*(16), 5261–7.

Wei, G., Kloepper, J. W., & Tuzun, S. (1991). Induction of systemic resistance of cucumber to Colletotrichum orbiculare by select strains of plant growth-promoting rhizobacteria, *Phytopathology, 81*, 1508–1512.

Weller, D. M. (2007). Pseudomonas biocontrol agents of soilborne pathogens: looking back over 30 years. *Phytopathology*, *97*(2), 250–6.

Whipps, J. M. (2001). Microbial interactions and biocontrol in the rhizosphere. *Journal of experimental botany*, *52*, 487–511.

White, J. G. (1990). Mycostop--a novel biofungicide based on Streptomyces griseoviridis. *Brighton Crop Protection Conference-Pests and Diseases, 1*, 221-226.

Wolf, A., Fritze, A., Hagemann, M., & Berg, G. (2002). Stenotrophomonas rhizophila sp. nov., a novel plant-associated bacterium with antifungal properties. *International journal of systematic and evolutionary microbiology*, *52*(6), 1937–44.

Yeung, N., Cline, M. S., Kuchinsky, A., Smoot, M. E., & Bader, G. D. (2008). Exploring biological networks with Cytoscape software. *Current protocols in bioinformatics, Chapter 8*, Unit 8.13.

Yiridoe, E. K., Bonti-Ankomah, S., & Martin, R. C. (2005). Comparison of consumer perceptions and preference toward organic versus conventionally produced foods: A review and update of the literature. *Renewable Agriculture and Food Systems*, *20*(4), 193–205.

Yu, O., Shi, J., Hession, A. O., Maxwell, C. A., McGonigle, B., & Odell, J. T. (2003). Metabolic engineering to increase isoflavone biosynthesis in soybean seed. *Phytochemistry*, *63*(7), 753–63.

Zachow, C. (2010). Strain-specific colonisation pattern of Rhizoctonia antagonists in the root system of sugar beet, *FEMS microbiology ecology, 74*(1), 124-35,1–34.

Zachow, C., Tilcher, R., & Berg, G. (2008). Sugar beet-associated bacterial and fungal communities show a high indigenous antagonistic potential against plant pathogens, *Microbial Ecology, 55*, 119–129.

Zangh, L. and Birch, G. R. (1997). The gene for albicidin detoxification from Pantoea dispersa encodes an esterase and attenuates pathogenicity of Xanthomonas albilineans to sugarcane, *Proceedings of the National Academy of Science, 94*, 9984–9989.

Zuanazzi, J.A.S., Clergeot, P.H., Quirion, J.C., Husson, H.P., Kondorosi, A., and Ratet, P. (1998). Production of Sinorhizobium meliloti nod gene activator and repressor flavonoids from Medicago sativa roots. *Molecular Plant-Microbe Interactions, 11*(8), 784–794.

List of abbreviations

%	percentage
°C	degree centigrade
A	absorption
ACN	acetonitrile
BCAs	bacterial control agents
BLAST	basic local alignment search tool
cfu	colony forming unit
CLSM	confocal laser scanning microscopy
cm	centimetre
conc	concentrated
CTAB	cetyl trimethylammonium bromide
DAD	diode array detector
ddH2O	double distilled water
DMSO	dimethlsulfoxid
DNA	deoxyribonucleic acid
dNTP	desoxyribonukleosid-5‘‘-triphosphate
E.C.	electrical conductivity
e.g.	exempli gratia
ESI	electron spray isonisation
et al.	et alteri
Fig.	Fig.
h	hour
H_2O	water
HCl	hydrogen chloride
HNO_3	nitric acid
HPLC	high performance liquid chromatography
HPTLC	high performance thin layer chromatography
kb	kilo base

l	litre
LB	lysogeny broth
LC	liquid chromatography
m	milli
M	molar
m/z	mass-charge ratio
mcf	moisture correction factor
MeOH	methanol
min	minute
MS	mass spectrometer
MS	mass sepctrum, mass spectrometry
MW	molecular weight
n	nano
NaCl	sodium chloride
NaOH	sodium hydroxide
NCBI	national center for biotechnology information
O.C.	organic carbon
O.M.	organic matter
ONC	overnight culture
Pa	Pascal
PBS	phosphate-buffered saline
PCR	polymerase chain reaction
PGPBs	plant growth promoting bacteria
pH	negative decimal logarithm of the hydrogen ion activity in a solution
pH	pondus hydrogenii
qPCR	quantitative real-time PCR
r	ribosomal
Rf	retention factor.
RNA	ribonucleic acid
rpm	rounds per minute

Rt	retention time
SDS	sodiumdodecylsulfate
sec	second
SSCP	single-strand conformation polymorphism
T.K.	total phoshphorous
T.N.	total nitrogen
T.P.	total potassium
TAE	tris-acetate-EDTA
TBE	tris-borate-EDTA
TEMED	N,N,N,N-tetramethylethylendiamin
Tris	tris-hydroxymethyl-amminomethan
UPGMA	unweighted pair group method with arithmetic mean
USDA	united states department of agriculture
UV	ultraviolet
V	volt
VOCs	volatile organic compounds
λ	wavelength
µ	micro

List of Figures

List of Tables